Evaluation of Analysis Methods used for the Assessment of I-walls Stability

Liselle Vega-Cortés

Thesis submitted to the faculty of the
Virginia Polytechnic Institute and State University
in partial fulfillment of the requirements for the degree of

Master of Science
in
Civil Engineering

Thomas L. Brandon, Chair
George M. Filz
James K. Mitchell

December 4, 2007
Blacksburg, Virginia

Keywords: Slope Stability, OCR

Evaluation of Analysis Methods used for the Assessment of I-walls Stability

Liselle Vega-Cortés

(ABSTRACT)

On Monday, 29 August 2005, Hurricane Katrina struck the U.S. gulf coast. The storm caused damage to 169 miles of the 284 miles that compose the Hurricane Protection System (HPS) of the area. The system suffered 46 breaches due to water levels overtopping and another four caused by instability due to soil foundation failure. The Interagency Performance Evaluation Task Force (IPET) conducted a study to analyze what happened on the I-wall breach of the various New Orleans flood control structures and looked for solutions to improve the design of these floodwalls.

The purpose of the investigation, describe in this document, is to evaluate different methods to improve the analysis model created by IPET, select the best possible analysis techniques, and apply them to a current cross-section that did not fail during Hurrican Katrina. The use of Finite Element (FE) analysis to obtain the vertical total stress distribution in the vicinity of the I-wall and to calculate pore pressures proved to be an effective enhancement. The influence of overconsolidation on the shear strength distribution of the foundation soils was examined as well.

Dedication

To

my beloved husband

Juan Ramón Ortiz-Ortiz

Thank you for giving me the most beautiful gifts of all…your love.

In loving memory of all the victims who passed away during the Virginia Tech shootings in April 16, 2007. You will never be forgotten.

Acknowledgements

First, I would like to thank God for being by my side and giving me the strength that I needed to finish my goal.

I also want to thank all of the members of my committee for encouraging me to finish what I started on Fall 2006, Juan's and I biggest dream, the Master of Science in Civil Engineering degree. I would like to give special thanks to Dr. Thomas Brandon, for serving as my committee chair and for teaching me that the most important thing is to learn.

I would also like to thank my family, friends, and people around the world that during the most difficult time of my life cheered me up and told me not to give up. Without all the support, I would not be able to finish. Thank you.

Table of Contents

List of Figures

List of Tables

Introduction

On Monday, 29 August 2005, Hurricane Katrina struck the U.S. gulf coast. Hurricane Katrina, with a Category 3 status and maximum sustained winds of 127 mph at the time of landfall, brought rainfall of over 14 inches in 24 hours (IPET 2007).

The effects of the storm were being felt in the New Orleans area during the early morning hours. Of the 284 miles of levees and floodwalls that compose the Hurricane Protection System (HPS) of the area, 169 miles were damaged. The system suffered 50 breaches, being 46 of them due to water levels overtopping. Four other breaches were caused by instability due to soil foundation failure.

A study was conducted by the Interagency Performance Evaluation Task Force (IPET) to understand what happened during and after the storm and seek solutions to the design problems presented on the levees and floodwalls system. An analysis method was created by IPET to simulate what happened on the I-wall breach of the 17th Street Outfall Canal, as well as other I-walls in the New Orleans flood control system. This breach at 17th Street occurred due to a shear failure in the soil beneath the I-wall.

The purpose of this investigation is to examine the assumptions used in the IPET analyses and to provide suggestions on how to enhance the analyses. Twelve separate cases were analyzed. The conditions varied in the analyses included the following:

(1) Canal water elevation
(2) Method of calculating vertical total stress
(3) Method of calculating pore pressures
(4) Consolidation condition of foundation soils.

The examination of the different analysis assumptions was performed on a cross section based on an east bank cross section for the 17th Street Outfall Canal reported in the IPET report. However, these analyses are not intended to fully represent the soil conditions and loading conditions resulting in the failure of the 17th Street I-wall, but only to gain an insight on the influence of analysis assumptions on the calculated factor of safety.

After the examination of the east bank cross section was made, the resulting analysis techniques were applied to a representative west bank cross section that did not fail during Hurricane Katrina. The analysis techniques presented in this thesis may serve as a guide to future design and analysis methods used for I-wall flood control structures.

1. History of 17th Street Outfall Canal

The city of New Orleans was originally located near the Mississippi River on high ground. Due to continuing development, expansion of the city has been necessary throughout the years (IPET 2007). This expansion has led to difficult construction sites mainly composed of marshlands and the never-ending fight with flooding as an outcome of annual precipitation or storm surge by tropical hurricanes. This situation brought to attention the necessity of having a proper hurricane protection system.

1.1 New Orleans Hurricane Protection System

The Hurricane Protection System (HPS), outlined on the map in Figure 1, includes approximately 350 miles of protective structures, 56 miles of which are floodwalls. The majority of the floodwalls are I-walls with small sections of T-walls and a very small number of L-walls (IPET 2007).

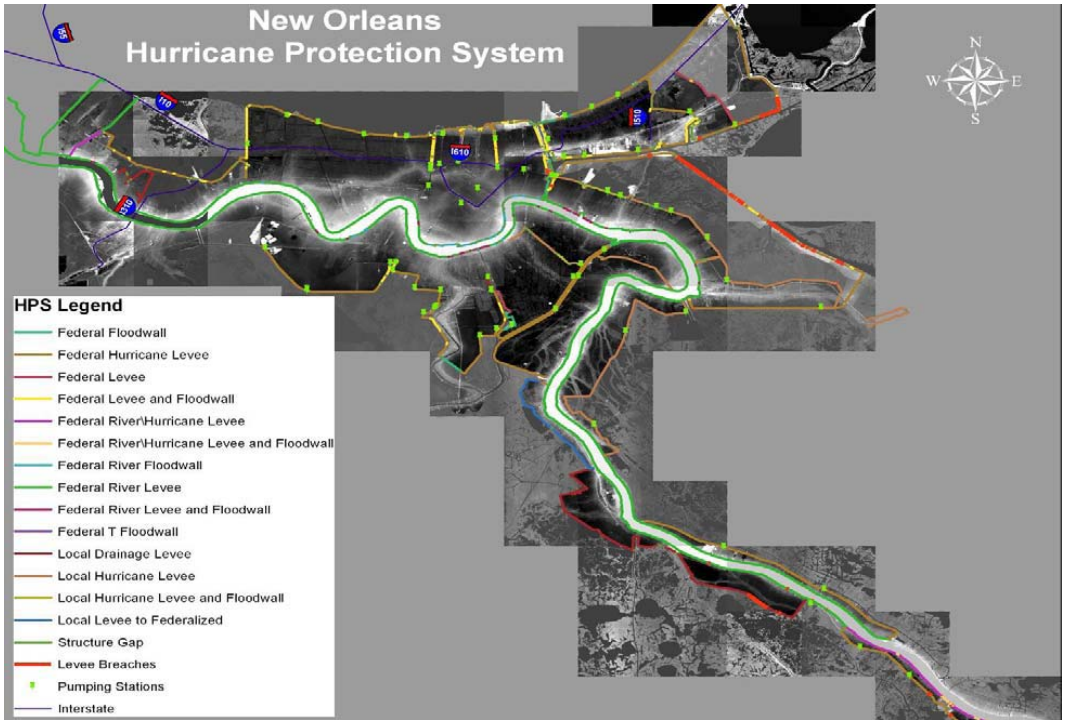

Figure 1: New Orleans Hurricane Protection System (IPET 2007)

The HPS is divided into three major hurricane and flood protection regions: Lake Pontchartrain and Vicinity, West Bank and Vicinity, and New Orleans to Venice, shown on Figure 2. For each project, different hurricane characteristics where used for design.

Figure 2: Hurricane and flood protection projects (IPET 2007)

For Lake Pontchartrain and Vicinity and West Bank and Vicinity, the Standard Project Hurricane (SPH) was selected as the design hurricane because of the urban nature of the project area. The SPH was defined as a hypothetical hurricane intended to represent the most severe combination of hurricane parameters that is reasonably characteristic of a specified region (IPET 2007). The Lake Pontchartrain and Vicinity region covers four parishes in southeast Louisiana: St. Bernard, Orleans, Jefferson, and St. Charles.

1.2 Location of the 17th Street Outfall Canal

The storm water drainage of Orleans Parish is composed of three outfall canals: the 17th Street Outfall Canal, the London Avenue Canal, and the Orleans Avenue Canal. The 17th Street Outfall Canal follows the Orleans/Jefferson Parish line. It runs parallel to the London Avenue Canal and the Orleans Avenue Canal and is oriented generally in the north-south direction (Department of the Army 1990). It extends 3 miles from Pump Station No. 6 near Interstate Highway 10 to its confluence with Lake Pontchartrain (IPET 2007). A diagram showing the location of the 17th Street Outfall Canal is presented in Figure 3. In

addition, a more detailed location map of the 17th Street Outfall Canal is shown on Figure 4.

Figure 3: Location of 17th Street Outfall Canal (Department of the Army 1990)

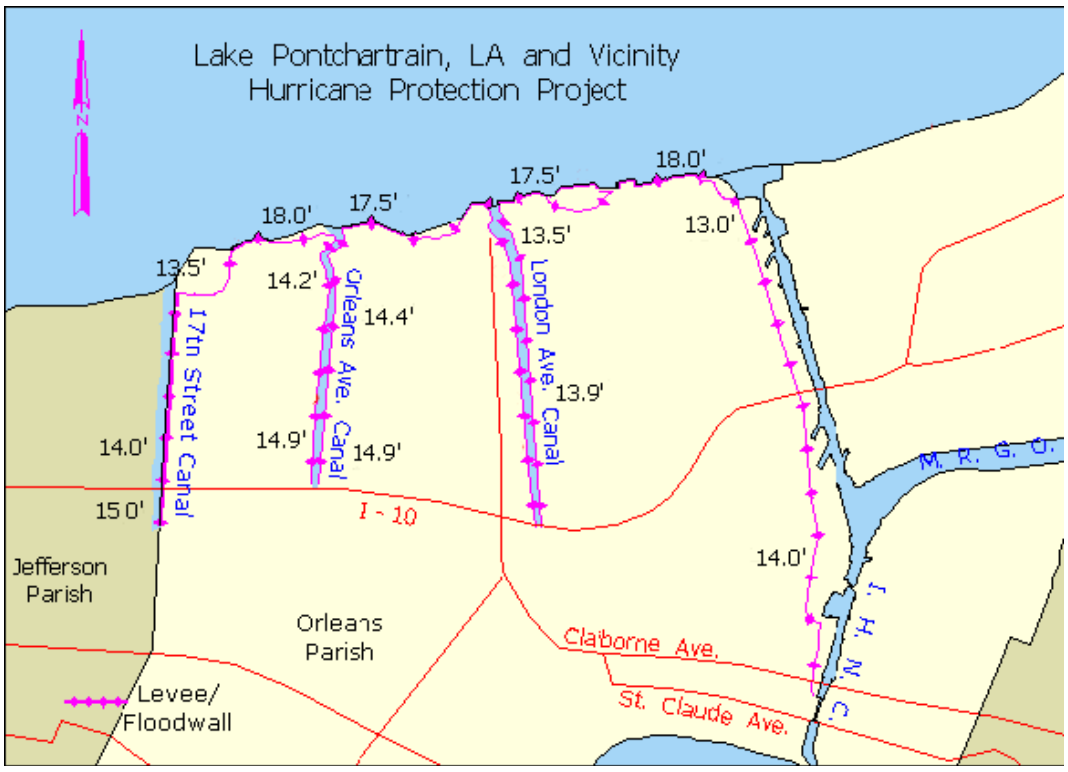

Figure 4: Location of the 17th Street Outfall Canal (IPET 2007)

1.3 Characteristics of the 17th Street Outfall Canal

The 17th Street Outfall Canal is one of the major outfall canals that serve the city of New Orleans and a portion of Jefferson Parish. The purpose of the 17th Street Outfall Canal and all other components of the Lake Pontchartrain and Vicinity Hurricane Project is to protect areas around Lake Pontchartrain from flooding due to storm surge or rainfall produced by a hurricane. This canal was dug in 1871, with original dimensions of 50 feet wide and 16,500 feet long. The dimensions of the canal increased over the years to comply with the capacity requirements imposed by the expansion of the developed areas. At the time of Hurricane Katrina's landfall, the bottom invert elevation was -18.0 feet NGVD (Department of the Army 1990).

In 1898, the construction of the first portion of Pumping Station No. 6 was completed to control the rainfall runoff in the area (Department of the Army 1990). This pumping station is located 2.4 miles south of the canal's outfall at Lake Pontchartrain (Department of the Army 1990). The original capacity of this station was 1,000 cubic feet per second (cfs). The station has been expanded since then to accommodate the need of additional drainage

as the developed areas increased. By the time of Hurricane Katrina's landfall, the capacity of this station was 9,630 cfs, which would make it one of the largest low head lift stations in the world (Department of the Army 1990).

For the 17th Street Outfall Canal, the design water level was obtained from the "Hurricane Protection Project Reevaluation Study" (Department of the Army 1984), and it was revised in subsequent Design Memoranda. The water surface elevation was set at 11.5 ft according to the National Geodetic Vertical Datum (NGVD) at Lake Pontchartrain, which is the still-water level in the lake for SPH conditions (IPET 2007). Prior to Hurricane Katrina, the return levee of the canal was considered to be an effective enough barrier to prevent major flood exchange between East Jefferson Parish and the west New Orleans area.

When a significant precipitation event occurs, the Sewerage and Water Board of New Orleans (S & W B) activate their pumps to drain the rainwater out of the city into the 17th Street Outfall Canal, which discharge into Lake Pontchartrain, as shown in Figure 5. It should be noted that the USACE pumps and the floodwall shown in the figure were added after Hurrican Katrina. At the time of the failure, it was not possible to isolate the outfall canals from Lake Pontchartrain.

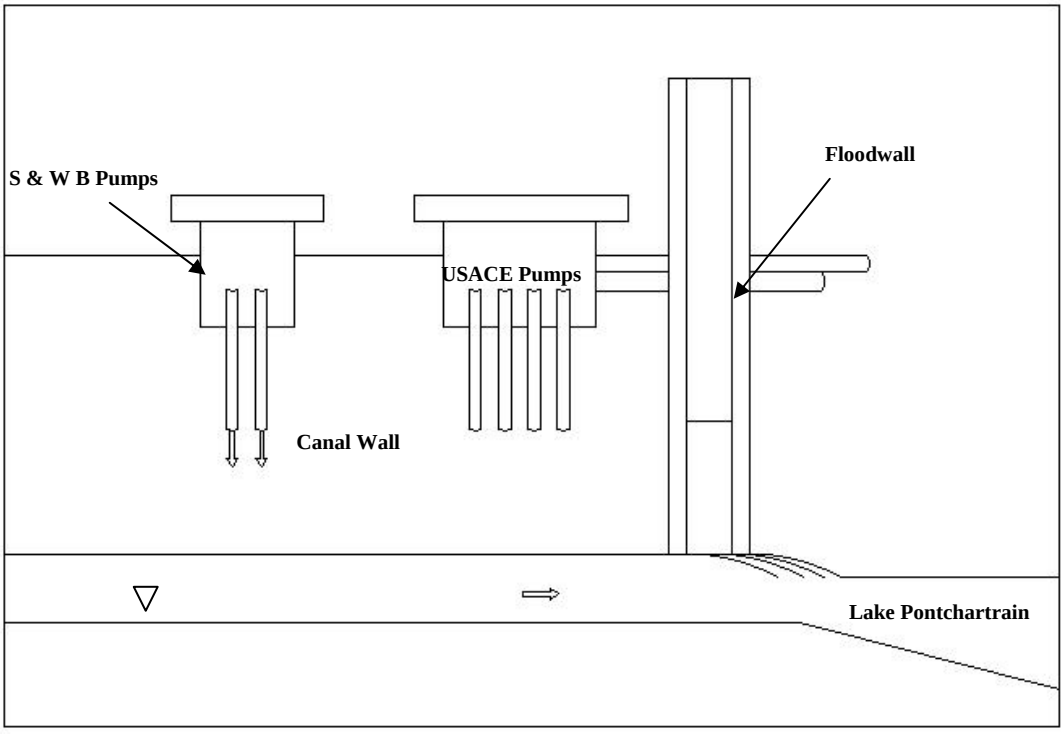

Figure 5: Diagram showing activation of S & W B Pumps during a precipitation event

Hurricane winds can produce storm surge, which can move water from the lake into the canal and cause flooding in the city. To avoid flooding, when the water in the lake increases to a dangerous level, the floodgates in the canal are closed preventing more water from coming in. This step is shown in Figure 6.

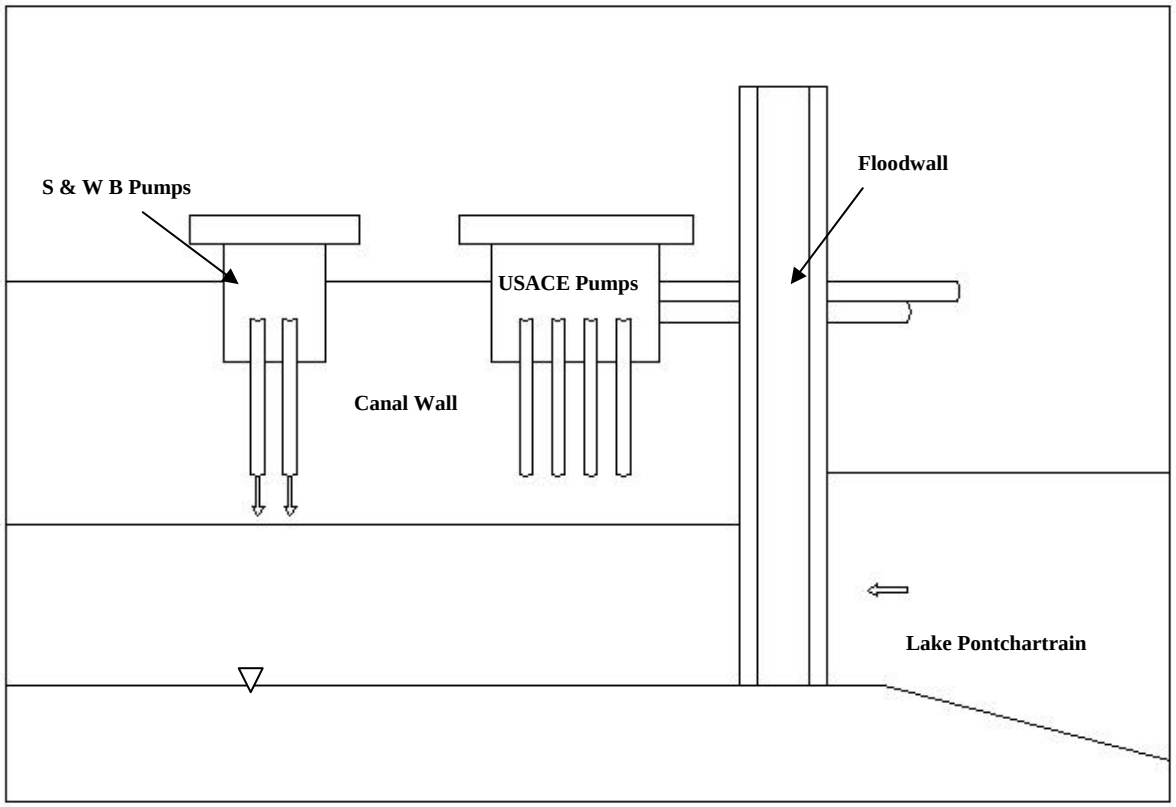

Figure 6: Diagram showing the closing of the floodgate in the canal

After the floodgates are closed, pumped rainfall water starts to accumulate inside the canal increasing the water level. An additional set of pumps are activated by the United States Army Corps of Engineers (USACE) to drain the water out of the canal into the lake once again. This step is illustrated in Figure 7. After the level of water in both the lake and the canal has reached a safe level, the floodgate is opened and the original flow of water restored.

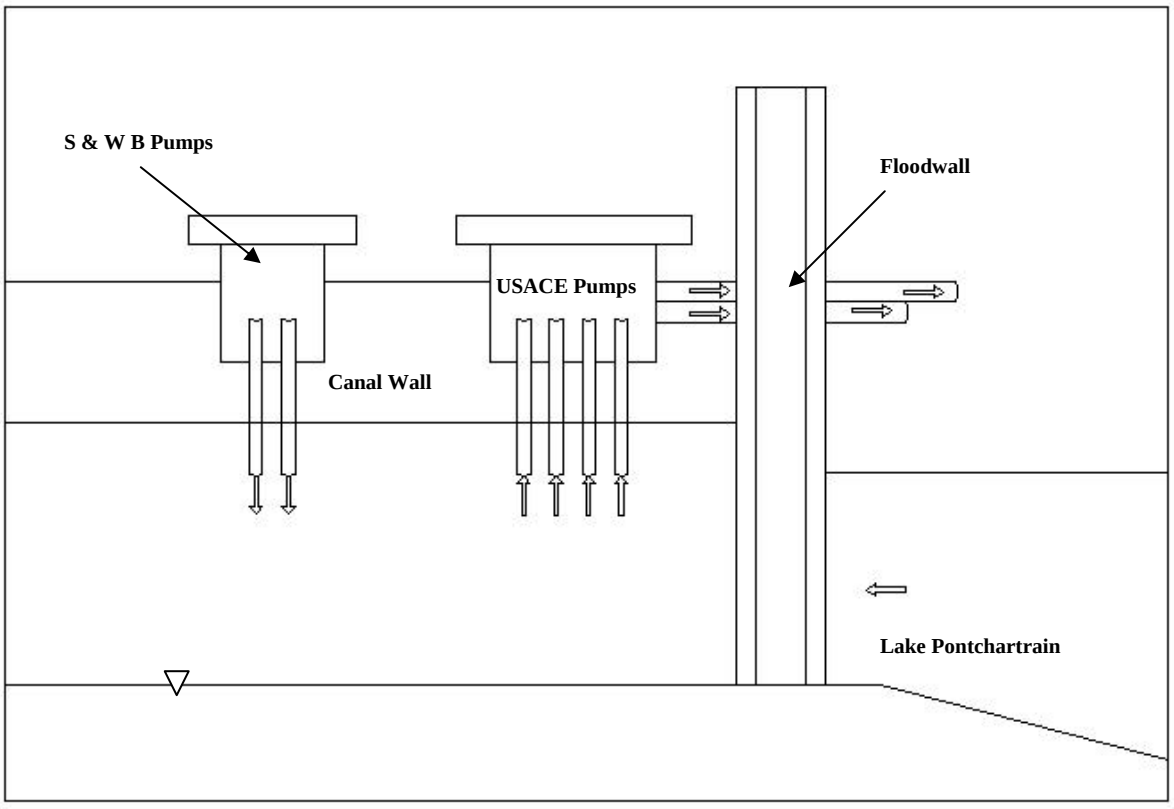

Figure 7: Diagram showing activation of USACE pumps to drain water out of the canal

1.4 Foundation Conditions

The engineering properties of the sediment beneath the 17th Street Outfall Canal vary greatly. Generally, the subsurface consists of Holocene deposits varying in depth to approximately 60 ft and underlain by Pleistocene deposits (IPET 2007). The area of the breach (described in detail on Chapter 2) consists mainly of marsh-swamp deposits that are underlain by lacustrine deposits which are variable in thickness. These lacustrine deposits are comprised predominantly of fat clays (CH). Figure 8 shows a cross section of the 17th Street Outfall Canal and its foundation conditions. The design characteristics of the 17th Street Canal will be discussed further on Chapter 3.

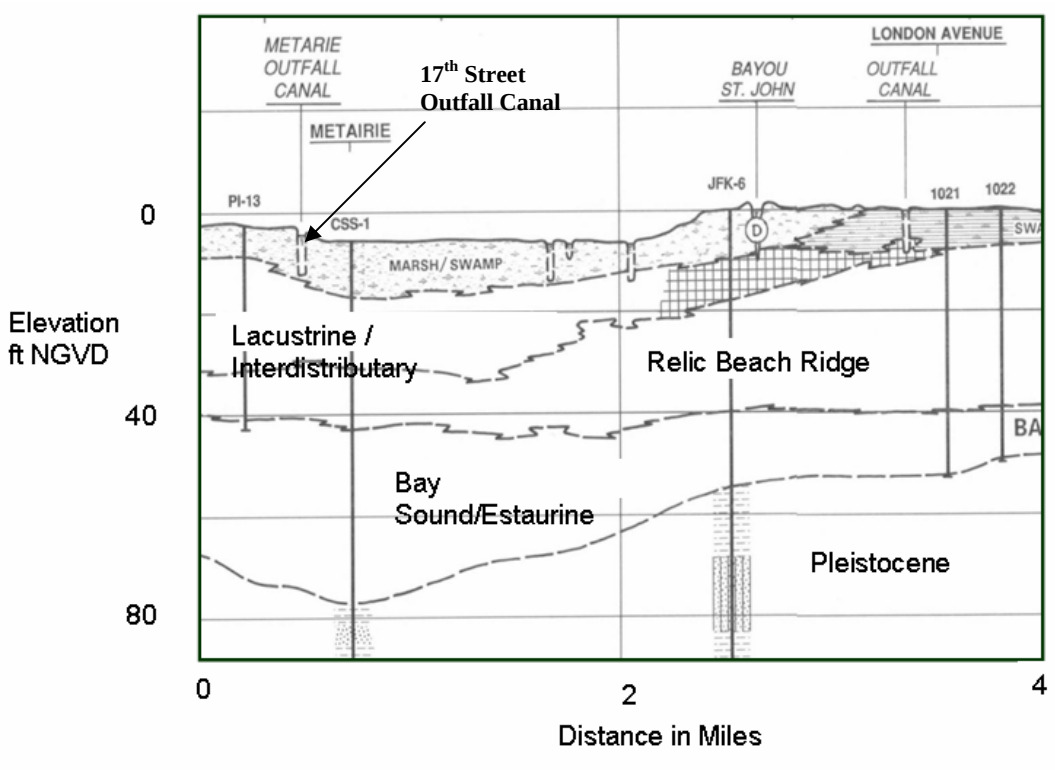

Figure 8: Cross section of 17th Street Outfall Canal with foundation conditions extending west to east across eastern Jefferson Parish and into western Orleans Parish (IPET 2007)

2. Description of failure during Hurricane Katrina

On Monday, 29 August 2005, Hurricane Katrina struck the U.S. gulf coast. The effects of the storm were being felt in the New Orleans area during the early morning hours. Of the 284 miles of levees and floodwalls, 169 miles were damaged (IPET 2007). There were two principal causes for the breaches: erosion due to overtopping and instability due to soil foundation failure. On the 17th Street Outfall Canal a breach occurred due to a shear failure in the foundation clays resulting in instability of the floodwall. Figure 9 shows the locations of the major breaches in Orleans Parish. Figure 10 shows an aerial view of the breach in the floodwall along the east side of the 17th Street Outfall Canal.

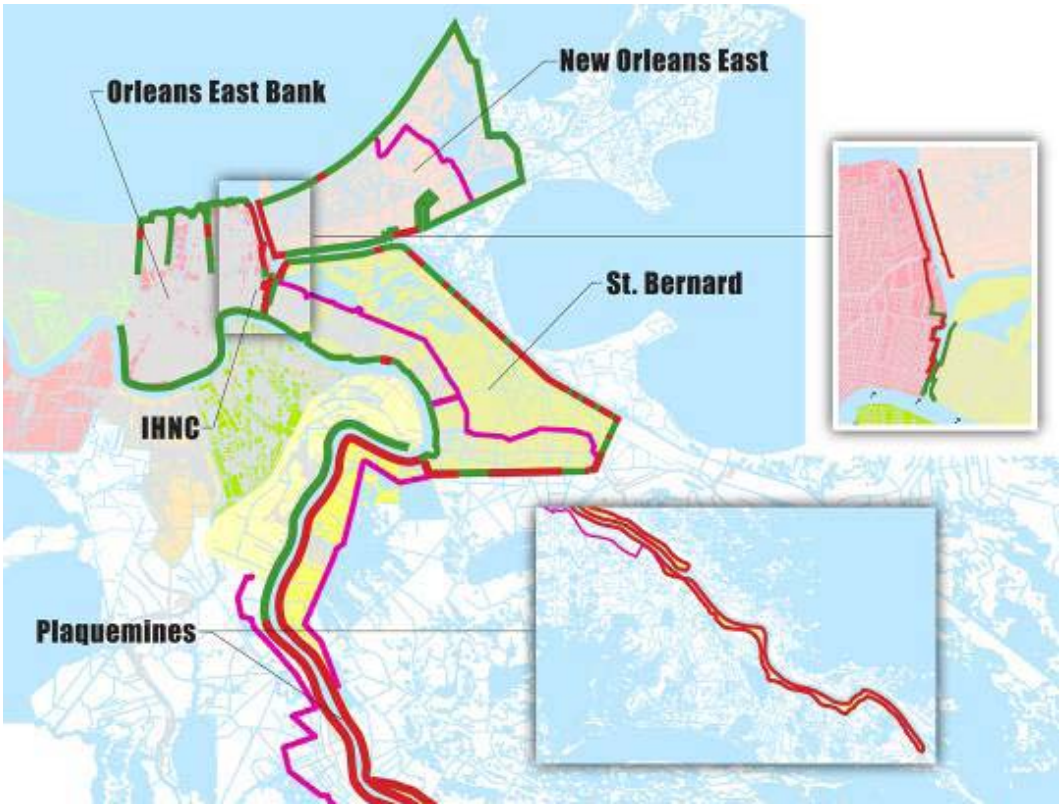

Figure 9: Major breaches in Orleans Parish (IPET 2007)

Figure 10: Aerial view of breach in floodwall on east side of 17th Street Outfall Canal (IPET 2007)

2.1 Hurricane Katrina

Hurricane Katrina was a considerably large storm. When the storm made landfall in Louisiana, it had a maximum sustained surface wind speed of 127 knots, which corresponded to Category 3 strength in the Saffir-Simpson scale. Hurricane Katrina brought 14 inches of rainfall in a 24 hour period, serverely loading the Hurricane Protection System of Louisiana. Even though Hurricane Katrina struck on the early hours of the 29th of August, the effects of the storm on the water levels were being felt hours prior to its landfall. Figure 11 shows a diagram with the total rainfall amounts produced by Hurricane Katrina.

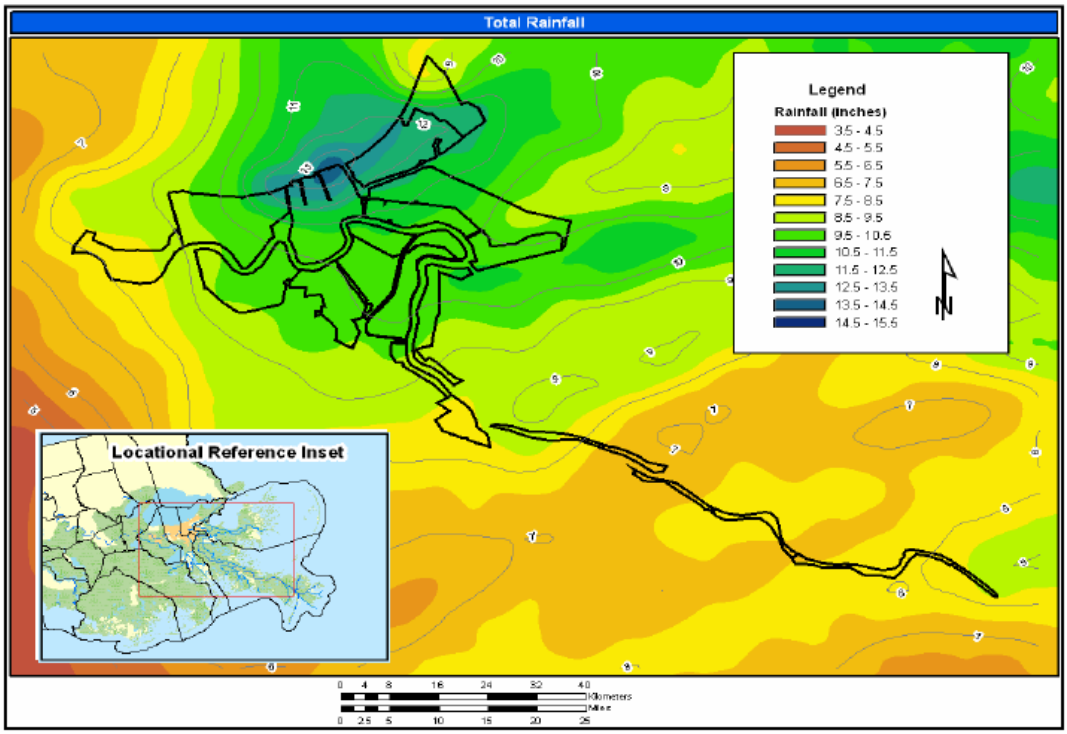

Figure 11: Hurricane Katrina total rainfall amounts (IPET 2007)

The time-history of the surge levels was predicted by IPET by using a model with a very high-resolution computational grid, because Hurricane Katrina destroyed all of the gauging instruments to measure water conditions. Predicted surge levels ranged from about 10 to 12 feet along the south shore of Lake Pontchartrain to 20 feet along the Plaquemines Levees (IPET 2007). Figure 12 shows the maximum surge levels predicted for Hurricane Katrina by IPET. These predicted values were compared to the high water marks leaved by Hurricane Katrina and were in close agreement in most cases.

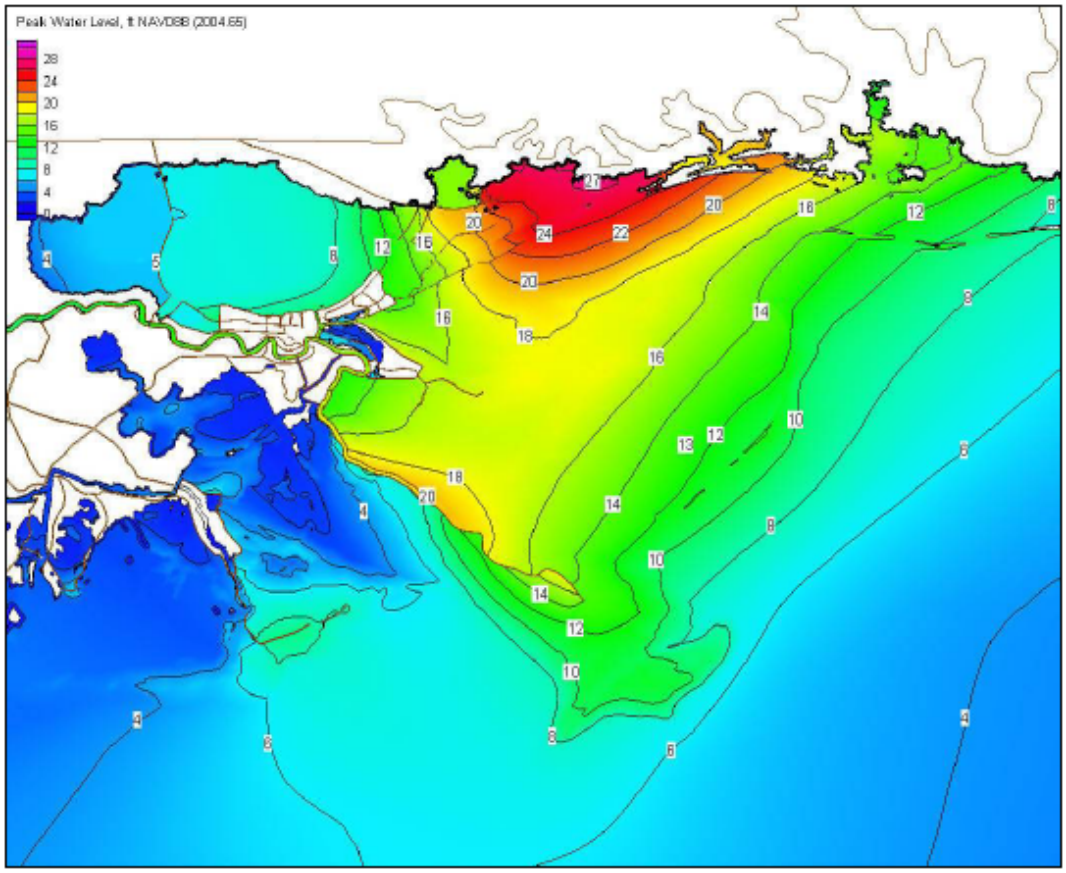

Figure 12: Maximum surge levels predicted by IPET

The water level is not only affected by rainfall, but by wave environment due to winds as well. In Lake Pontchartrain, the maximum significant wave heights ranged from 3 to 9 feet. Figure 13 shows a diagram with the maximum modeled significant wave height and mean direction.

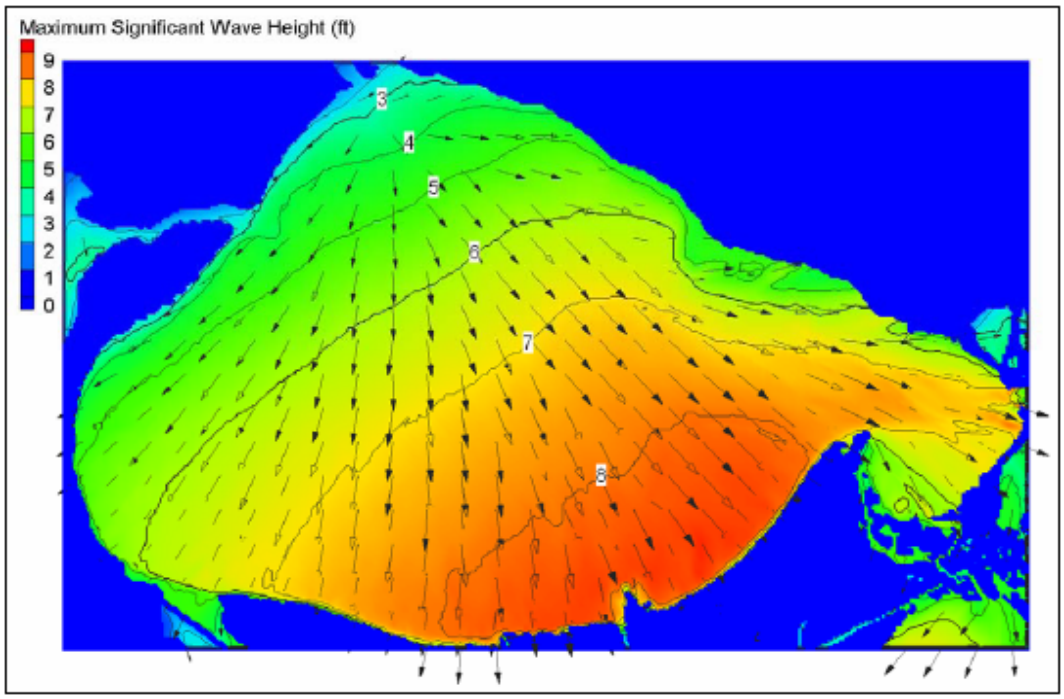

Figure 13: Maximum modeled significant wave height and mean direction

The wave height generated by Hurricane Katrina, in many cases, differed considerably from the design assumptions. The period of Hurricane Katrina generated waves agreed with the design assumptions for waves generated in Lake Pontchartrain in the 6 to 7 second range. However, for St. Bernard and Plaquemines Levees the generated waves were three times the design wave periods. Figure 14 shows a diagram with the modeled peak wave period that corresponds to the maximum wave height.

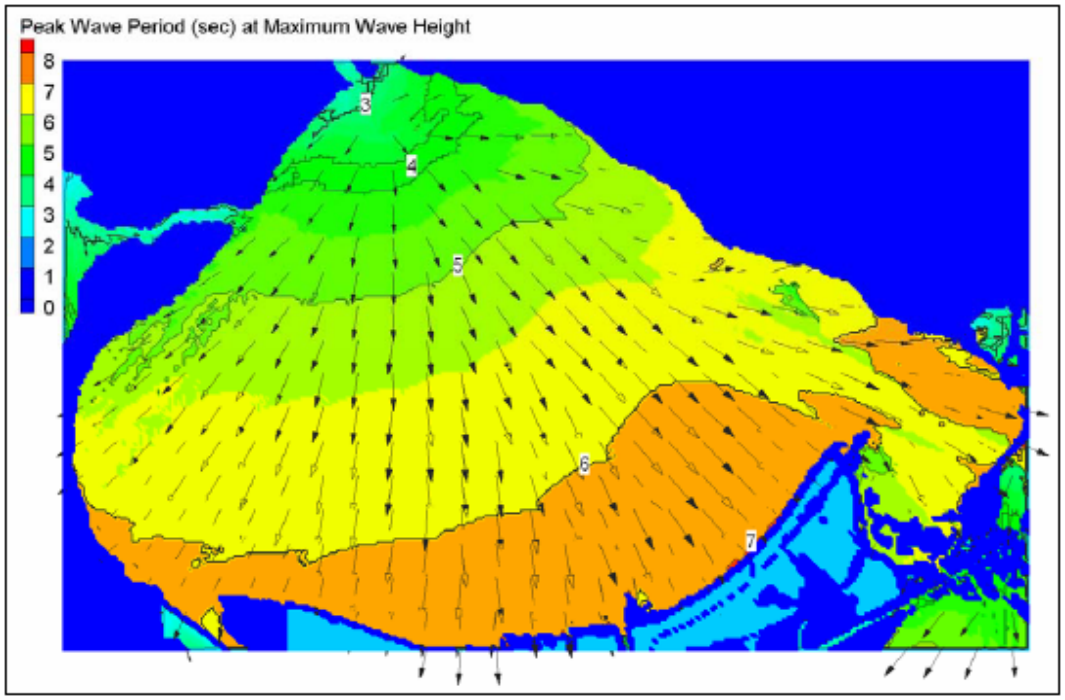

Figure 14: Modeled peak wave period that corresponds to the maximum wave height

Figure 15 shows a comparison between the surge generated by Hurricane Katrina and the values used for design.

Figure 15: General surge level values used for design (D) and estimated from Katrina (K) (IPET 2007)

The surge levels, generated by Hurricane Katrina, on the east side of New Orleans were significantly greater than the values assumed for design, while on Lake Pontchartrain the values were nearly the same.

2.2 Timeline of Events

From eye-witness reports, field investigations, and stability analyses, it appears that the breach process started around 0630hr. At that time, the static water level was estimated to have been from 7 to 8 ft, and possibly 1 to 2 ft higher due to wave effects at the time of the catastrophic breach. Figure 16 shows the hydrograph at 17th Street Outfall Canal. The data was collected by IPET and is based on photographs and observed information.

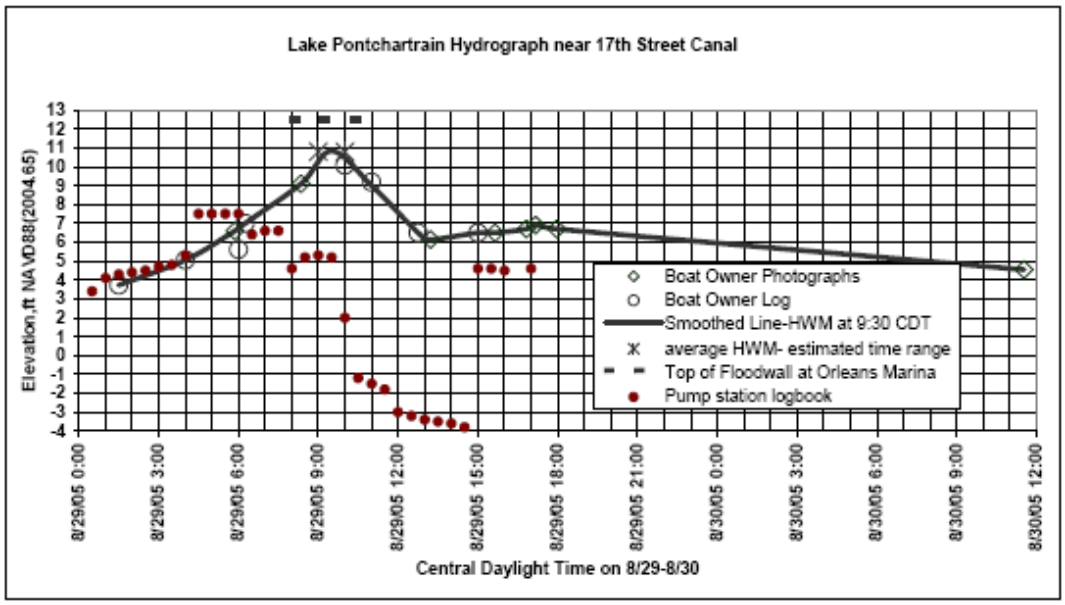

Figure 16: Constructed hydrograph at 17th Street Outfall Canal entrance (IPET 2007)

The reported water levels at the pump station differ significantly from the constructed hydrograph for the 17th Street Canal entrance, especially on the morning and afternoon of the 29th of August. However, the derived hydrograph at the Lake and the pump station log are in fair agreement before 4:00AM of that same day.

No overtopping had occurred and the design water elevations had not been reached at the time of levee failure (IPET 2007). This process is shown on the following figure.

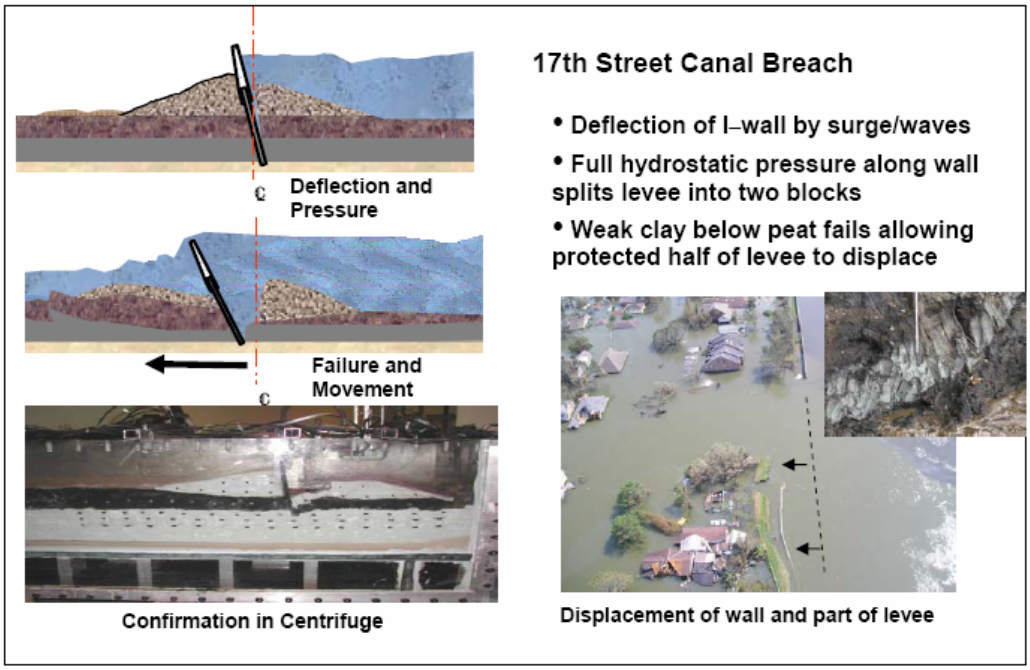

Figure 17: Description of failure on 17th Street Canal breach (IPET 2007)

Post-Katrina studies showed that the crest of the levee on the canal side remained in place after the breach, but the levee and floodwall moved about 40 ft laterally during the failure, and the floodwall was tilted toward the landside at about 45 degrees after the failure (IPET 2007).

Shortly after the hurricane, an emergency closure of the breach had to be made and water levels had to be drawn down. During this process, a significant discovery was made when large blocks of marsh were exposed from exploration trenches. The marsh blocks were attached to a clay layer of approximately 1-ft thick and observations were made of the location of the failure plane. The field investigation showed that the failure plane of the slide block was within the clay under the levee, and the failure plane came upward through the marsh layer further landward (IPET 2007). The following figure shows an exposed failure plane with marsh and clay layers.

Figure 18: Exposed failure plane with a marsh layer between two clay layers (IPET 2007)

Field evidence, analyses, and physical model tests concluded that the breach was due to instability caused by shear failure within the clay in the foundation beneath the levee and the I-wall, with a rupture surface that extended laterally beneath the levee, and exited upward through the marsh layer (IPET 2007). From analyses, the undrained shear strength was found to be lower beneath the levee slopes and beyond the toe than beneath the levee crest, where the clay had been compressed under higher pressure. This spatial variation in shear strength is important in understanding the foundation soil behavior, for it affected greatly the stability. Another factor that influenced the stability was a gap that formed between the wall and the levee fill on the canal side of the wall. This allowed water pressure to act on the wall below the surface of the levee, thus decreasing the stability of the floodwall.

3. Results of IPET Analysis

The Interagency Performance Evaluation Task Force (IPET) was established by the Chief of Engineers, soon after Hurricane Katrina, to determine the facts concerning the performance of the Hurricane Protection System (HPS) in New Orleans and southeast Louisiana during the hurricane (IPET 2007).

Composed by more than 300 experts, the IPET members compared the original design of the HPS with the actual conditions present during Hurricane Katrina. They also evaluated the performance of the levees and floodwalls under the forces generated by the effects of the hurricane.

Information regarding the geometry of the sections to be analyzed, as well as the physical properties of the subsurface materials in the sections is necessary to be able to do stability and seepage analysis. The IPET team performed the analyses using the original design information contained in previously published technical studies, as well as test results from post-Katrina exploration (IPET 2007).

During the analyses, expertise and experience from the investigators were used to make the correct assumptions. The American Society of Civil Engineers (ASCE) and the National Research Council (NRC) provided technical reviews to ensure that correct information and methods were used. However, it is possible to refine the assumptions used by IPET and to perform more advanced analyses. In this section the results of the limit equilibrium stability analyses using the IPET Strength Model will be discussed.

Using the borings and soil types information from the General Design Memorandum No. 20 (USACE 1990), as well as new borings, the subsurface stratigraphy was determined. It consisted mainly of marsh-swamp deposits underlain by lacustrine clay deposits. This information was compiled in 1990, as an upgrade of the New Orleans levee system was scheduled. From laboratory consolidation tests, the clay layer was found to be normally consolidated. Figure 19 shows a diagram of a cross section of the breach in 17th Street

Outfall Canal before failure occurred. Table 1 gives the elevation of the contact between the various soil layers, and the general consistency of the soil types.

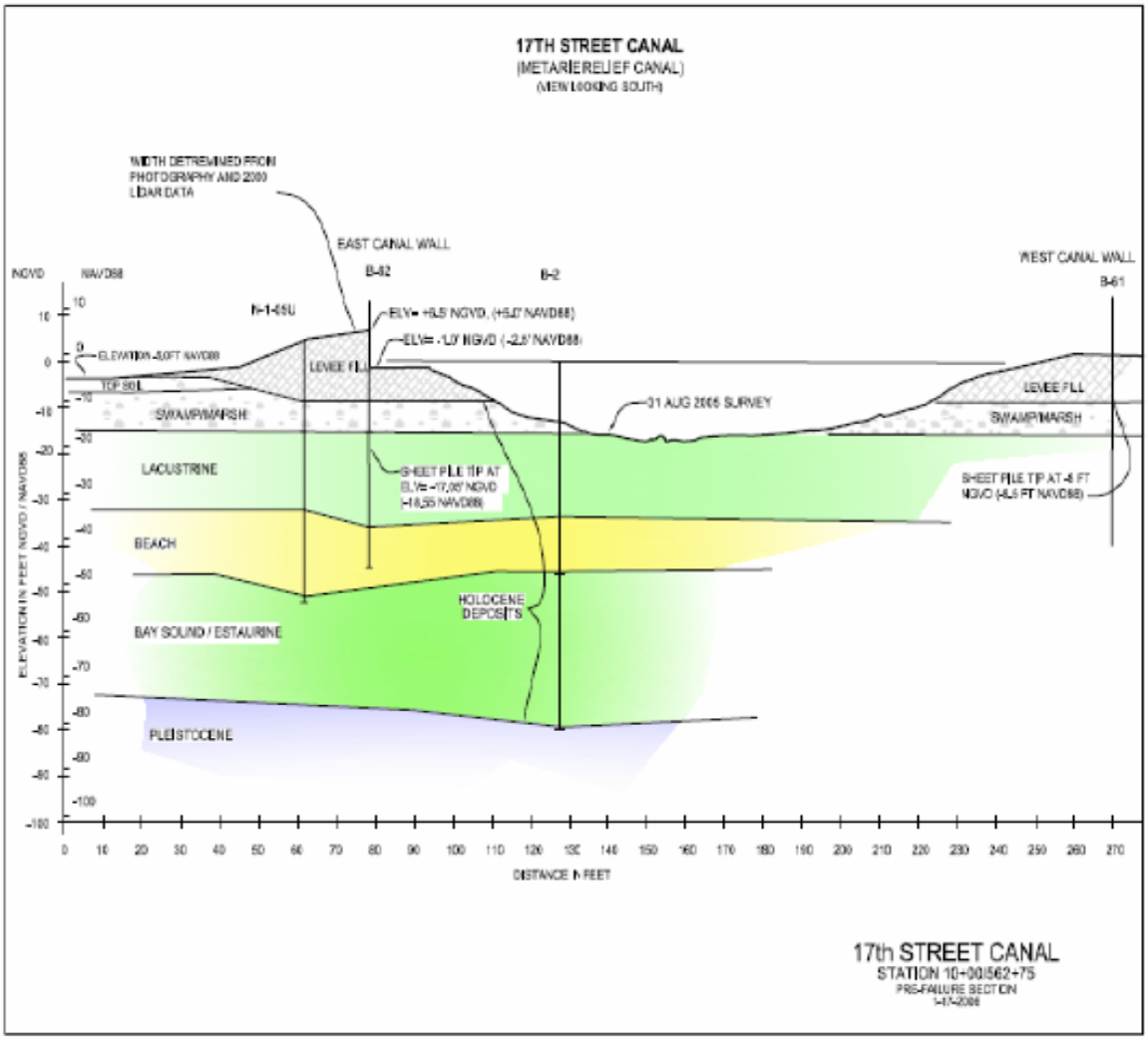

Figure 19: Diagram of breach cross section on 17th Street Outfall Canal before failure (IPET 2007)

Table 1: Subsurface stratigraphy information on breach area (IPET 2007)

Layer	Approximate Elevation of Top of Layer (NGVD)	Approximate Elevation of Bottom of Layer (NGVD)	Soil Type	Consistency
Embankment	6.5	-10	Clayey (CL's and CH)	Stiff
Marsh	-10	-15	Organic/Peat	Very Soft
Lacustrine	-15	-35	Clays (CH)	Very Soft
Beach Sand	-35	-45	Sand	
Bay Sound/Estuarine	-45	-75	Clayey (CH)	Stiff to Very Stiff
Pleistocene	-75		Clays-Generally CH with some sand	Stiff

3.1 Mode of failure

The IPET analyses were performed for undrained conditions in the levee fill, the marsh layer, and the clay beneath the marsh layer, to evaluate the stability. Assuming undrained conditions is reasonable owing to the short times involved as the event developed. The dissipation of excess pore pressures during the rise of the water level in the canal would have been negligible because of the low permeability of the materials, thus having a minor influence on stability (IPET 2007).

3.1.1 Effective stresses

In both, the IPET analyses and the original design, effective stresses were calculated based on simple vertical effective overburden pressure using this equation:

$$\sigma_v' = \gamma \cdot z - u \text{ , where}$$

σ_v' =vertical effective stress

γ =effective unit weight of soil layer

z =depth to the point to be analyzed

u = pore pressure at location of stress calculation

The IPET analyses were performed on cross sections at Stations 8+30, 10+00, and 11+50, as reported in the initial GDM. The geometry of these cross sections will be discussed in a further section.

3.1.2 Undrained shear strength

The undrained shear strength values used to create the IPET analyses came from different sources: Unconfined Compression (UC) tests, Unconsolidated Undrained (UU-1) tests performed using one confining pressure only, conventional UU tests, and cone penetration tests with pore pressure measurements (CPTUs) (IPET 2007). Due to the rapid nature of the loading, and the low permeability of the levee, marsh, and clay soils, undrained strengths were deemed important in the IPET analyses.

3.1.3 Undrained Shear Strength of the Fill Material

The fill was assumed to be saturated, thus, a S_u = c and ϕ_u = 0 strength interpretation was used (IPET 2007).

The range of the shear strength values obtained from the laboratory tests was from 120 psf to more than 5,000 psf, so choosing an average value was discarded due to high levels of scatter in the data. An undrained shear strength value of S_u = 900 psf was selected as a representative value based on the data from UU tests. It should be noted that the shear strength of the fill material has very little impact on the factor of safety.

3.1.4 Undrained Shear Strength of the Marsh Layer

As mentioned before, the marsh layer was assumed to be an undrained condition for the IPET analyses and, from soil exploration, was found to be stronger beneath the levee crest than at the toe and beyond the toe of the levee. The layer is then behaving in accordance with the conditions to which it was exposed, because at the toe and beyond the toe of the levee, the layer was compressed under a lower stress than beneath the levee crest, where the marsh layer is additionally loaded by the weight of the levee.

The range of the shear strength values obtained was from 50 psf to about 920 psf. An undrained shear strength value of S_u = 300 psf was selected as a representative value beneath the levee toe and beyond, and S_u = 400 psf beneath the levee crest (IPET 2007).

3.1.5 Undrained Shear Strength of the Clay Layer

For this layer the best representative values were those obtained from the CPTU tests. To obtain the undrained shear strength from these tests, Mayne's method (Mayne 2003) was used. This method was found to give more reasonable values of undrained shear strength than if constant values of the cone factors were used (IPET 2007). When plotting the variations of the undrained shear strength with depth, a value of 11 psf per foot of depth was found to be representative of the data. Based on a saturated unit weight of 109 pcf, an undrained strength ratio of 0.24 was obtained and used to calculate the undrained shear strength values.

3.1.6 Undrained Shear Strength of the Sand Layer

As previously mentioned, there is a layer of sand beneath the clay, but it does not affect the stability analyses. A value of the friction angle (ϕ') was estimated from correlations with the data from the Cone Penetration Tests to be 35 degrees, and this value was used in all analyses.

3.1.7 Comparison between IPET Strength Model and Original Design

If we compare the undrained shear strengths selected for the IPET analyses with those selected in the original design we will see that, for the fill and marsh layers, the undrained shear strengths used for IPET analyses differ greatly from the ones used in the original design. A value of S_u = 900 psf was selected as a representative value for the fill layer, but a S_u value of 500 psf was used in the original design (IPET 2007). It should be noted that the shear strength of the levee fill has little impact on the stability analyses. For the marsh layer, values of S_u = 400 psf beneath the levee crest and S_u = 300 psf beneath the levee toe were used for the IPET analyses, but a S_u = 280 psf was selected as representative value at all locations on the original design (IPET 2007). The original design used a maximum strength of S_u = 380 psf for the clay layer at all locations. For the clay layer beneath the levee crest, the original design strengths are very close to the IPET Strength Model, but at the toe of the levee the strengths used in the original design are considerably higher than the strengths from the IPET analyses (IPET 2007). Figure 20 shows a comparison between the strengths used in the original design and the ones used in the IPET analyses at the three cross sections that were evaluated.

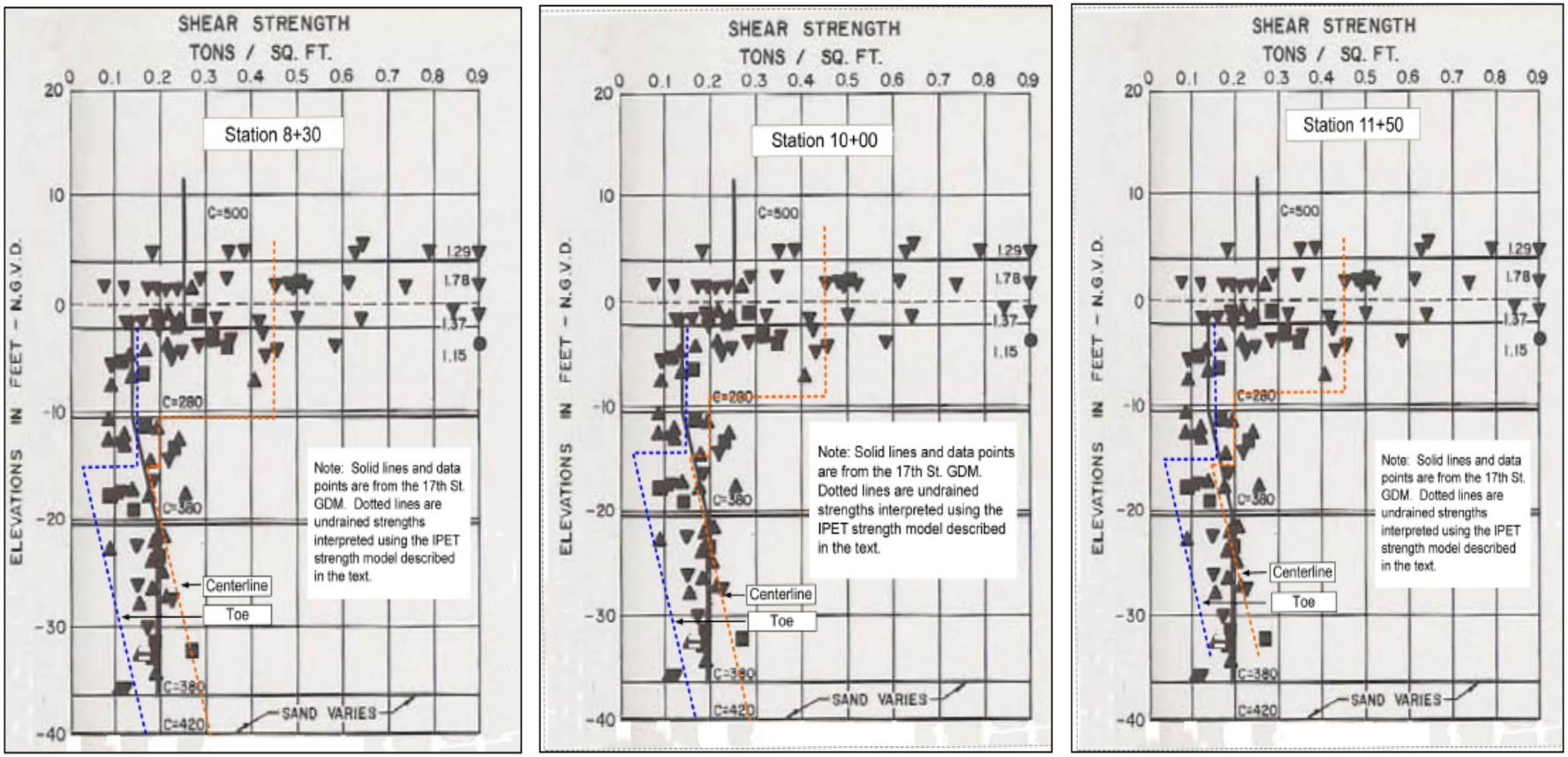

Figure 20: Comparison of undrained shear strengths from original design with IPET analyses (IPET 2007)

In Figure 20, the black solid lines represent the undrained shear strength interpretation for the original design; meanwhile the red and blue dotted lines represent the undrained shear strength interpretation for the IPET analyses at the crest and toe, respectively. The undrained shear strength relationships are similar in all three cross sections. Beneath the crest, the undrained shear strength values for the clay layer are nearly the same, while at the toe, the IPET analyses used significantly lower values of undrained shear strength compared to the original design.

3.2 Factors of safety

The hurricane protection structures of the 17th Street Outfall Canal consisted of reinforced concrete I-wall floodwalls encasing the top of sheet piles (IPET 2007). Three transverse cross sections through the levee breach were analyzed. The three sections were developed at Station 8+30, Station 10+00, and Station 11+50. Figure 21 shows the geometry of the cross sections analyzed by IPET.

The original levee stability analyses were performed using the New Orleans District Method of Planes (IPET 2007). The Method of Planes consists of resolving the forces into horizontal components and computing the factor of safety as:

$$FS = \frac{\Sigma F_R}{\Sigma F_D}$$

where:

FS = factor of safety

ΣF_R = sum of resisting forces

ΣF_D = sum of driving forces

This method is based on equilibrium of a soil mass above a slip surface that consists of an active wedge, a neutral block, and a passive wedge. Stability of the levees was analyzed for a minimum factor of safety (FS) of 1.30 for the highest water level in the canal (IPET 2007). The analyses considered potential failure surfaces for drained shear to the floodside and undrained shear to the protected side of the levee. Analyses to the protected side considered the canal water level as the *still water level*.

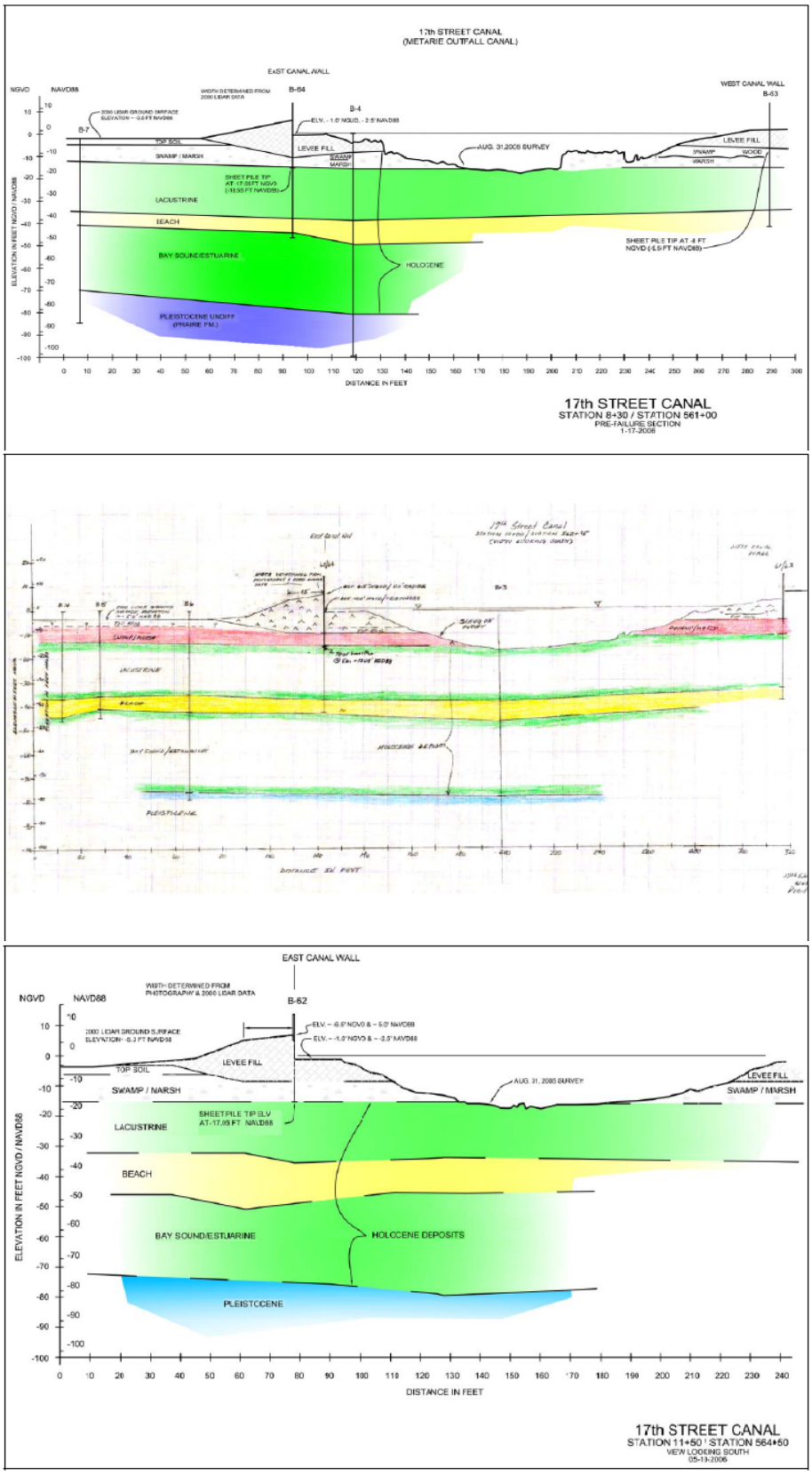

Figure 21: Geometry of cross sections 8+30, 10+00, and 11+50 analyzed by IPET

As part of the research, stability analyses were performed using the same procedures as adopted in the IPET report. The calculation of the undrained shear strength values was made using a spreadsheet and was verified with hand calculations. The following figure shows the undrained shear strength data obtained from these analyses at crest.

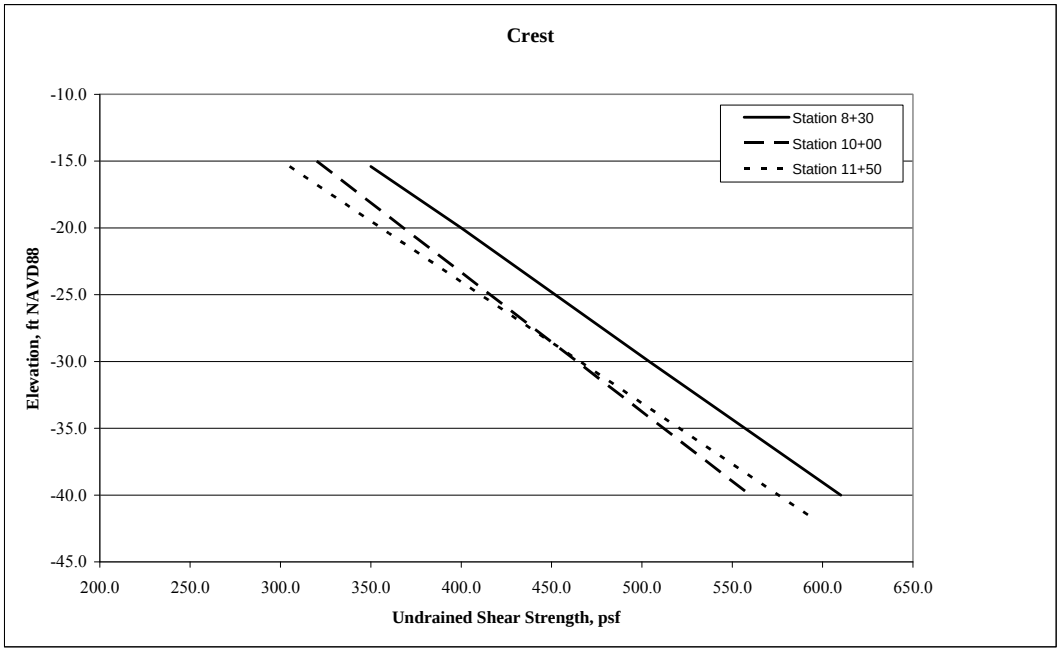

Figure 22: Undrained shear strength values from IPET Analyses at crest

On Figure 22, Station 8+30 is represented by a solid line, while Station 10+00 and Station 11+50 are represented by a dashed line and a dotted line, respectively. At crest, the undrained shear strength of clay layer ranged approximately from 300 psf to 600 psf. Meanwhile, at the toe the values ranged approximately from 40 psf to 350 psf. Figure 23 shows the undrained shear strength data relationships used in the IPET analyses at the toe of Stations 8+30, 10+00, and 11+50 using the same representation as discussed previously.

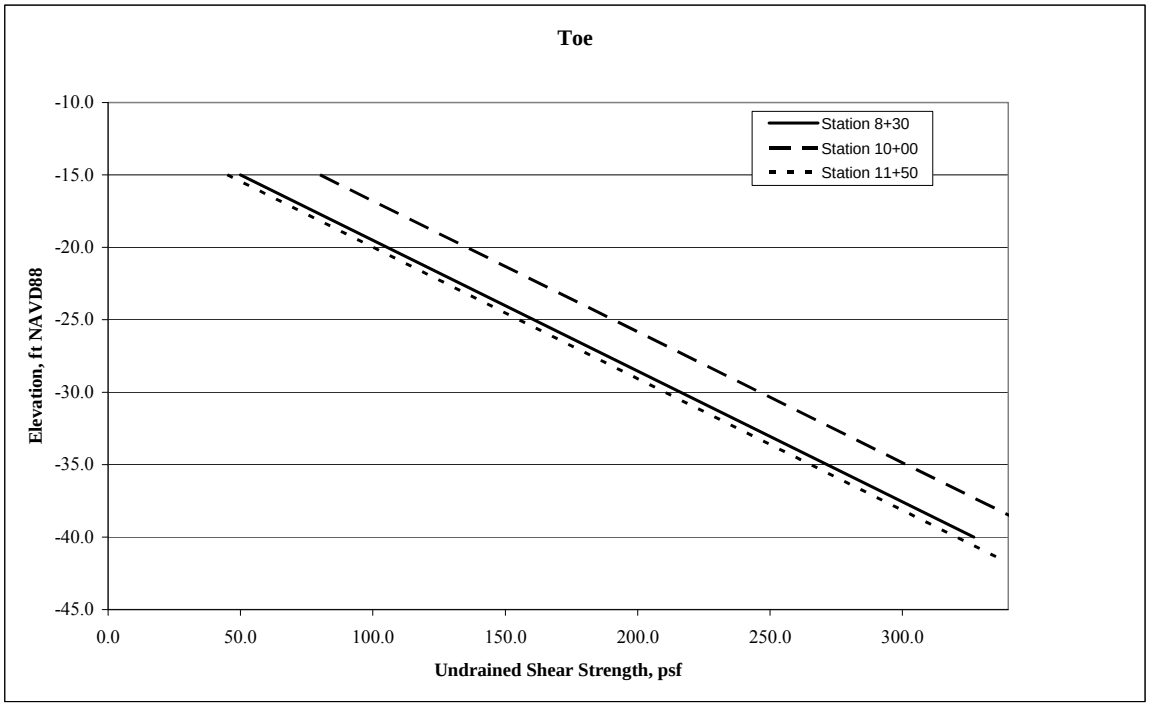

Figure 23: Undrained shear strength values from IPET Analyses at toe

The shear strengths beyond the toe toward the protected side were essentially equal to those at the toe. The following figure shows the undrained shear strength values for the IPET analyses beyond the toe for Stations 8+30, 10+00, and 11+50.

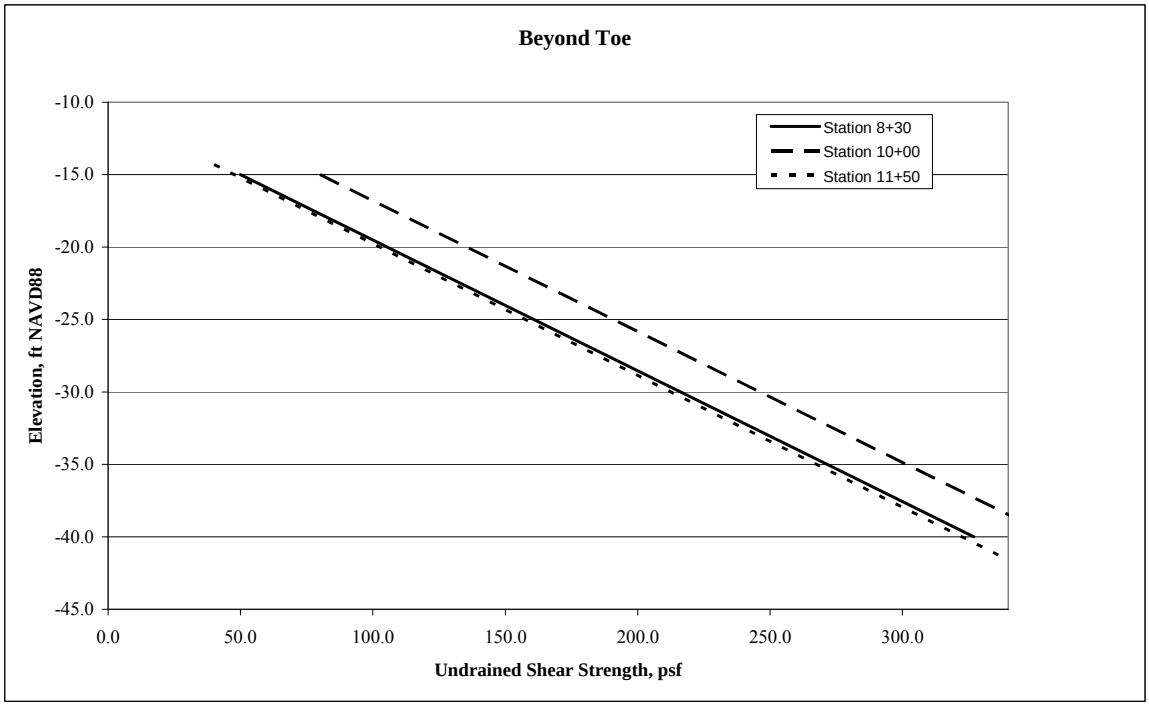

Figure 24: Undrained shear strength values from IPET Analyses beyond toe

Limit equilibrium analyses were performed to analyze the stability of the levee and I-wall. The stability analyses were made using Spencer's method (Spencer 1967), with the computer program *Slide* (Rocscience 2006). This profile used was the northern section of the 17th Street Outfall Canal where the breach occurred, at Station 11+50. These stability analyses evaluated seven different cases, taking into account the effects of different canal water levels. The previously calculated undrained shear strengths values were used in the *Slide* file and the factors of safety were obtained at canal water elevations of 6 ft, 7 ft, 8 ft, 9 ft, 10 ft, and 12.5 ft NAVD88. The canal water elevation that produces a factor of safety of 1.0 was also obtained. The following figure shows the factor of safety, calculated by *Slide*, using Spencer's for a canal water level (CWL) of 6 ft

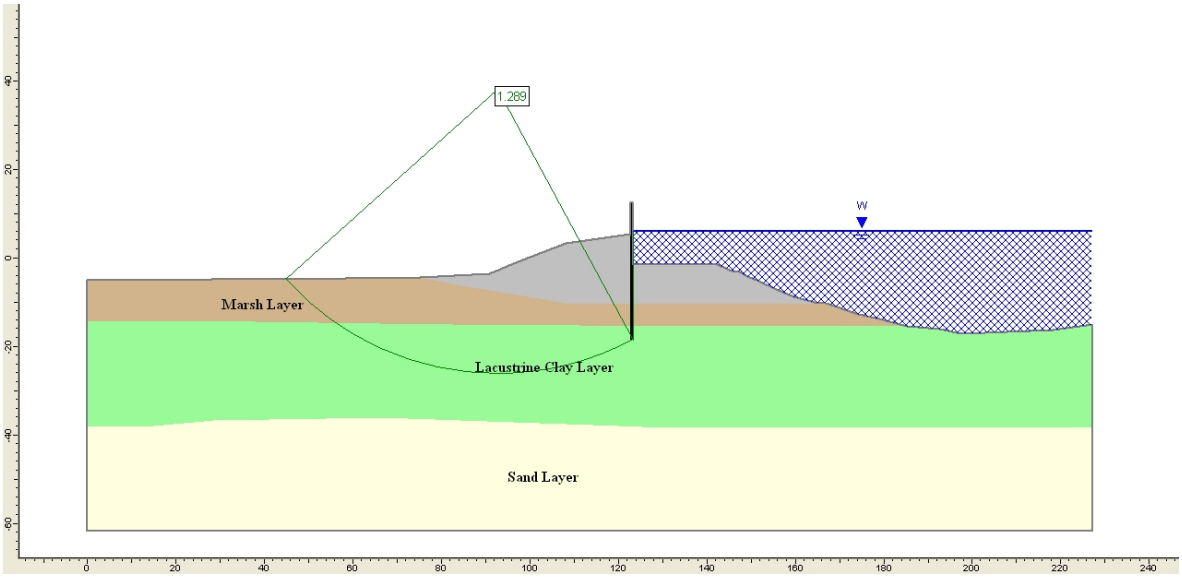

Figure 25: Factor of safety calculated by *Slide* for CWL = 6 ft in Station 11+50

The *Slide* figures showing the critical circles at different canal water levels are given in Appendix C.

The following table shows the values of factors of safety obtained from the stability analyses using the IPET strength model. A comparison of these results with the original analyses will be discussed in a later section.

Table 2: Factors of safety obtained from stability analyses on IPET Strength Model in Station 11+50

Case	Canal Water Elevation (ft) NAVD88	FS
1	6.0	1.289
2	7.0	1.207
3	8.0	1.125
4	9.0	1.049
5	9.67	1.000
6	10.0	0.977
7	12.5	0.821

From the stability analyses made by the IPET team, the following conclusions were drawn:

- The calculated factors of safety decreased as the elevation of the water level on the canal side of the wall increased.
- Smaller factors of safety were calculated when it was assumed that a gap existed between the wall and the soil on the canal side of the wall, with hydrostatic water pressures acting within this gap, increasing the load on the wall. The calculated factors of safety are about 25% lower when it is assumed that a separation or gap develops.
- Use of noncircular slip surfaces reduced the calculated factors of safety by about 5% as compared with those calculated when using circular slip surfaces. (IPET 2007)

IPET concluded that it seems likely that a gap formed between the wall and the soil on the canal side of the wall. This gap should have affected greatly the stability of the wall, because when it filled with water, it should have increased the hydrostatic pressure along the wall, causing a deflection of the wall and moving it away from the levee. This was confirmed by field observations and is consistent with the results of stability analyses. The canal water elevation calculated for a factor of safety equal to 1.0 for stability analyses that include a gap behind the wall was 9.7 ft and this is the approximate level when the breach in the levee fully opened. Also, the factors of safety obtained for areas adjacent to the breach were higher than those calculated at the breach area.

3.2.1 Comparison Between New Orleans Method of Planes and Spencer's Method

To compare Spencer's method and the Method of Planes, the IPET team performed analyses on the original cross section used in the original design, but this time taking into

account the effect of different canal water levels and gaps next to the sheetpile wall. The following table shows the factors of safety obtained for these cases.

Table 3: Factors of safety obtained from analyses on original data using IPET approach

Case	Section	Gap	Canal Water Elevation (ft) NAVD88	FS
16	GDM 20	No	7.0	1.77
17	GDM 20	Yes	7.0	1.60
18	GDM 20	No	10.0	1.45
19	GDM 20	Yes	10.0	1.24
20	GDM 20	Yes	11.5	1.00

The factor of safety obtained in the original design using the Method of Planes for a canal water level of 10ft NAVD88 was 1.30, without considering the effect of a gap between the I-wall and the levee embankment. From Table 3, using Spencer's Method for the same conditions, the factor of safety obtained is 1.45. The Method of Planes is a conservative method and gives lower factors of safety than more accurate methods, such as Spencer's Method (IPET 2007). Spencer's Method solves for force and momemt equilibrium, and determines the inclination of the slide forces by iteration. The Method of Planes assumes the inclination of the resultants of the side forces and solves only for horizontal force equilibrium, thus Spencer's Method is more precise than the Method of Planes.

3.2.2 Comparison Between Original Design and IPET Analyses

The factor of safety obtained for the IPET Analyses for a canal water elevation of 10 ft NAVD88 and considering the effect of a gap between the I-wall and levee embankment was 0.977. Meanwhile for the original design under the same conditions, the factor of safety calculated was 1.24. The same pattern can be seen for the canal water level that corresponds to a factor of safety of 1.000. For the IPET Analyses, a canal water level of 9.67 ft was obtained, versus a canal water level of 11.5 ft for the original design. The canal water level from the stability analyses on the original design geometry does not agree with the eyewitness and field observations information.

In the original analyses, the wall was assumed to be in contact with the levee fill soil on the canal side, so the effect of a gap was not taken into account, while for the IPET analyses, the cases were analyzed with gaps. Another difference between the analyses is that for the original design the same strength for the clay was used beneath the levee slopes and for the levee toe. The IPET analyses used lower strengths beneath the levee slopes and beyond the

toe (IPET 2007). The presence of the gap and the difference in the shear strength interpretations were the greatest differences between the two analyses.

4. Assumptions in IPET Analysis

This section evaluates the assumptions made during the IPET analyses in order to select the best approach to enhance these analyses.

4.1 Static water table elevation

For the IPET analyses, as mentioned previously, the factors of safety were calculated at different canal water levels. From the analyses, some of the conclusions were that the higher the water levels in the canal, the lower the calculated factor of safety. In addition, the canal water level was varied to determine the static water level at which the calculated factor of safety would be equal to 1.0 and it was concluded that the best estimate of the water level at the time of failure, from field observations and eyewitness reports, was in good agreement with the water level for F = 1.00 determined using noncircular slip surfaces. In addition, the location of the phreatic surface used for the determination of pore pressures and effective consolidation stresses is important.

The approach used by the IPET team assumes a position of the phreatic surface for the calculation of effective stresses. The phreatic surface assumed to be at a canal water elevation of 0 ft, and extend horizontally toward the protected side. When the ground surface was lower than elevation 0 ft, the phreatic surface was assumed to be coincident with the ground surface. Assuming the phreatic surface may lead to unprecise approximations of pore water pressures. The use of a finite element program to determine the phreatic surface offers an alternative method to calculate the pore pressures. This can be done by setting constant head boundary conditions at the protected side boundary combined with a static canal water elevation. Establishing these conditions, will allow the finite element program to calculate the location of the phreatic surface and the resulting pore pressures.

Pore water pressures can be calculated knowing the position of the phreatic surface as the product of the pressure head and the unit weight of water. This method assumes vertical

equipotential contours. With the finite element method, the pore pressures are determined based on calculated equipotential contours influenced by the geometry of the problem.

4.2 Initial effective consolidation stress

The IPET analyses did not considered details of the stress distribution beneath the levee, which would result in "load spread" effects. These effects would have resulted in rotation of principal stresses beneath the levee, a lower total stress beneath the levee crest, and a higher total stress beneath the levee toe (IPET 2007). The reason to disregard the "load spread effects" was that it would have complicated the model. However, calculating the vertical stress without taking into consideration the "load spread effects" will lead to a mis-calculation of the stresses, due to the assumption that the levee is an infinite fill that stress does not dissipate with depth. Using the IPET approach, the stresses at the toe were underestimated, while beneath the crest, the stresses were overestimated. In this thesis, the finite element method was used to determine the vertical stresses. This allows a better accommodation of the geometry of the problem. The use of finite element analysis should give more accurate stresses than the IPET approach.

4.3 OCR conditions

All of the IPET analyses were made assuming that the clay was normally consolidated. Consolidation tests conducted both before and after Hurricane Katrina have shown that the soil is normally consolidated beneath the crest, but possibly overconsolidated at the toe and beyond the toe. Overconsolidation can be logically be produced by a couple of mechanisms. For example, if the water table drops a few feet and then increases to the original elevation, this would result in an increase in OCR, as shown in Figure 26.

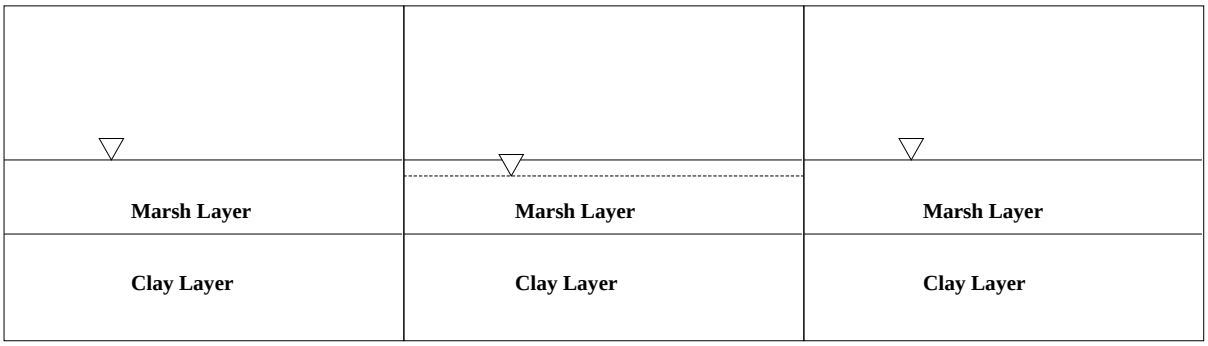

Figure 26: Overconsolidation due to change in water table elevation

An additional mechanism would be if new soil is deposited on top of the ground surface, and then the marsh or clay layer compresses until the top of the new soil is at the same elevation of the water table. Figure 27 shows a diagram with this mechanism of overconsolidation.

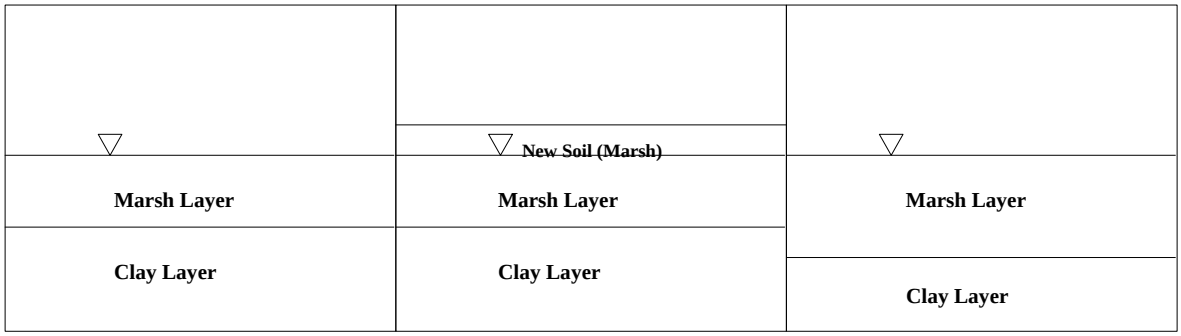

Figure 27: Overconsolidation due to new soil deposit on top of ground surface

In both of these mechanisms, the increase in stress is result of the difference between the buoyant and total unit weight of the soil. Assuming that the soil was normally consolidated would result in lower values of undrained shear strength than for the overconsolidated case due to the difference in the undrained strength ratio. The influence of overconsolidation was incorporated into the analysis by using the following equation developed by Jamiolkowski, et. al. (1985):

$$\frac{S_u}{\sigma_v'} = 0.24 OCR^{0.8}, \text{ where}$$

S_u =undrained shear strength

σ_v' =vertical effective stress

OCR =overconsolidation ratio

4.4 Undrained strength determination

The undrained shear strength values can be affected by the following factors:

- Location of phreatic surface
- Assumption of infinite versus finite levee embankment fill.
- Assumption of normally consolidated versus overconsolidated conditions.

All of these factors affect the calculated undrained shear strength in the lacustrine clay layer, thus impacting the calculated factor of safety.

5. Enhancements to the IPET Analyses

Analyses similar to those performed by IPET were completed to examine the effect of the various analysis assumptions. Different methods were developed to take into account the stress dissipation with depth and the geometrical characteristics of the levee in order to investigate the impact of the assumptions made in the original IPET Analyses. In addition, the analyses were made assuming that the lacustrine clay layer was normally consolidated at the crest and overconsolidated at the toe and beyond. The following table lists the analysis cases, including the original IPET Analysis, discussed in previous chapters:

Table 4: Methods used to enhance IPET Analysis

Name	Phreatic Surface Elevation (ft) NAVD88	Pore Pressure	Total Stress	OCR
IPET Analysis	Assumed at 0 ft or ground surface	Calculated from $\gamma_w \cdot z$	Calculated from $\gamma \cdot z$	1.0
IPET Analysis With Assumed OCR	Assumed at 0 ft or ground surface	Calculated from $\gamma_w \cdot z$	Calculated from $\gamma \cdot z$	1.0 under crest 1.2 under toe and beyond
IPET Analysis With Calculated OCR	Assumed at 0 ft or ground surface	Calculated from $\gamma_w \cdot z$	Calculated from $\gamma \cdot z$	Calculated based on settlement
Elastic Stress Distribution (ESD) With Static Water Table (SWT)	Assumed at 0 ft or ground surface	Calculated from $\gamma_w \cdot z$	Elastic Theory	1.0
ESD With SWT	Assumed at 0 ft or ground surface	Calculated from $\gamma_w \cdot z$	Elastic Theory	1.0 under crest 1.2 under toe and beyond
ESD With SWT	Assumed at 0 ft or ground surface	Calculated from $\gamma_w \cdot z$	Elastic Theory	Calculated based on settlement
ESD With Calculated Pore Pressures From Seepage Analysis	BC = El -5 ft	FE seepage analysis	Elastic Theory	1.0
ESD With Calculated Pore Pressures From Seepage Analysis	BC = El -5 ft	FE seepage analysis	Elastic Theory	1.0 under crest 1.2 under toe and beyond
ESD With Calculated Pore Pressures From Seepage Analysis	BC = El -5 ft	FE seepage analysis	Elastic Theory	Calculated based on settlement
ESD With Calculated Pore Pressures From Seepage Analysis	BC = El -7ft	FE seepage analysis	Elastic Theory	1.0
ESD With Calculated Pore Pressures From Seepage Analysis	BC = El -7 ft	FE seepage analysis	Elastic Theory	1.0 under crest 1.2 under toe and beyond
ESD With Calculated Pore Pressures From Seepage Analysis	BC = El -7 ft	FE seepage analysis	Elastic Theory	Calculated based on settlement

The canal water level was assumed at el. 0 ft, and extended horizontally at 0 ft to the protected side. When the ground surface was located below el. 0 ft, the phreatic surface was assumed to be at the ground surface, as shown in Figure 28.

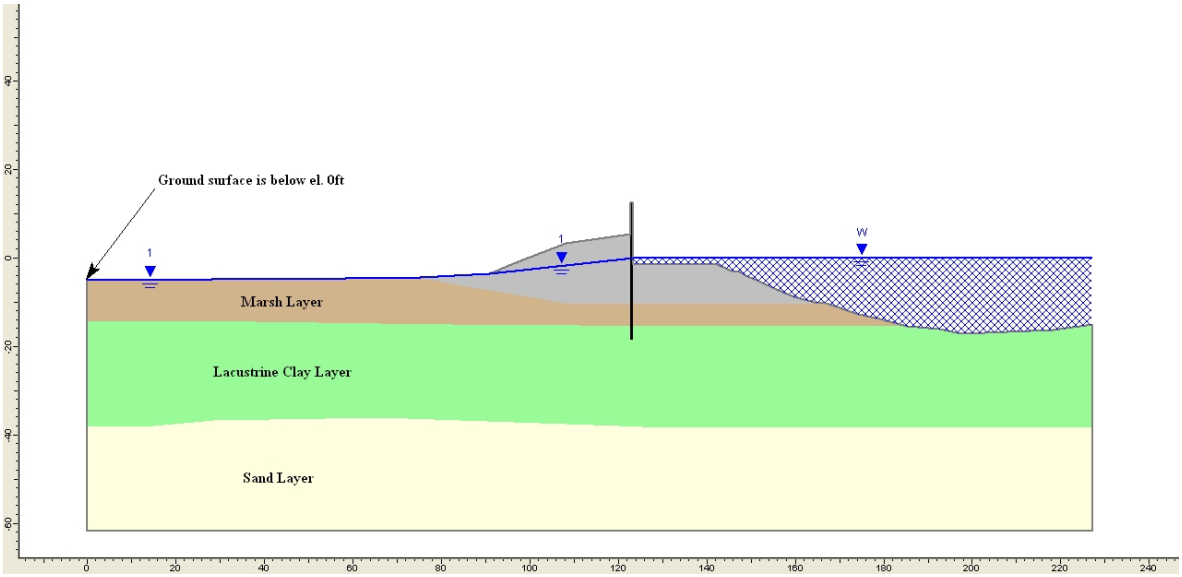

Figure 28: Diagram showing location of phreatic surface when ground surface is below el. 0ft

5.1 Finite Element Analysis of in situ stress conditions

Finite element (FE) analysis was used to determine the in situ vertical total stress conditions using a simple linear elastic model. This method allows the geometry of the levee to be accommodated, and should remove uncertainties included in the IPET method. In order to calculate the vertical effective stress, the pore pressures were calculated using three different methods. In the first method, a static water table location was assumed, and pore pressures were calculated from the equation:

$$u = \gamma_w z \text{, where}$$

$u =$ pore pressure

$\gamma_w =$ unit weight of water

$z =$ vertical depth below piezometric line

In the other two cases, the pore pressures were calculated from seepage analysis by establishing protected side constant head boundary conditions at elevation -5 ft (ground surface) and elevation -7 ft, and a flood side water elevation of 0 ft. The vertical effective stresses and factor of safety in all three cases were determined for normally consolidated and overconsolidated conditions within the lacustrine clay, as mentioned above.

FE analyses were performed on a cross section at Station 11+50. The cross section is

composed of a levee fill layer followed by a marsh layer. Beneath the marsh layer, there is a lacustrine clay layer followed by a sand layer and a bay sound clay layer. Figure 29 shows the cross section used in the FE analyses. Table 5 shows the material properties of the analyzed cross section.

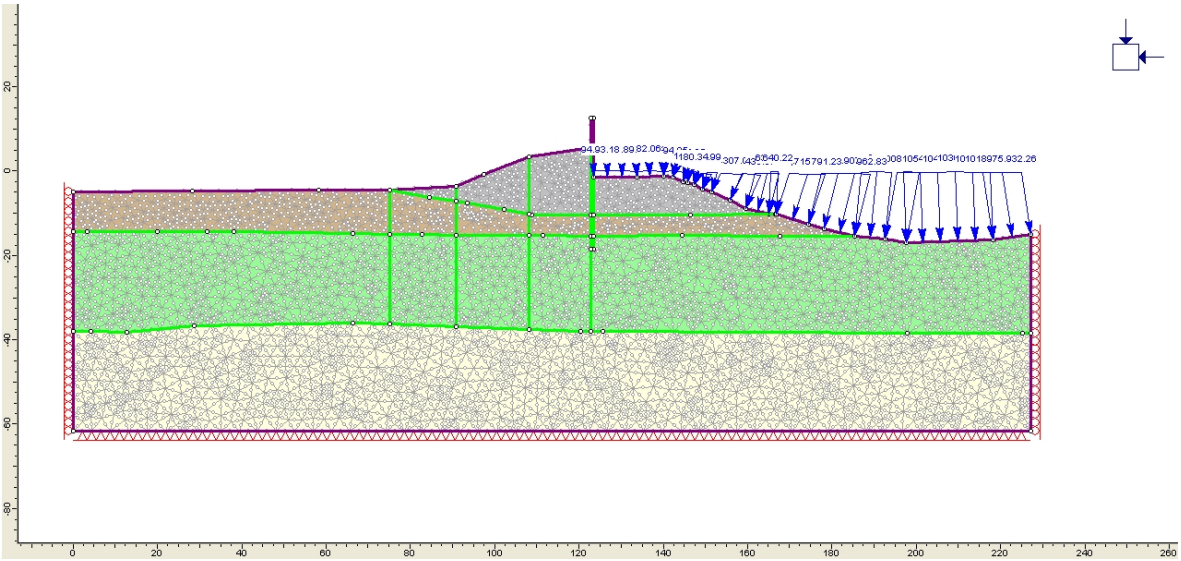

Figure 29: 17th Street Outfall Canal cross section used in FE analyses

Table 5: Material properties for 17th Street Outfall Canal FE Analysis

Material	Permeability (ft/s)	Poisson's Ratio	Unit Weight (pcf)	Cohesion (psf)	Friction Angle
Levee Fill	1×10^{-7}	0.49	109	900	0
Marsh	1×10^{-6}	0.49	80	219.3	35
Lacustrine Clay	1×10^{-7}	0.49	109	219.3	35
Sand	1×10^{-3}	0.40	120	0	35
Bay Sound Clay	1×10^{-7}	0.49	120	500	0
Sheetpile	1×10^{-99}	0.4	120	219.3	35

Six-noded triangles with approximately 1500 mesh elements were used in the analyses. The mesh element density was increased beneath the levee fill to improve the precision of the total stresses and pore pressures, thus the undrained shear strength values obtained.

The groundwater boundary conditions were set differently depending on the case to be analyzed, as it will be discussed further on each case.

5.1.1 Static Water Table

This case consists of using finite element analysis with total unit weights and a static water table (SWT) combined with elastic theory. Vertical effective stresses were calculated using *Phase2* software, provided by Rocscience. The vertical effective stresses obtained were used to calculate the undrained shear strength of the clay layer for normally consolidated conditions, using the following equation:

$$S_u = 0.24\sigma_v', \text{ where}$$

S_u = undrained shear strength

σ_v' = vertical effective stress

The calculated undrained shear strength values were then imported in a *Slide* file, to obtain the factor of safety against slope stability for different canal water levels. The factor of safety for slope stability was obtained for canal water elevations of 6 ft, 7 ft, 8 ft, 9 ft, 10 ft, and 12.5 ft. The canal water level that produces a factor of safety of 1.0 was also obtained. The difference between these cases and IPET analyses is that the Elastic Stress Distribution with SWT case calculated the vertical total stresses from FE method and IPET Analyses calculated them from vertical equilibrium. Discussion of results from stability analyses and a comparison of these two cases will be made further in Chapter 6.

The *Slide* cross sections showing the critical circles for the different canal water elevations are shown on Appendix C.

5.1.2 Seepage Analysis

In this section, two cases were analyzed using pore pressures calculated from seepage analyses. The first case was a canal side constant head boundary condition at el. 0 ft, and a protected side constant head boundary condition at el. -5 ft. The second case differed in that the protected side boundary conditions were set at el. -7 ft. Vertical effective stresses were obtained for these conditions, using *Phase2* software, and were used to calculate the undrained shear strength of the clay layer for normally consolidated conditions. The calculated undrained shear strength values were imported into *Slide* and factors of safety for slope stability were obtained for canal water levels of 6 ft, 7 ft, 8 ft, 9 ft, 10 ft, and 12.5 ft. The canal water level that produces a factor of safety of 1.0 was also obtained.

5.1.2.1 Boundary conditions at -5 ft

In this case, the hydraulic boundary conditions in the *Phase2* file were set at el. –5 ft NAVD88 on the protected side of the cross section. This is approximately equal to the ground surface elevation at the limit of the protected side domain. This case would differ from the original IPET analysis in that the total stresses were calculated by linear elastic theory and the pore pressures were calculated using a finite element seepage analysis. In this case, the phreatic surface is obtained by the program instead of being assumed. Discussion of the results from the stability analyses and a comparison of this case with IPET analysis will be made further in Chapter 6.

The *Slide* cross sections showing the critical failure circle for different canal water levels for this case are given in Appendix C.

5.1.2.2 Boundary conditions at -7 ft

For this case, the hydraulic boundary conditions in the *Phase2* file were set at el. –7 ft NAVD88 on the protected side of the cross section. This equates to a water table being about two feet below the ground surface at the far protected side boundary. The same procedures as for the previous case were used and the factors of safety (FS) for slope stability were obtained at different CWLs. The differences between this case and IPET analysis are the same as stated for the previous case. At a same canal water elevation, the factors of safety obtained from IPET analyses are marginally lower than those obtained for this analysis. A discussion of the results from the stability analyses and a comparison of this case with the IPET analyses will be made further in Chapter 6.

The *Slide* cross sections showing the critical failure circle for different canal water levels for this case are given in Appendix C.

5.2 Overconsolidation of clay layer

As mentioned before, the IPET analyses assumed that the lacustrine clay layer was normally consolidated. Laboratory test data suggest that the clay may have a small degree of overconsolidation from the toe to the protected side boundary. Figure 30 shows OCR values obtained from laboratory consolidation tests, using Casagrande's Method (Casagrande 1936) and Becker's Method (Becker et. al. 1987), at the toe of the

embankment. The laboratory consolidation tests were made on samples from Stations 560+50 and 564+50.

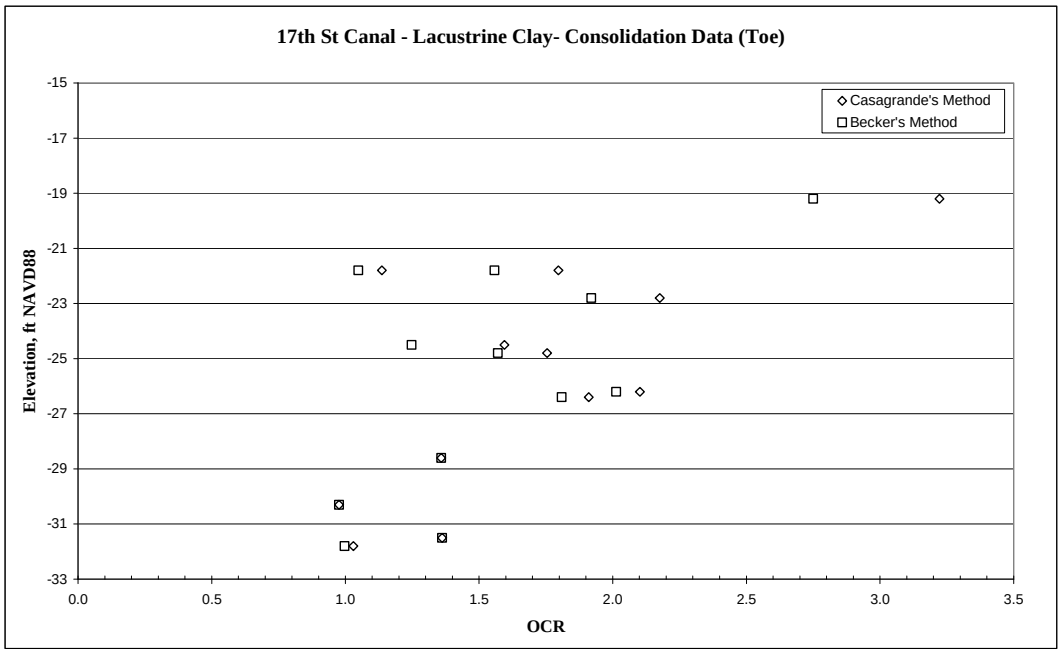

Figure 30: OCR values from laboratory consolidation tests at toe

At the toe and beyond, OCR values ranged from 1.0 to 3.2, with the highest concentration of values between 1.5 and 2.0, showing a lot of scatter in the data. Meanwhile, at crest OCR values ranged from 0.6 to 1.34, with the average about at 1.0. Figure 31 shows the OCR values obtained from laboratory consolidation tests at crest.

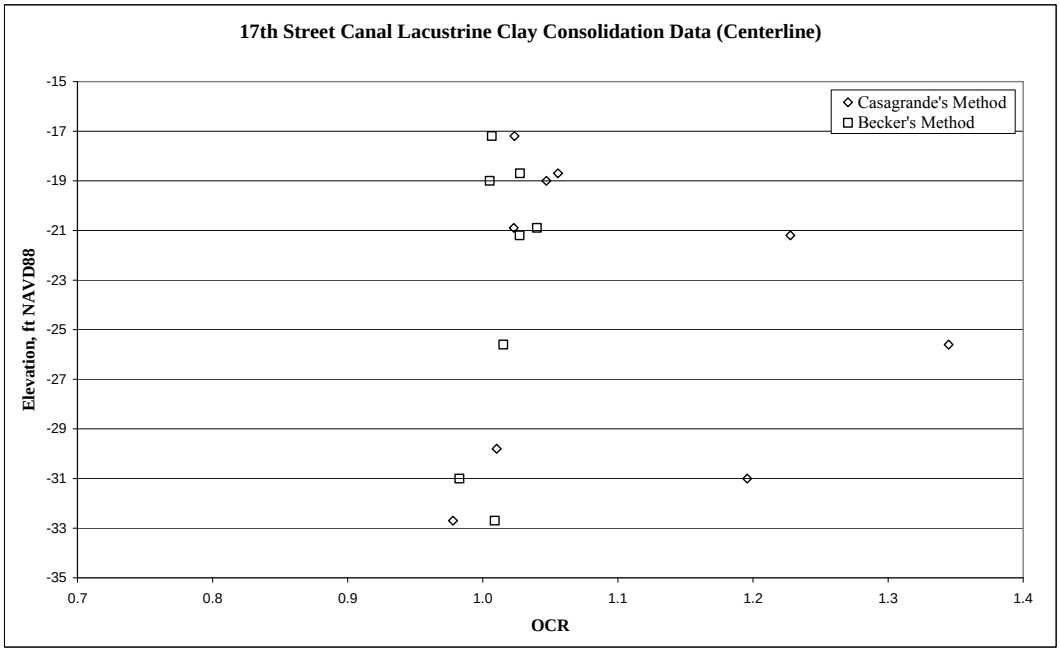

Figure 31: OCR values from laboratory consolidation tests at crest

Analyses were performed on the same cross section for overconsolidation conditions, as described subsequently.

5.2.1 Mechanisms of Overconsolidation

Different situations can lead to some overconsolidation of the lacustrine clay layer. One mechanism is that the water table elevation decreases and then increases. Another situation could be that new soil is deposited on top of the ground surface, compressing one or both of the underlying layers until the top of the new soil layer is at the same elevation as the water table. After examining ways to implement the effect of overconsolidation to the analyses, two approaches were used. The first approach was to assume an OCR value of 1.0 under the crest and 1.2 under the toe of the levee, with a linear variation in between. The second approach was to calculate the OCR value based on the assumption of adding a new layer of soil to the profile. Both approaches will be discussed in more detail below.

5.2.1.1 Analyses with assumed OCR values

Based on the results of consolidation analyses, OCR values of 1.2 were assumed at the toe and beyond. Under the crest of the levee, an OCR value of 1 was assumed. The OCR value was assumed to linearly vary between the toe and the crest. The value of OCR was assumed to be constant with depth. The undrained shear strength (S_u) was calculated, based on the OCR value using the following equation (Jamiolkowski, et.al. 1985):

$$S_u = 0.24\sigma'_v OCR^{0.8},$$

as previously discussed. Using the undrained shear strengths values obtained from this approach, stability analyses were conducted to obtain the factor of safety for slope stability for the various method descrived earlier used to calculate the total stress and the pore pressures. The critical circles for the different analysis cases are shown in Appendix C. Table 6 shows the values of factor of safety (FS) obtained for this approach at CWLs of 6 ft, 7 ft, 8 ft, 9 ft, 10 ft, and 12.5 ft, as well as the CWL that corresponds to a factor of safety of 1, for all cases. A discussion of the results from the stability analyses will be given in Chapter 6.

Table 6: FS for different CWL for IPET analysis and ESD cases for assumed OCR values of 1 to 1.2

IPET Analysis		Total Stress calculated with Elastic Theory. Pore pressure calculated assuming static water table		Total Stress calculated with Elastic Theory. Pore pressure calculated using FE Method BC el. -5ft		Total Stress calculated with Elastic Theory. Pore pressure calculated using FE Method BC el. -7ft	
CWL	Factor of Safety	CWL	Factor of Safety	CWL	Factor of Safety	CWL	Factor of Safety
6ft	1.324	6ft	1.246	6ft	1.404	6ft	1.544
7ft	1.236	7ft	1.156	7ft	1.309	7ft	1.438
8ft	1.149	8ft	1.073	8ft	1.216	8ft	1.335
9ft	1.068	8.94ft	1.000	9ft	1.129	9ft	1.239
9.92ft	1.000	9ft	0.996	10ft	1.050	10ft	1.147
10ft	0.994	10ft	0.922	10.65ft	1.000	11.88ft	1.000
12.5ft	0.831	12.5ft	0.767	12.5ft	0.877	12.5ft	0.958

5.2.1.2 Analyses with calculated OCR values

An estimation of an OCR profile was possible with the assumption of adding a new layer of soil to the profile. Initial conditions consisted of a marsh layer of 9.3 ft thick, followed by a lacustrine clay layer of 23.8 ft thick, for which the initial vertical effective stress (σ_{v_o}') was calculated. Figure 32 shows the initial soil profile.

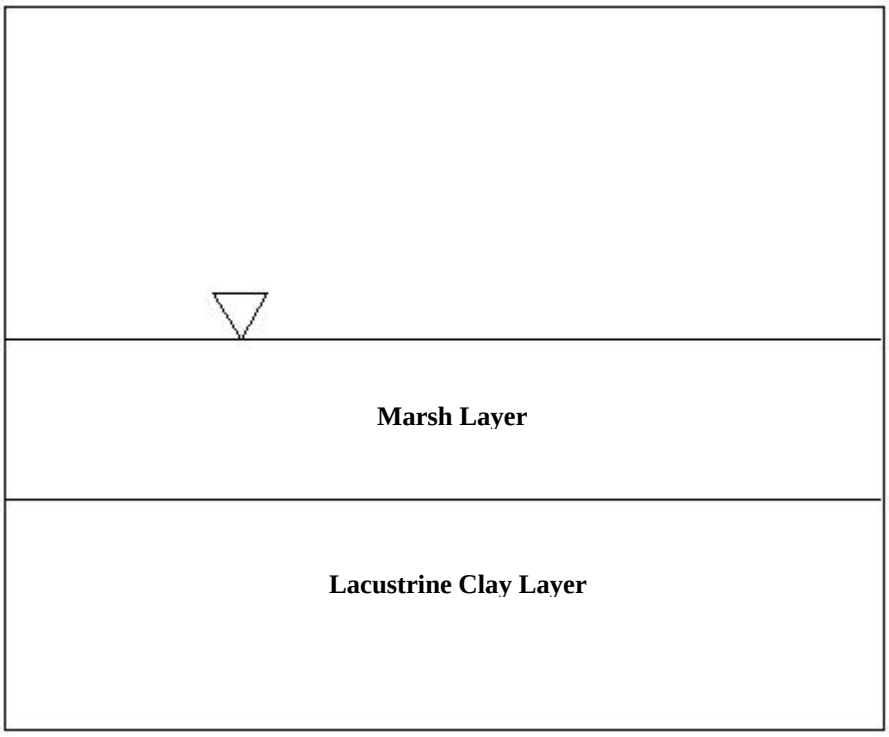

Figure 32: Initial soil profile

The vertical effective stress (σ_v') was then calculated after adding one foot of marsh to the profile, as shown on Figure 33.

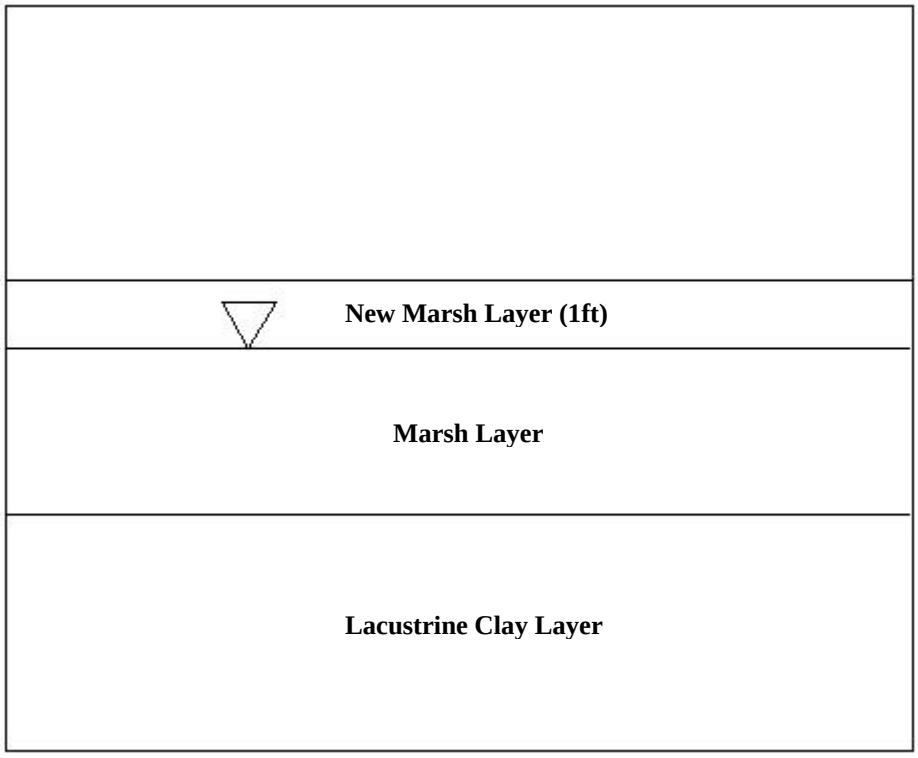

Figure 33: Addition of one foot of marsh to original soil profile

After a very long time, the lacustrine clay layer compressed until the top of the marsh layer was at the same elevation of the water table. Figure 34 shows the soil profile for this condition.

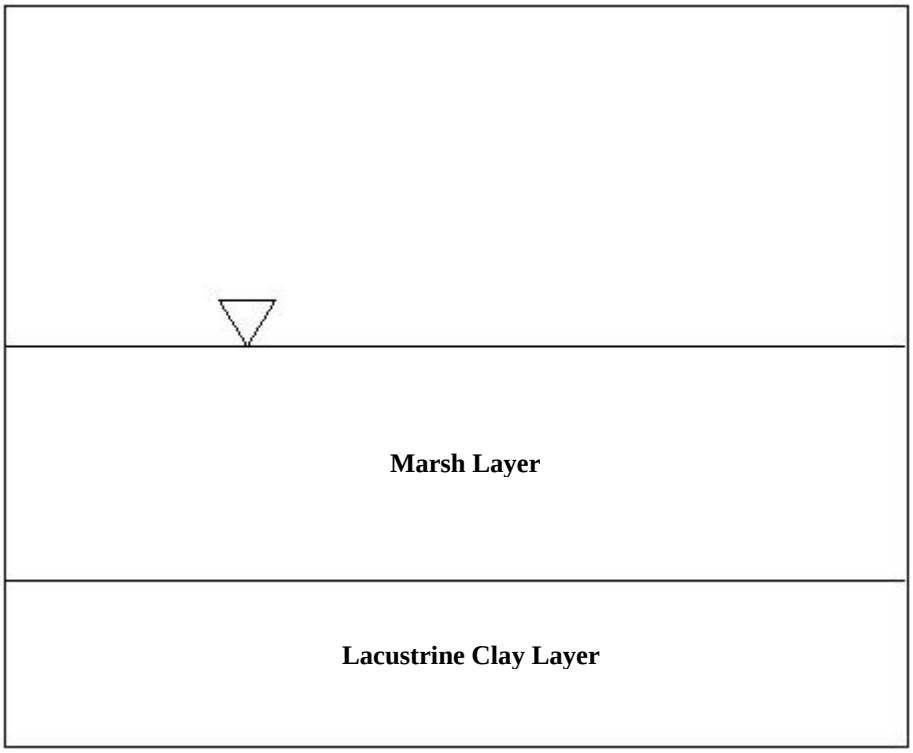

Figure 34: Soil profile after consolidation

Calculation of final vertical effective stress (σ_{v_f}') was also made for this condition and, since the final vertical effective stress (σ_{v_f}') was smaller than the vertical effective stress (σ_v') due to the addition of one foot of soil, the preconsolidation pressure (σ_p') was said to be equal to the vertical effective stress (σ_v'). Then, it is assumed that the levee fill is placed, and the vertical effective stress obtained from the various methods of analysis was compared to the preconsolidation pressure (σ_p'). If the calculated vertical effective stress owing to the presence of the levee was greater than the preconsolidation pressure (σ_p'), the soil was assumed to be normally consolidated and an OCR value of 1 was used. Meanwhile, if the vertical effective stress was less than the preconsolidation pressure, then the soil was assumed to be overconsolidated and the OCR was calculated from the following equation:

$$OCR = \frac{\sigma_p'}{\sigma_{v_o}'}, \text{ where}$$

$OCR =$ overconsolidation ratio

$\sigma_p' =$ preconsolidation pressure

σ_{v_o} '= initial vertical effective stress

Stability analyses were performed using the undrained shear strength obtained with this approach to calculate the factor of safety for slope stability for total stress and pore pressure determinations described previously. The *Slide* cross sections showing the critical failure circles for different canal water levels are shown in Appendix C. The Table 7 shows the values of factor of safety (FS) obtained for this approach at for CWLs of 6 ft, 7 ft, 8 ft, 9 ft, 10 ft, and 12.5 ft, as well as the CWL that corresponds to a factor of safety of 1, for all cases:

Table 7: FS for different CWL for IPET analysis and ESD cases for calculated values of OCR

IPET Analysis		Total Stress calculated with Elastic Theory. Pore pressure calculated assuming static water table		Total Stress calculated with Elastic Theory. Pore pressure calculated using FE Method BC el. -5ft		Total Stress calculated with Elastic Theory. Pore pressure calculated using FE Method BC el. -7ft	
CWL	Factor of Safety	CWL	Factor of Safety	CWL	Factor of Safety	CWL	Factor of Safety
6ft	1.318	6ft	1.231	6ft	1.386	6ft	1.491
7ft	1.233	7ft	1.148	7ft	1.296	7ft	1.400
8ft	1.148	8ft	1.067	8ft	1.204	8ft	1.301
9ft	1.069	8.87ft	1.000	9ft	1.120	9ft	1.212
9.92ft	1.000	9ft	0.990	10ft	1.043	10ft	1.127
10ft	0.995	10ft	0.919	10.57ft	1.000	11.64ft	1.000
12.5ft	0.833	12.5ft	0.765	12.5ft	0.872	12.5ft	0.942

Plots of OCR versus depth were made to compare the OCR values assumed and calculated for all methods with the values obtained from the results of consolidation tests. At crest, all of the techniques used an OCR value of 1, but at the toe and beyond values are different depending on the technique and OCR approach used. Figure 35 shows the comparison of OCR values of all the techniques with OCR from laboratory consolidation tests at the toe.

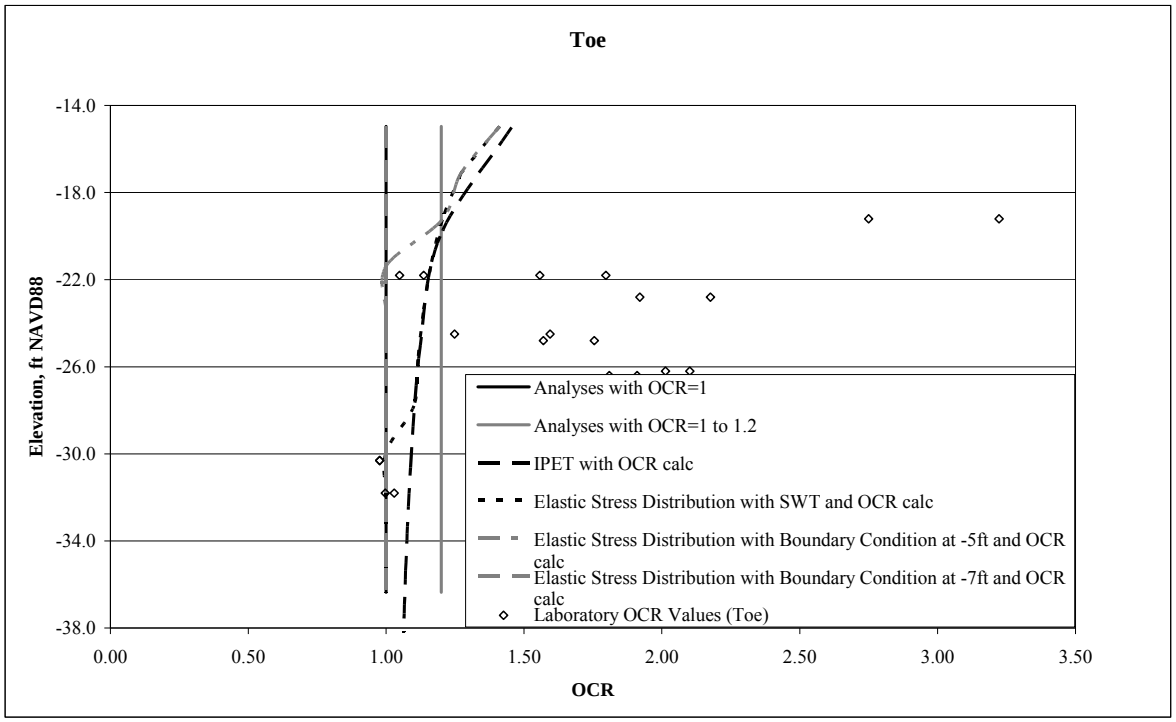

Figure 35: OCR versus depth comparison plot at toe

Since considerable scatter exits in the laboratory test data, there isn't a discernible trend of OCR vs. depth for which to compare to. The methods based on based on calculating an OCR variation with depth resulting from water table fluctuations or soil deposition and subsequent settlement tend to show a decrease in OCR with depth, which is the general trend observed in the laboratory test data.

6. Results of Analyses

6.1 Influences on calculated factor of safety values

As previously described in Chapter 4, the IPET analyses involved assumptions regarding the water table elevation, initial total stress, and consolidation conditions; all of which affect the undrained shear strength in the lacustrine clay layer. Enhancements to the IPET analyses were made to better simulate field conditions and to improve the accuracy of the analyses. A description of how these enhancements affected the values of factor of safety obtained is given in this section.

6.1.1 FE stresses versus static stresses (vertical equilibrium)

One of the assumptions made for the IPET analyses was to use the total vertical stress equal to the overburden pressure at all the locations in the cross section. Beneath the crest, the levee was approximated as an infinite fill, instead of finite fill, leading to overestimation of the stress, because the stress would dissipate with depth. Figure 36 shows a diagram for these conditions.

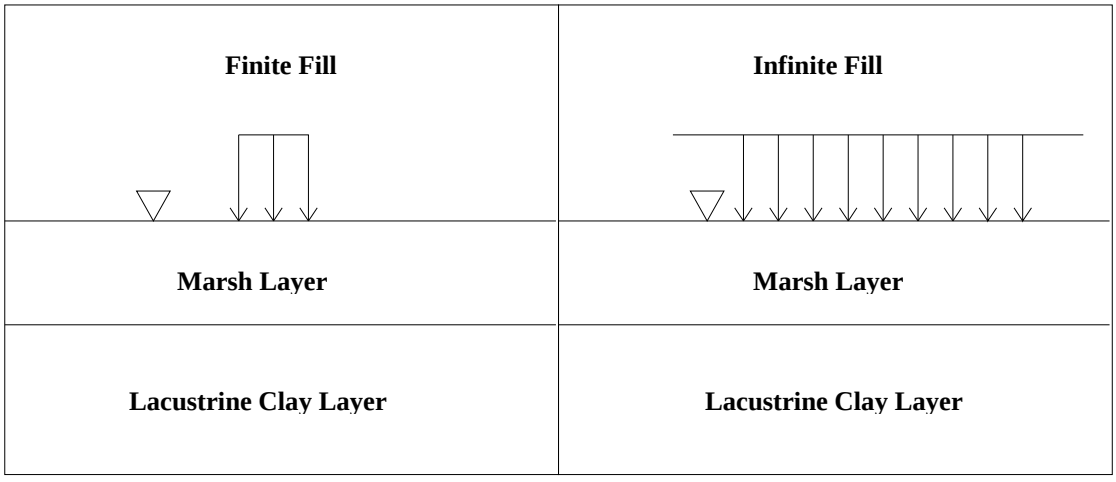

Figure 36: Diagram showing infinite and finite fill conditions

Meanwhile, beneath the toe, the stress was underestimated, because the proximity of the levee was not considered. As explained by Duncan etal. (2007), by using this assumption, redistribution of stress within the foundation from the center toward the toe of the levee is

ignored. That actual effective stress beneath the toe, and thus the shear strength, would be higher if the proximity to the levee fill was considered.

To more accurately calculate the vertical total stress values, it is recommended to use elastic theory, because it better approximates the geometry of the cross section, therefore providing a more realistic analysis. The following table shows the factors of safety obtained using vertical equilibrium and FE analysis for different CWLs. The canal water level that produces a factor of safety of 1 was also obtained.

Table 8: Factors of safety from FE stresses and static stresses for OCR=1

IPET Analyses Total stress calculated assuming vertical equilibrium Pore pressure calculated assuming static water table		Total Stress calculated with Elastic Theory Pore pressure calculated assuming static water table	
CWL (ft) NAVD88	**FS**	**CWL (ft) NAVD88**	**FS**
6.00	1.289	6.00	1.208
7.00	1.207	7.00	1.127
8.00	1.125	8.00	1.048
9.00	1.049	8.65	1.000
9.67	1.000	9.00	0.975
10.00	0.977	10.00	0.909
12.50	0.821	12.50	0.755

If a comparison is made between the cases with stresses calculated from FE and the method with static stresses at a same canal water level, the factors of safety obtained from FE cases are less than those obtained from static stresses. For the geometry analyzed, it appears that the load-spread effects of the levee fill are important. The smaller stress calculated under the levee with elastic theory overshadows the larger stress calculated beneath the toe of the levee. For other cross sections analyzed by IPET, these two effects appeared to balance out (IPET 2007).

Another comparison can be made between the canal water level obtained for a factor of safety of unity and the canal water level when the breach fully opened, suggested by the hydrograph in Figure 37. Calculating the total stress based on elastic theory resulted in a CWL about 1 ft less than that calculated using vertical equilibrium. Based on eyewitness reports, the breach fully open around 9:00AM, when the water level in the canal was between 9.5 ft and 10.5 ft. Owing to the uncertainty of the CWL at the exact time of failure due to indeterminate wave action, these results are roughly equivalent to those obtained by IPET.

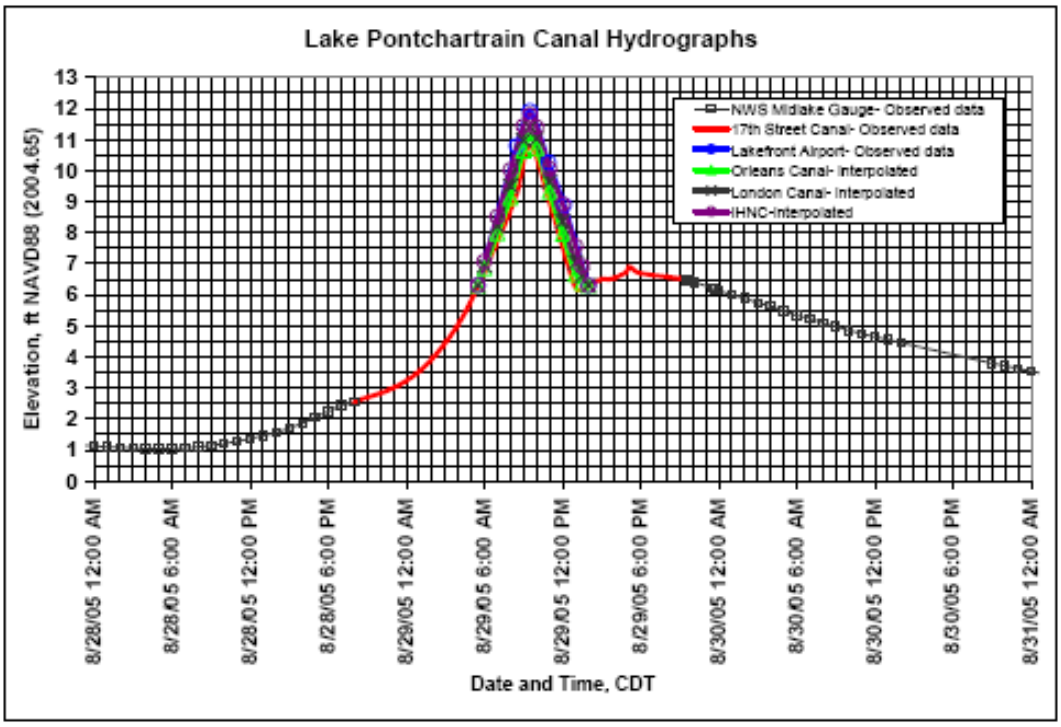

Figure 37: 17th Street Outfall Canal Hydrograph

6.1.2 Static water table versus seepage analysis

In the IPET analyses, the pore pressures were calculated assuming a horizontal water table $\gamma_w z$ approach. Analyses were performed as part of this thesis using pore pressures calculated by the finite element method. It should be noted that the calculated pore pressures are sensitive both to the position of the the protected side hydraulic boundary, and the assigned boundary conditions.

Two cases were analyzed to isolate the effect of calculating the pore pressures using a steady-state seepage analysis. In both of these cases, the total stresses were calculated using elastic theory. These cases were Elastic Stress Distribution with the protected side Boundary Conditions set at el. -5ft (ESD w BC-5ft) and Elastic Stress Distribution with the protected side Boundary Conditions set at el. -7ft (ESD w BC-7ft). In both of these cases, the protected side boundary was about 120 ft from the I-wall. The following table shows the factors of safety obtained from these analyses.

Table 9: Factors of safety from static water table and seepage analysis for OCR=1.

IPET Total stress calculated assuming vertical equilibrium Pore pressure calculated assuming static water table		Total Stress calculated with Elastic Theory Pore pressure calculated from finite seepage analysis with boundary conditions at -5ft		Total Stress calculated with Elastic Theory Pore pressure calculated from finite seepage analysis with boundary conditions at -7ft	
CWL (ft) NAVD88	**FS**	**CWL (ft) NAVD88**	**FS**	**CWL (ft) NAVD88**	**FS**
6.00	1.289	6.00	1.364	6.00	1.491
7.00	1.207	7.00	1.276	7.00	1.400
8.00	1.125	8.00	1.188	8.00	1.301
9.00	1.049	9.00	1.107	9.00	1.212
9.67	1.000	10.00	1.031	10.00	1.127
10.00	0.977	10.44	1.000	11.64	1.000
12.50	0.821	12.50	0.865	12.50	0.942

In general, the pore pressures obtained from the steady-state finite element seepage analyses were lower than those obtained for a static water table position and vertical head contours. The lower pore pressures resulted in higher values of effective stress, hence higher strengths in the lacustrine clay layer. If a comparison is made between the cases with static water table and cases with seepage analysis at a same canal water level, the factors of safety obtained from the static water table case are smaller than the ones obtained from seepage analysis. The calculated pore pressures decrease with a reduction in the head assigned to the protected side hydraulic boundary. Accordingly, the factor of safety increases with decreasing head at the protected side boundary.

Figure 38 shows pore pressure contours for the two different boundary conditions. As evident from the figure, the phreatic surface is lower for the protected side boundary condition set at el. -7 ft than when the boundary condition is set to el. -5 ft.

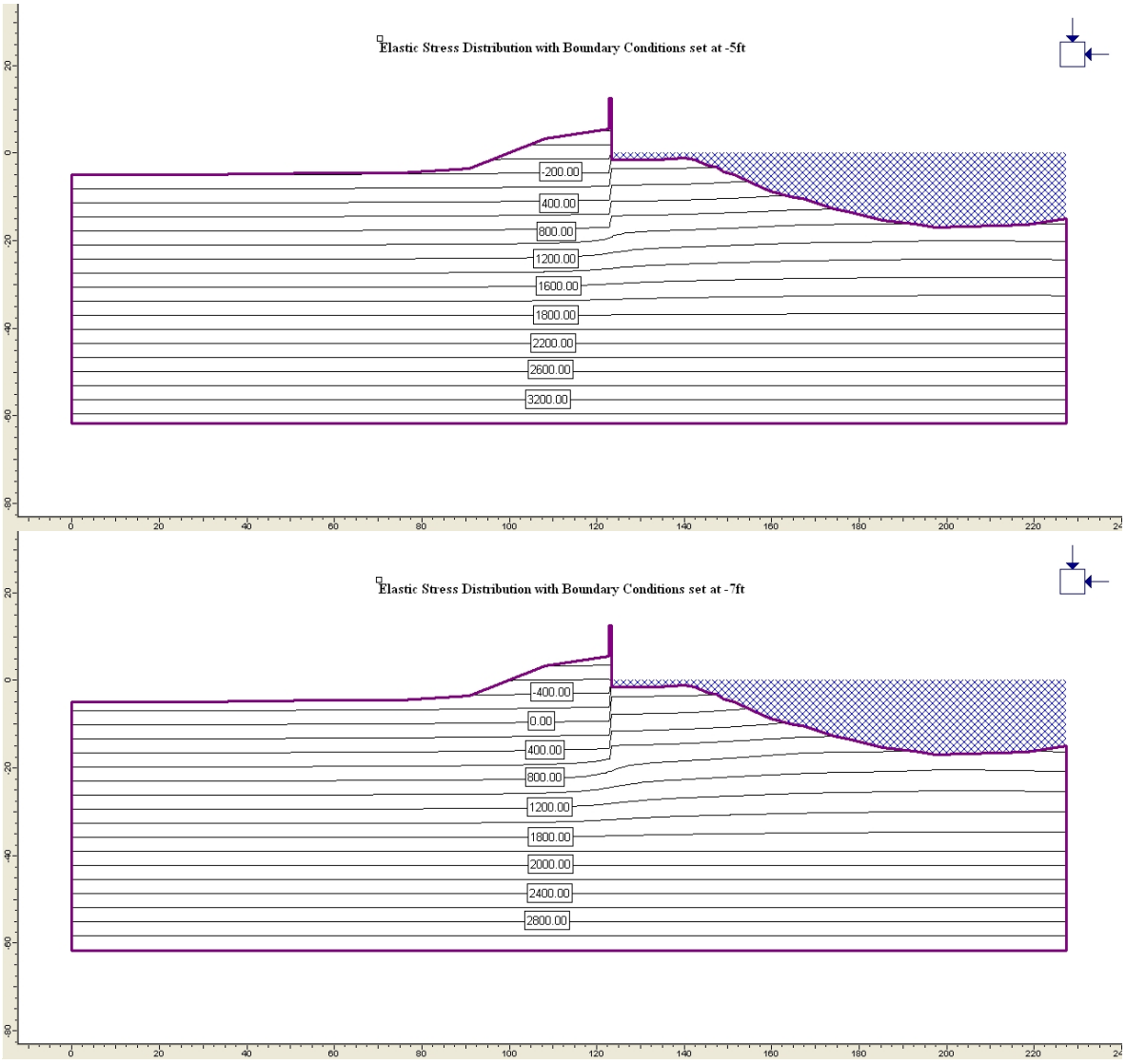

Figure 38: Pore pressure diagrams for cross section at 17th Street Outfall Canal

Comparing the CWL obtained for a factor of safety of unity to the hydrograph in Figure 37, the results of the analysis with the boundary conditions set at el. – 5 ft (10.4 ft) agrees well with the eyewitness reports of a CWL between 9.5ft and 10.5ft when the breach fully opened.

As stated earlier, the values of pore pressure calculated from the steady state seepage analysis are sensitive to the position of the constant head boundary. If the distance between the contant head boundary and the I-wall is decreased, for the same value of head at the boundary, the pore pressures decrease, and the factor of safety increases.

6.1.3 Influence of canal water elevation

As would be expected, the calculated factor of safety decreases with increasing canal water level. Raising the canal water level from 6 ft to 10 ft results in a reduction in the factor of safety varying from about 0.30 to 0.36. Figure 39 shows the variation of the factor of safety with canal water elevations for normally consolidated conditions.

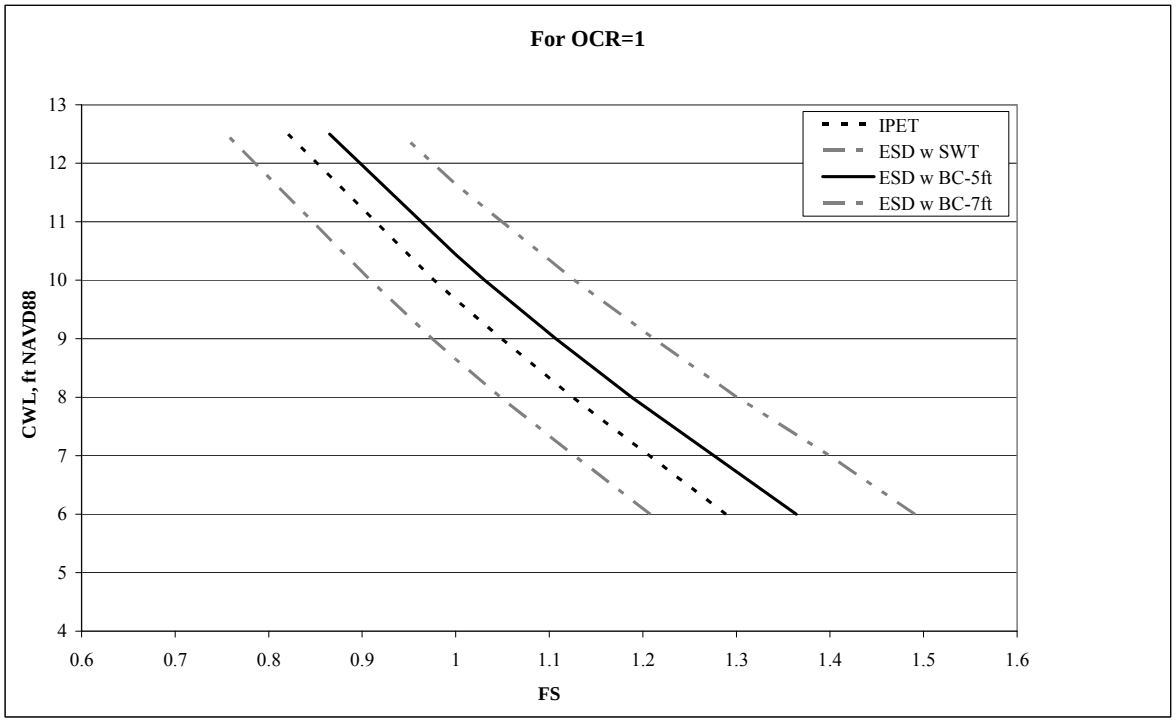

Figure 39: Factors of safety at different Canal Water Levels (CWL) for OCR=1

It is important to mention that all of these analyses assumed that there was a gap between the sheetpile and levee embankment. The IPET analyses demonstrated the significant importance of this assumption. As previously discussed in Chapter 3, there is a high probability that a gap formed during the 17th Street Outfall Canal failure and the gap was one of the main causes of the failure. As the water rose against the I-wall, as the gap formed, the load on the wall increased, because the water pressures in the gap were higher than the earth pressures that were in effect before the gap formed (Duncan et al. 2007).

6.1.4 Influence of OCR

The IPET analysis assumed that the clay layer was normally consolidated, but consolidation tests results indicate that the lacustrine clay may have been overconsolidated beneath the toe and beyond. To take this into consideration two approaches were used. In

the first approach, the OCR was assumed to be 1.0 under the crest and 1.2 under the toe of the levee, with a linear variation in between. This is indicated as *OCR = 1 to 1.2* on Figure 40. The second approach involved obtaining values of OCR versus depth assuming a loading-settlement scenario prior to levee construction. This is indicated as *OCR calc* on Figure 40. Figure 40 shows the variation of the factor of safety with canal water elevations for all cases using the first overconsolidation approach.

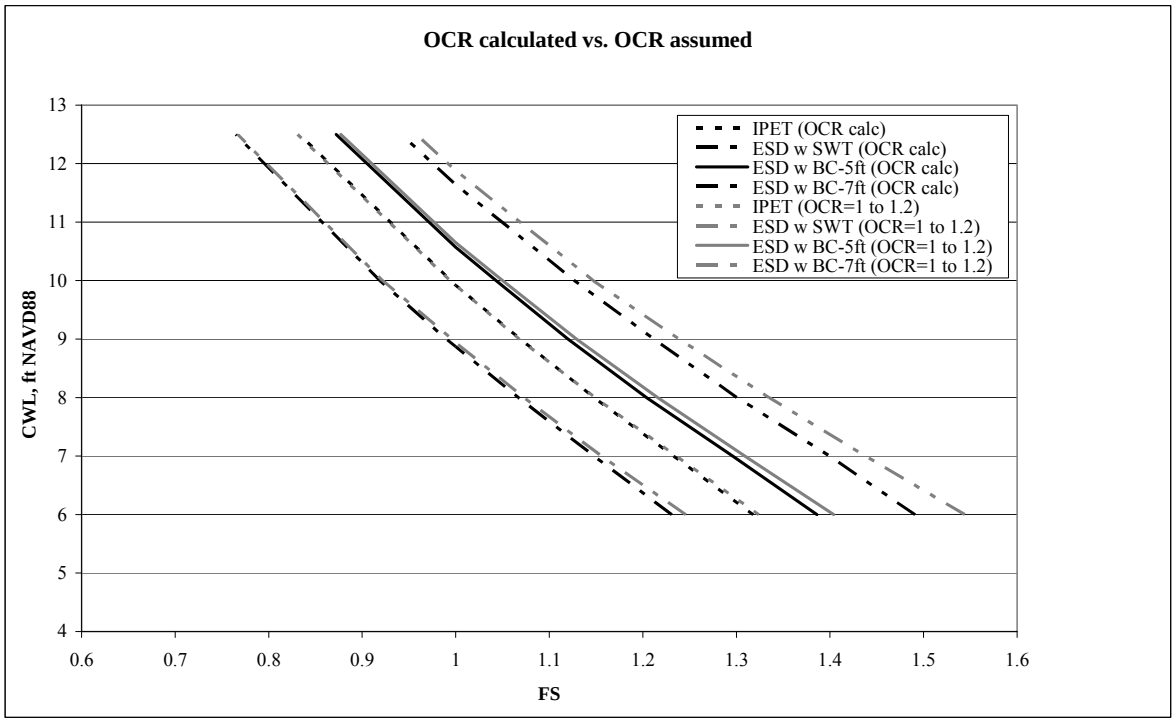

Figure 40: Factors of safety against CWL for all cases for the two OCR approaches

There does not appear to be a significant difference in the calculated factor of safety values using the two different OCR approaches. As stated previously, there was much scatter in the laboratory-determined values of OCR, so it was not possible to definitively conclude that one approach was better than the other. It seems certain that the lacustrine clay is normally consolidated beneath the crest of the levee, but the OCR variation with depth at the toe is uncertain.

Even though results presented here are inconclusive, it is recommended that the effects of overconsolidation be included in subsequent analyses. It may be that with careful consolidation testing, more reasonable variations of OCR versus depth can be determined.

6.2 Agreement with laboratory test data

Undrained shear strength (S_u) versus depth plots were made to compare the predicted values obtained from the results of the IPET analysis and the Elastic Stress Distribution (ESD) cases with the laboratory test results. These methods differ in the calculated values of the vertical effective stress, thus different shear strengths would be expected to result. Figure 41 shows the undrained shear strength comparison for all methods at crest assuming normally consolidated conditions. Plotted on the figure are results from unconfined compression tests and unconsolidated-undrained triaxial tests that were performed both prior to and after Hurrican Katrina.

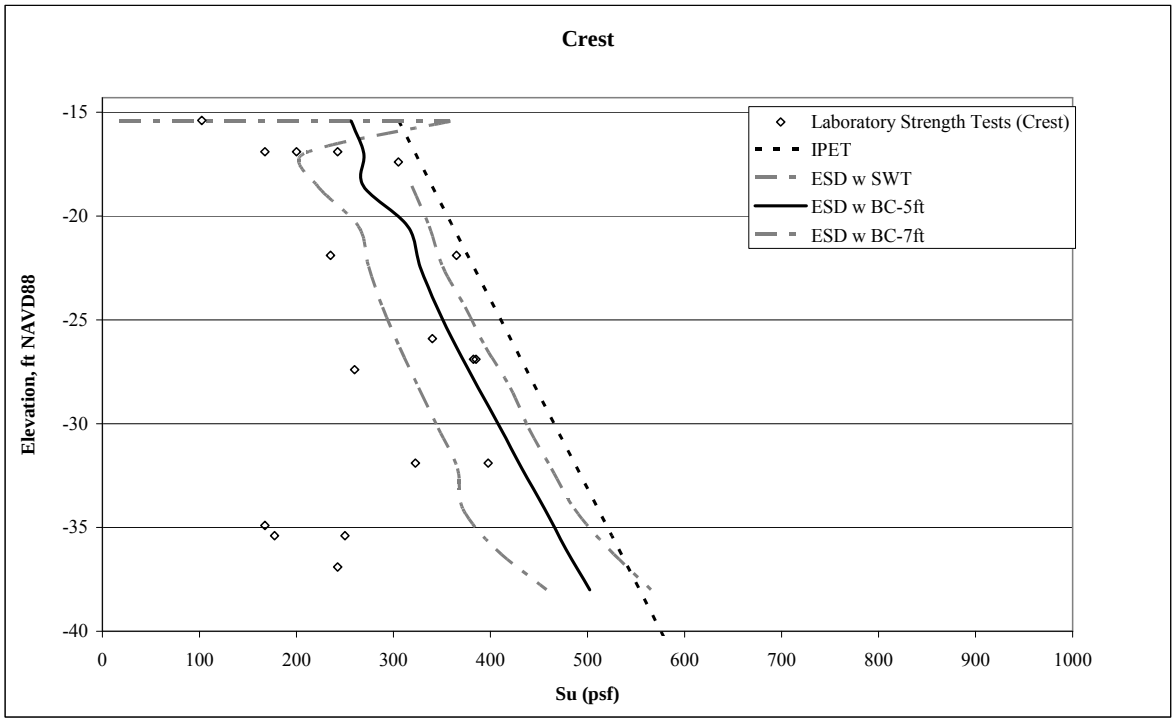

Figure 41: Undrained shear strength versus depth comparison at crest

From the plot, undrained shear strength values for IPET analyses varied linearly with depth ranging from about 300 psf to 600 psf. Caculating the total stresses using elastic theory, and determining the pore pressures using a static water table resulted in the lowest strength distribution, from about 200 psf to 450 psf. The methods using elastic theory combined with a steady-state seepage analysis were in between the methods using a static water table. Considerable scatter exists in the laboratory test data, and it is difficult to conclude that on method is superior to the others. However, the methods that resulted in the lowest shear strengths seem to agree better with the laboratory data.

It should be noted that the finite element analyses produced erratic total stresses right at the tip of the sheetpile (el. -15.5 ft). This is thought to be an artifact of the analysis. Refining the finite element mesh at this location seemed to partially solve the problem. Undrained shear strength values were also compared at the toe. Figure 42 shows the undrained shear strength comparison.

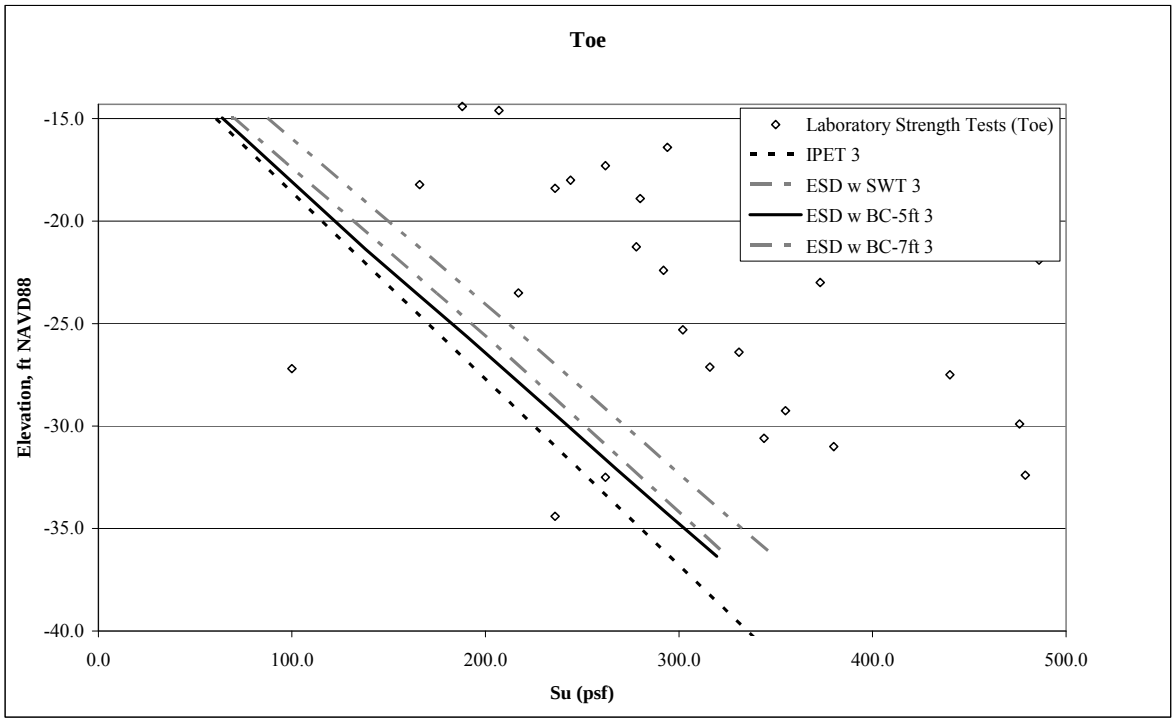

Figure 42: Undrained shear strength versus depth comparison at toe

In general, all methods seem to result in undrained shear strengths that are lower than those measured using laboratory tests. Considerable scatter exists in the the laboratory test data, but the higher laboratory strengths imply that the soil may be overconsolidated beneath the toe of the levee. In addition, the borings specified to be drilled at the toe of the levee may have been located slightly toward the flood side of the toe, which would also result in higher undrained shear strengths.

Figure 43 shows the calculated undrained shear strengths at 55 to 75 ft from the levee toe. Plotted on this figure for reference are the laboratory shear strengths measured for toe borings. At this location, the lacustrine clay layer does not feel the effects of the presence of the levee. As expected, there is not a large difference the in calculated shear strengths from the different methods.

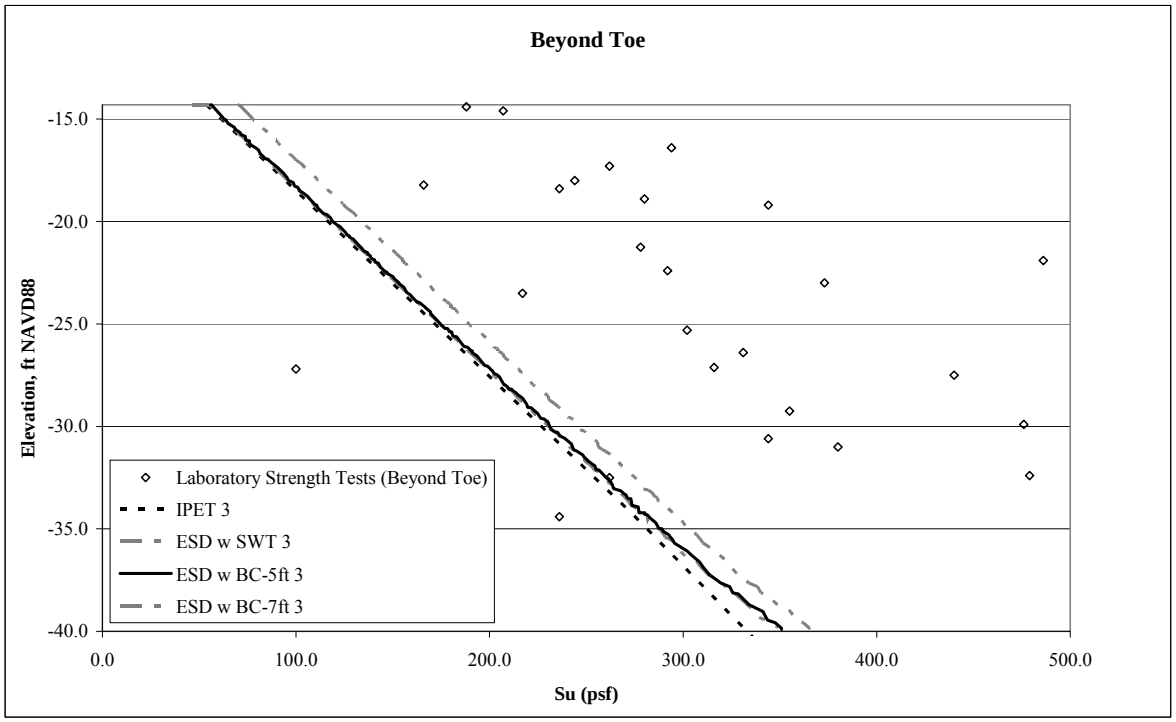

Figure 43: Undrained shear strength versus depth comparison beyond toe

From previous analyses, the following elements seem appropriate for future analyses:

- Vertical total stresses should be calculated using a linear elastic finite element model. This method accurately considers the "load-spread" effect of the levee fill, and should provide reasonably accurate total stress values.
- Steady-state seepage analyses should be conducted to determine pore pressures. Appropriate hydraulic boundary conditions should be accurately defined for these analyses.
- If laboratory tests indicate that the soil is overconsolidated at the toe, then the increase in shear strength owing to overconsolidation should be incorporated into the analysis.

The application of the recommended analysis elements on a section of the west bank of the 17th Street Outfall Canal will be discussed in detail in the next chapter.

7. Application of results to Current 17th St. I-wall Sections

In previous chapters, it was concluded that the analysis methods of I-walls can be improved using elastic stress distribution theory combined with steady state seepage analysis. Now, this analysis technique will be applied to a current cross section located on the west bank of the canal. This section did not fail during Hurricane Katrina and was not analyzed by IPET.

7.1 Laboratory and field test data

The west bank section is located on the Jefferson Parish side of the 17th Street Outfall Canal. The section of interest is between stations from 555+70 to 569+80. Figure 44 shows a soil profile made using the original field data.

Unconfined compression tests and unconsolidated-undrained triaxial tests were conducted on undisturbed samples taken from the levee fill, marsh, and lacustrine clay layers. For the levee fill, an undrained shear strength of 900 psf was used in the analysis. It should be noted that the shear strength of the levee fill material has little impact on the calculated factors of safety.

For the marsh material, laboratory test data showed undrained shear strength values of around 500 psf beneath the levee crest and 300 psf beneath the toe and beyond. Figure 45 presents a *Slide* image showing the cross section used in the analysis.

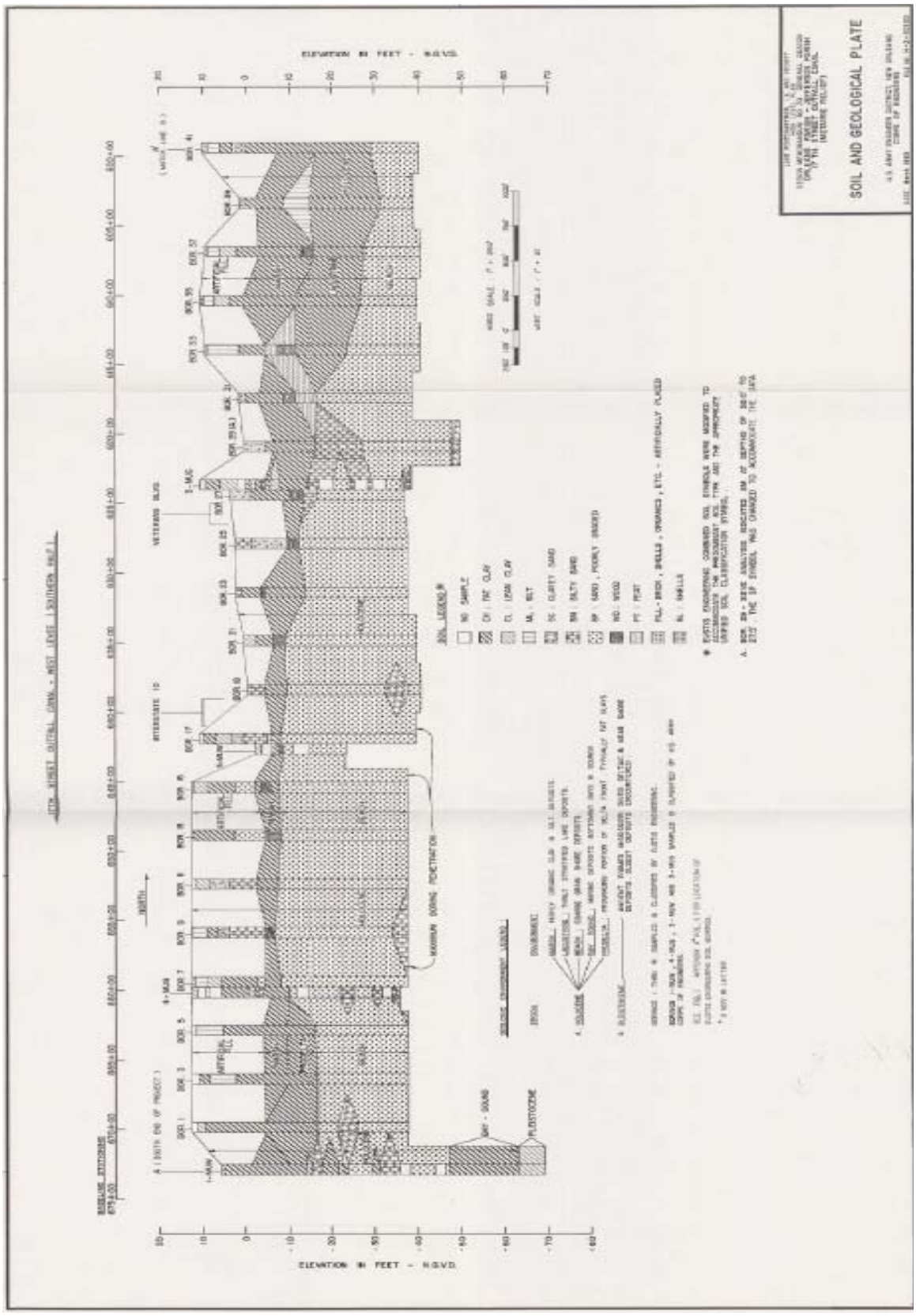

Figure 44: Profile of section of interest at 17th Street Outfall Canal West Bank

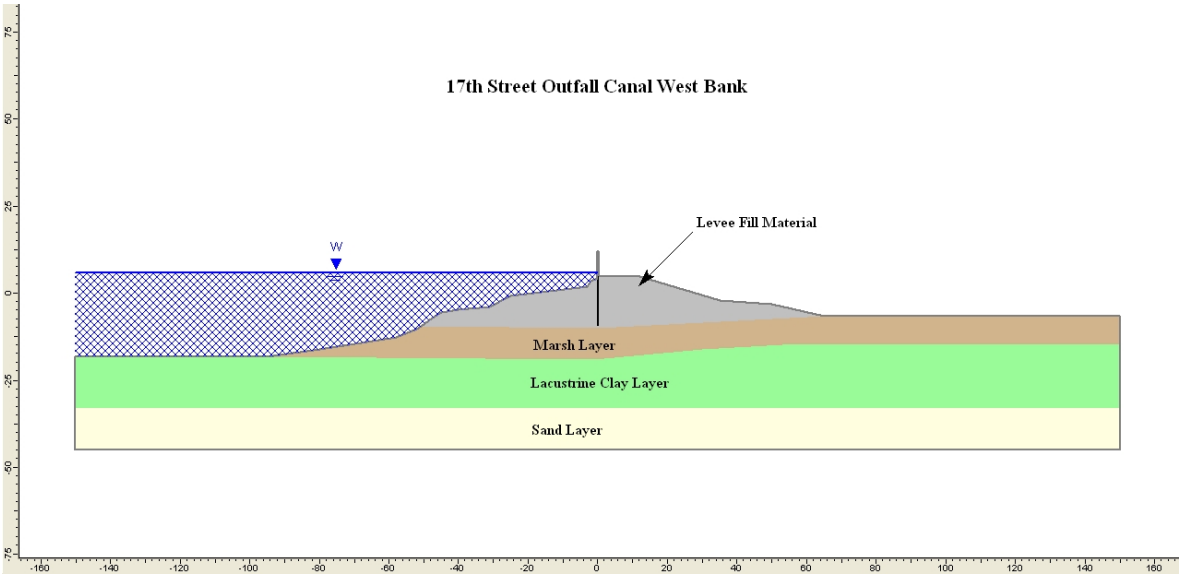

Figure 45: Soil profile of section of interest on west bank

Vertical total stresses in the clay layer were obtained from FE analysis using *Phase 2* software. Pore pressures were determined using a steady-state seepage analysis. This analysis assumed a CWL at el. 0 ft, and a protected side constant head boundary condition of -7 ft. The vertical effective stresses were used to calculate the undrained shear strength values. The same material properties, as for the cross section in the 17th Street Outfall Canal East Bank, were used and are shown on Table 10.

Table 10: Material properties for 17th Street Outfall Canal FE Analysis

Material	Permeability (ft/s)	Poisson's Ratio	Soil Unit Weight (pcf)	Tensile Strength (psf)	Cohesion (psf)	Friction Angle
Levee Fill	$1X10^{-7}$	0.49	109	900	900	0
Marsh	$1X10^{-6}$	0.49	80	0	219.3	35
Lacustrine Clay	$1X10^{-7}$	0.49	109	0	219.3	35
Sand	$1X10^{-3}$	0.40	120	0	0	35
Bay Sound Clay	$1X10^{-7}$	0.49	120	500	500	0
Sheetpile	$1X10^{-99}$	0.4	120	0	219.3	35

For the FE analysis a uniform mesh composed of 6 noded triangles was used with approximately 1500 mesh elements. The mesh element density was increased in the vicinity of the sheet pile tip to improve the precision of the stress values obtained.

The vertical position of the protected side boundary was set at -7 ft to represent what was used in the Elastic Stress Distribution with Boundary Conditions set at -5 ft (ESD w BC-5 ft).

The clay layer was found to be normally consolidated beneath the crest and overconsolidated beneath the toe and beyond, just as for the east bank based on laboratory consolidation test results.

Estimation of OCR was possible with the assumption of adding a new layer of soil to the profile, just as it was made for the east bank section as previously discussed in section 5.2.1.2. Initial conditions consisted of a marsh layer of 8.5 ft thick, followed by a lacustrine clay layer of 18.3 ft thick, for which the overconsolidation ratio (OCR) was calculated.

Determination of the undrained shear strength was made using the calculated values of OCR and applying those values to the following equation (Jamiolkowski et. al. 1985):

$$S_u = 0.24\sigma_v' OCR^{0.8}$$

The sample calculations made for the undrained shear strength determination are presented on Appendix B.

7.2 Safe Water Level (SWL) determination

Stability analyses were made on the west bank of the 17th Street Outfall Canal for canal water levels of 6 ft, 7 ft, 8 ft, 9 ft, 10 ft, and 12.5 ft. The canal water level corresponding to a factor of safety of 1.4 was also obtained. It is important to know the canal water level that produces a factor of safety of 1.4, because it will control the operation of the pumps during future hurricanes. *Slide* was used to run the stability analyses, as for the east bank. The following table presents the factors of safety obtained at different canal water levels for this set of analyses compared to the ones obtained for the east bank cross section with the same technique.

Table 11: Factors of safety at different Canal Water Levels (CWL) for west bank

West Bank		East Bank	
CWL (ft) NAVD88	**FS**	**CWL (ft) NAVD88**	**FS**
3.39	1.400	6.00	1.386
6.00	1.306	7.00	1.296
7.00	1.267	8.00	1.204
8.00	1.223	9.00	1.120
9.00	1.178	10.00	1.043
10.00	1.132	10.57	1.000
12.50	1.003	12.50	0.872

Figure 46 shows a *Slide* image with the critical circle and the factor of safety calculated for a canal water level of 6 ft on the section of interest in the west bank. The *Slide* figures are shown on Appendix C.

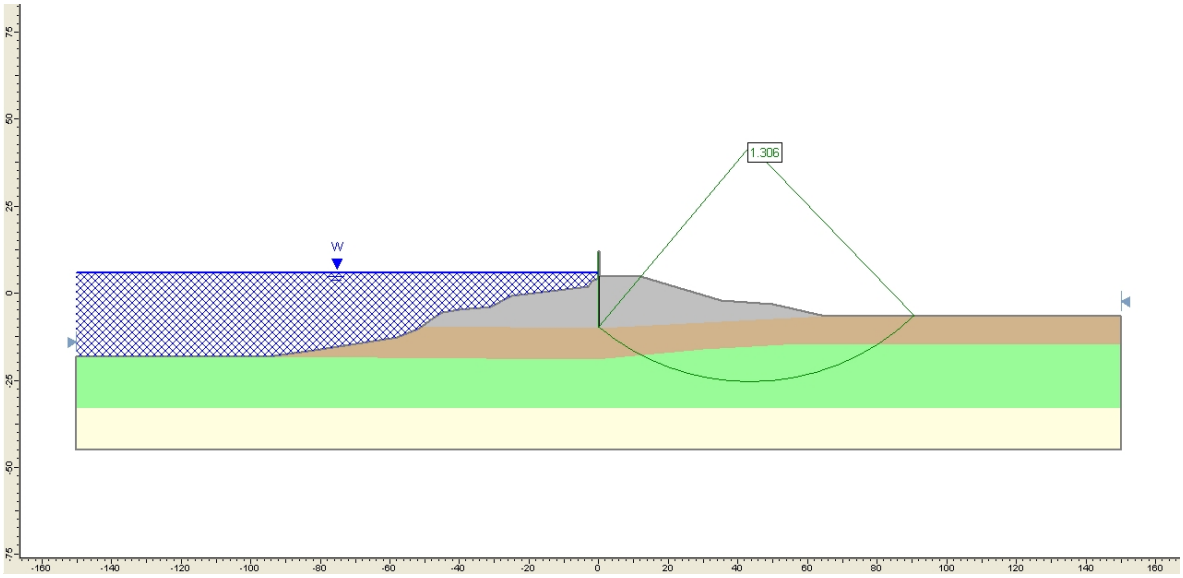

Figure 46: Factor of safety calculated by Slide for analysis at CWL = 6 ft for west bank section.

7.2.1 Agreement with laboratory consolidation and strength results

Undrained shear strength versus depth plots were made at crest to compare the laboratory strength results with the values obtained from the analysis of the west bank. Figure 47 shows the undrained shear strength comparison plot for the lacustrine clay layer at crest. In general, the calculated shear strength is less than the measured shear strength.

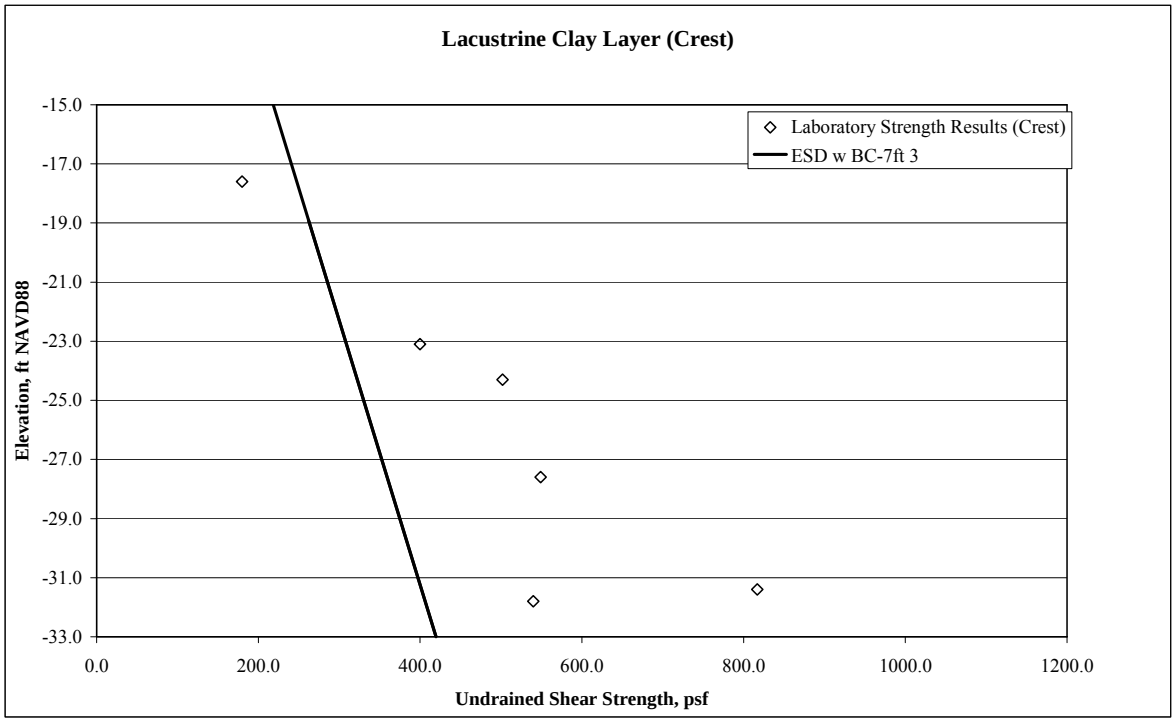

Figure 47: Su versus depth comparison plot at crest for lacustrine clay layer

Shown in Figure 48 are the calculated and measured undrained shear strengths in the lacustrine clay layer at the toe. As was the case with the east bank analysis, the calculated shear strengths are less than the measured shear strength. This implies that the clay may be overconsolidated beneath the toe. Also, the toe borings were made through about two feet of levee fill, so that the true effective stress at the sample locations would be higher than that calculated in the analysis.

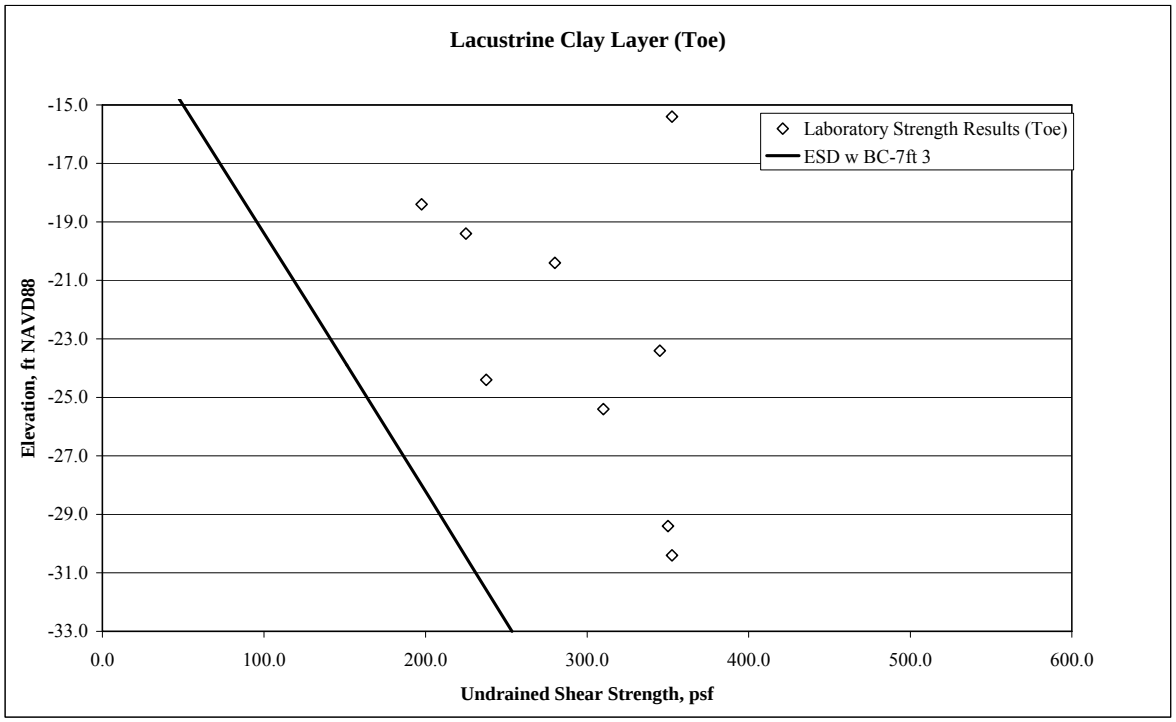

Figure 48: Su versus depth comparison plot at toe for lacustrine clay layer

Figure 49 shows the undrained shear strength comparison for the lacustrine clay layer at a location 75 ft beyond the toe. As would be expected, the calculated undrained shear strengths are less than the measured values.

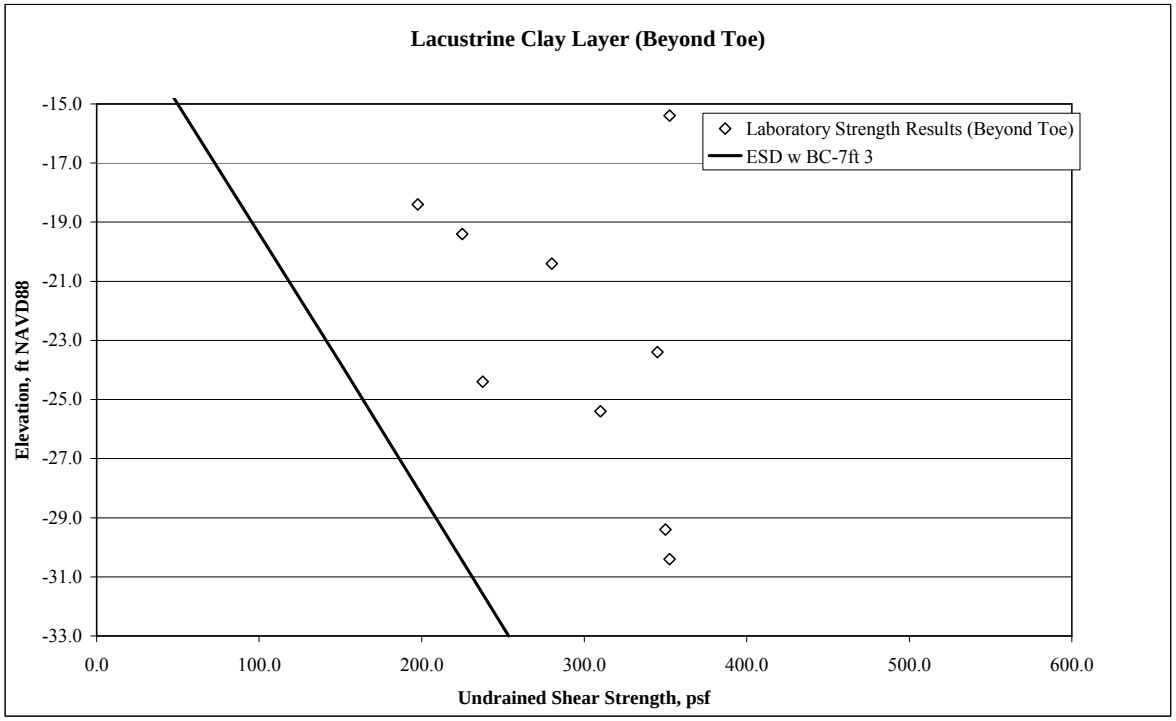

Figure 49: Su versus depth comparison plot beyond the toe for lacustrine clay layer

A comparison between the overconsolidation ratio (OCR) values obtained from computations and laboratory consolidation test results was also made. The comparison of OCR values in the clay layer beneath the crest is shown in Figure 50.

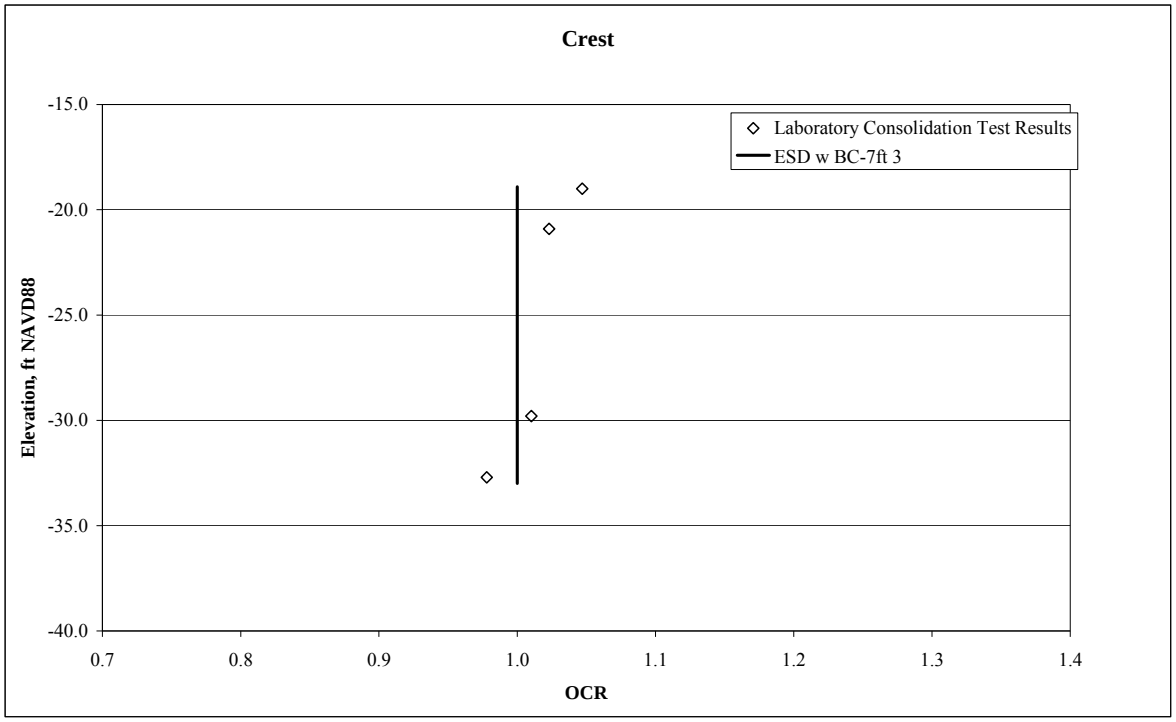

Figure 50: OCR versus depth comparison plot at crest

As can be seen from the plots, normally consolidated conditions were obtained at crest using the assumption of adding one foot of soil to the original soil profile. These conditions seem to agree with laboratory consolidation tests.

Figure 51 shows the OCR comparison at the toe and beyond.At the toe and beyond, there is not sufficient data to define a proper trend for the OCR values obtained in the analyses. Nevertheless, OCR values from laboratory consolidation tests are higher than those calculated. As was the case for the shear strength results, the proximity of the borings relative to the toe may have affected the laboratory test results.

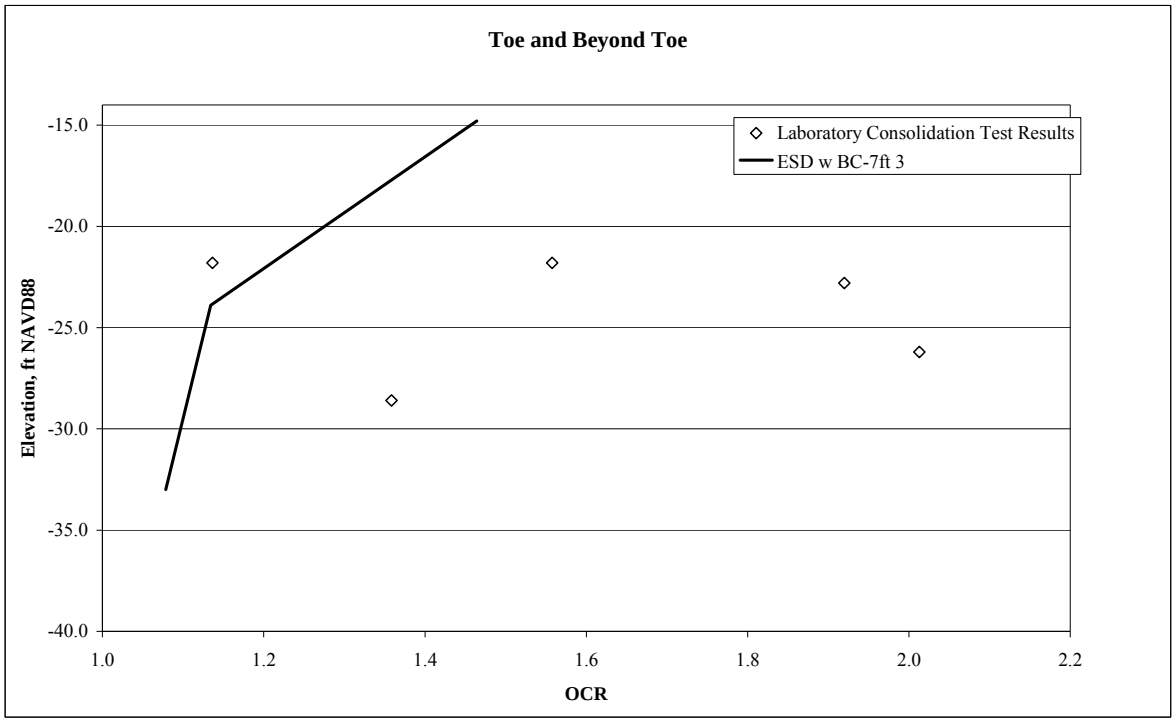

Figure 51: OCR versus depth comparison plot at toe and beyond the toe

8. Summary and Conclusions

The 17th Street Outfall Canal is located in New Orleans between Jefferson Parish and Orleans Parish. The subsurface conditions in the area of the canal consists of Holocene deposits varying in depth to approximately 60 ft and underlain by Pleistocene deposits.

On the 17th Street Outfall Canal a breach occurred during Hurricane Katrina due to instability of the floodwalls. The area of the breach consists mainly of marsh-swamp deposits underlain by lacustrine clay deposits.

Soon after the hurricane, the Interagency Performance Evaluation Task Force (IPET) was established by the Chief of Engineers, to determine the facts concerning the performance of the Hurricane Protection System (HPS) in New Orleans and southeast Louisiana during the hurricane.

The undrained shear strength and factor of safety values from the IPET analyses were compared with the values used in the original design and the following was found:

- A value of $S_u = 900$ psf was selected as a representative value for the levee fill layer in the IPET analyses versus an $S_u = 500$ psf used in the original design.
- Values of $S_u = 400$ psf beneath the levee crest and $S_u = 300$ psf beneath the levee toe were used in the IPET analyses for the marsh layer, but a $S_u = 280$ psf was selected as representative value at all locations on the original design.
- Under the crest of the levee, the original design strengths for the lacsutrine clay agreed with the IPET analyses. For locations beneath the toe and beyond, the strength values in the original design were considerably larger than those used by IPET.
- Stability analyses in the original design were made using the New Orleans District Method of Planes, while the IPET analyses used Spencer's Method incorporated into the *Slide* software.
- The IPET analyses evaluated the formation of a gap between the soil and the I-wall. The results of these analyses support that concept that the gap was the cause for the instability of the wall. The original design did not include the presence of a gap.

- The factor of safety obtained for the original design geometry and shear strengths, using Spencer's method, was approximately 30% higher than the one obtained using the Method of Planes.

Even though the analyses performed by IPET were found to be useful when examining the possible causes for the instability of the wall and identified some of the problems with the original design, there were some simplifying assumptions that were incorpated into the analyses. Some of the assumptions made by IPET were:

- The phreatic surface was assumed to be at el. 0 ft or at the ground surface.
- The clay was assumed to be normally consolidated, while the laboratory consolidation test results indicated that the soil was a little overconsolidated beneath the toe and beyond.
- IPET did not considered details of the stress distribution beneath the levee, which would result in "load spread" effects. The total stress calculated beneath the toe of the levee would be too large, and the total stress calculated beneath the toe of the levee would be too small.

In this thesis, the effects of these assumptions were evaluated. Twelve cases were evaluated, taking into consideration the location of the phreatic surface, the use of linear elastic models with the finite element method to calculate the vertical total stress, the use of a steady-state seepage analysis to calculate the pore pressures, and a consideration of overconsolidation within the lacustrine clay layer. Calculated undrained shear strength and OCR values obtained were compared with laboratory data. Calculating stresses using a linear elastic finite element method coupled with pore pressures determined from a seepage analysis, combined with either calculated or assumed values of OCR, was found to be a significant improvement in the original IPET analysis method. Using the modified analysis method, a section of the west bank of the 17th St. Canal that did not fail during Hurricane Katrina was analyzed.

The west bank section of the canal was assumed to have the same unit weights as the east bank section. The undrained shear strength beneath the crest in the marsh layer was found to be a little higher.

As previously done for the east bank, calculated undrained shear strength and OCR values were compared with laboratory test results. Undrained shear strength and OCR values from laboratory test results are a little higher than the ones from Elastic Stress Distribution with Boundary Conditions set at -7ft with calculated values of OCR (ESD w BC-7ft 3). This difference between OCR values could have been the result behind the calculations of OCR from the assumption of adding one foot of soil to the original conditions. Perhaps, the effect of adding more than one foot of soil to the original conditions can be evaluated in future investigations.

In addition to the application of the method to obtain factors of safety, the canal water level corresponding to a factor of safety of 1.4 was also obtained, because it will control the operation of the pumps during future hurricanes. The canal water level obtained was 3.39 ft.

References

1. Becker, D. E., et. al. (1987). *Work as a criterion for determining in situ and yield stresses in clays,* Canadian Geotechnical Journal, No. 24, Vol. 4, pp. 549-564.

2. Casagrande, A. (1936). *The determination of the pre-consolidation load and its practical significance,* Proceedings of the First International Conference of Soil Mechanics, Cambridge, Massachussetts, Vol. 3.

3. Davis, E.H. and Poulos, H.G. (1974). *Elastic Solutions for Soil and Rock Mechanics*, John Wiley and Sons, Inc, New York, pp. 407.

4. Duncan (1996). *State of the Art: Limit Equilibrium and Finite-Element Analysis of Slopes*, Journal of Geotechnical Engineering, pp. 6.

5. Duncan, et. al. (2007). *Stability of I-walls in New Orleans during Hurricane Katrina*, pp. 6.

6. Interagency Performance Evaluation Task Force (2007). *Performance Evaluation of the New Orleans and Southeast Louisiana, Volume 5 The Performance – Levees and Floodwalls,* New Orleans District, Corps of Engineers, p.1-53, 123-133.

7. Interagency Performance Evaluation Task Force (2007). *Performance Evaluation of the New Orleans and Southeast Louisiana, Volume 1 Executive Summary and Overview,* New Orleans District, Corps of Engineers, pp.147.

8. Interagency Performance Evaluation Task Force (2007). *Performance Evaluation of the New Orleans and Southeast Louisiana, Volume 5 The Performance – Levees and Floodwalls, Appendix 1*, New Orleans District, Corps of Engineers, pp.63.

9. Interagency Performance Evaluation Task Force (2007). *Performance Evaluation of the New Orleans and Southeast Louisiana, Volume 5 The Performance – Levees and Floodwalls, Appendix 2,* New Orleans District, Corps of Engineers, pp.45.

10. Interagency Performance Evaluation Task Force (2007). *Performance Evaluation of the New Orleans and Southeast Louisiana, Volume 5 The Performance – Levees and Floodwalls, Appendix 3,* New Orleans District, Corps of Engineers, pp.13.

11. Interagency Performance Evaluation Task Force (2007). *Performance Evaluation of the New Orleans and Southeast Louisiana, Volume 5 The Performance – Levees and Floodwalls, Appendix 4,* New Orleans District, Corps of Engineers, pp.31.

12. Interagency Performance Evaluation Task Force (2007). *Performance Evaluation of the New Orleans and Southeast Louisiana, Volume 5 The Performance – Levees and Floodwalls, Appendix 6,* New Orleans District, Corps of Engineers, pp.47.

13. Interagency Performance Evaluation Task Force (2007). *Performance Evaluation of the New Orleans and Southeast Louisiana, Volume 5 The Performance – Levees and Floodwalls, Appendix 10,* New Orleans District, Corps of Engineers, pp.29.

14. Interagency Performance Evaluation Task Force (2007). *Performance Evaluation of the New Orleans and Southeast Louisiana, Volume3 The Hurricane Protection System,* New Orleans District, Corps of Engineers, p. 1-283, 372-449.

15. Jamiolkowski et. al. (1985). *New developments in field and laboratory testing of soils*, Proceedings of the 11th International Conference on Soil Mechanics and Foundation Engineering, San Francisco, Vol. 1, pp. 57-153

16. Mayne, P.W. and Trevor, F (2004). *Undrained shear strength and OCR of marine clays from piezocone test results*, Geotechnical & Geophysical Site Characterization, Vol. 1, (Proc. ISC-2, Porto), Millpress, Rotterdam, 391-398

17. Spencer, E. (1967). *A method of analysis of the stability of embankments assuming parallel inter-slice forces*, Geotechnique, Institution of Civil Engineers, Great Britain, Vol. 17, No. 1, March, pp. 11-26.

18. United States Army Corps of Engineers (1990). *Design Memorandum No. 20 General Design, Orleans Parish, Jefferson Parish, 17th St. Outfall Canal Volume 1*, New Orleans District, Corps of Engineers, pp. 286.

19. United States Army Corps of Engineers (1990). *Design Memorandum No. 20 General Design, Orleans Parish, Jefferson Parish, 17th St. Outfall Canal Volume 2*, New Orleans District, Corps of Engineers, pp. 519.

20. United States Army Corps of Engineers (1990). *Design Memorandum No. 20 General Design, Orleans Parish, Jefferson Parish, 17th St. Outfall Canal Supplement No. 1*, New Orleans District, Corps of Engineers, pp. 549.

21. United States Army Corps of Engineers (2003). *Slope Stability Engineer Manual*, Corps of Engineers, Washington, DC, pp. 205.

Vita

Liselle Vega-Cortés was born in San Juan, Puerto Rico on April 9th, 1979. After graduating from high school, she attended the Polytechnic University of Puerto Rico and obtained a Bachelor of Science degree in Civil Engineering in 2005. While on Polytechnic University, she was an active member of student chapters, being vice-president of the American Society of Civil Engineers student chapter from 2002 to 2004. She was also part of the Civil and Environmental Engineering Department Honor Board from 1999 to 2005 and represented the student body in the Assesment Committee of the Middle States Association for Colleges and Schools for the Polytechnic University of Puerto Rico. In August, 2006, she enrolled Virginia Polytechnic Institute and State University to pursue a Master of Science degree in Civil Enginering in the Geotechnical Engineering program.

Appendix A

Phase 2 Figures and Output Data

Phase 2 Figures and Output Data: East Bank

ESD w SWT

Model

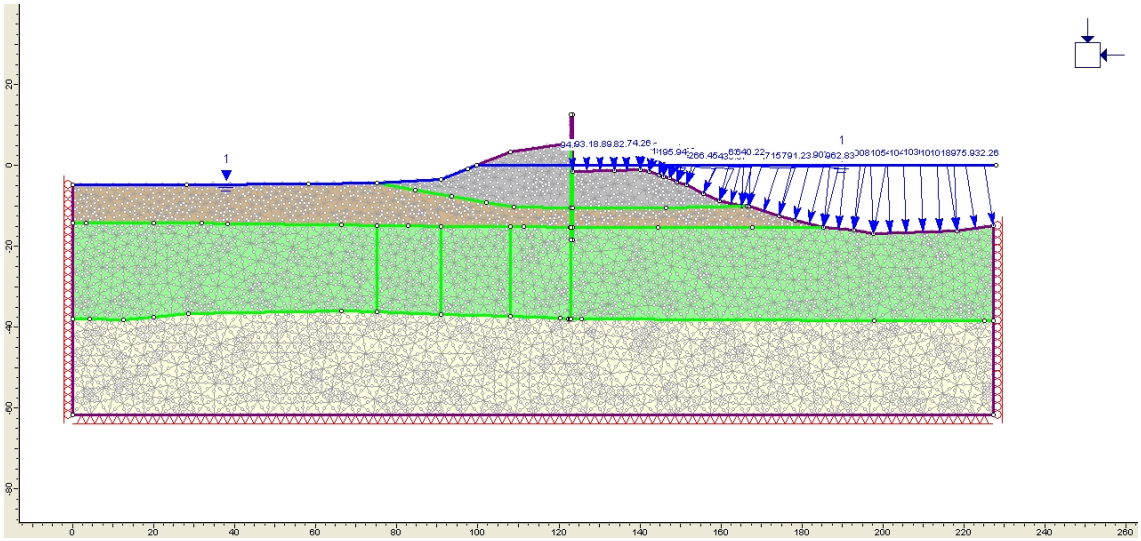

Figure A-1: Phase 2 Model for ESD w SWT

Vertical Effective Stress

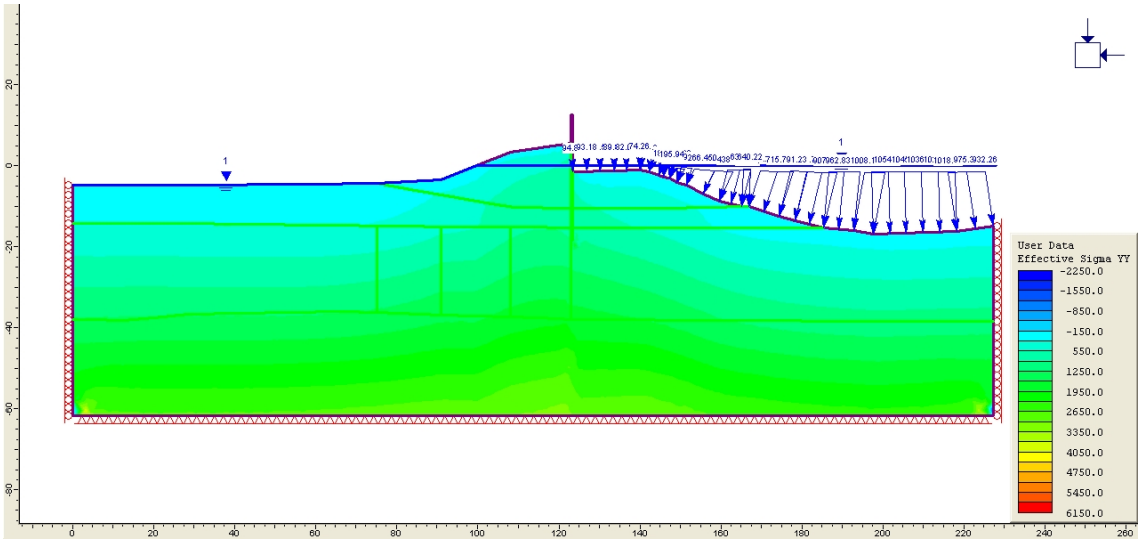

Figure A-2: Phase 2 Vertical Effective Stress figure for ESD w SWT

ESD w BC-5ft

Model

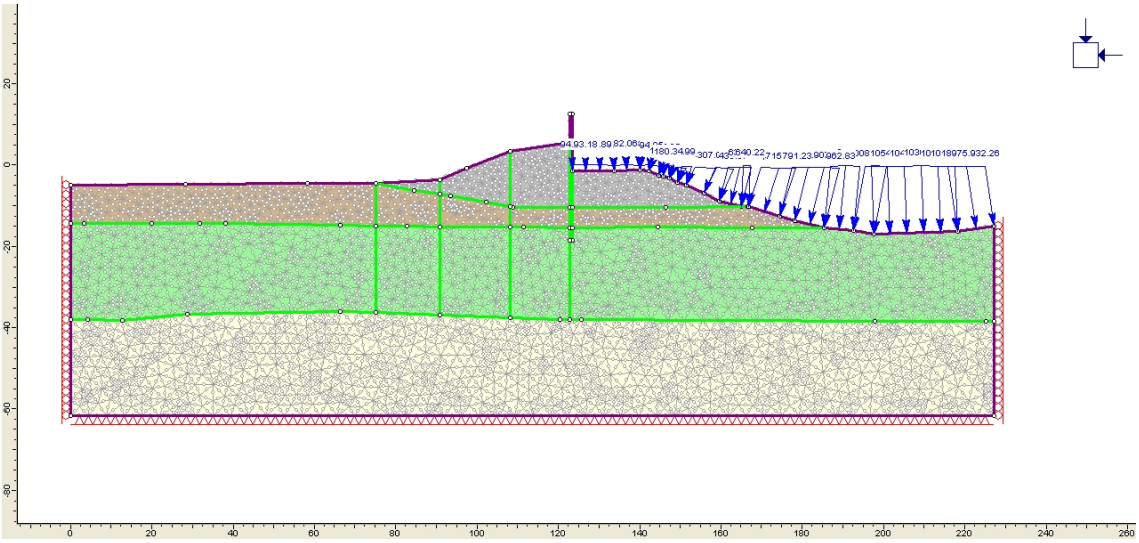

Figure A-3: Phase 2 Model for ESD w BC-5ft

Vertical Effective Stress

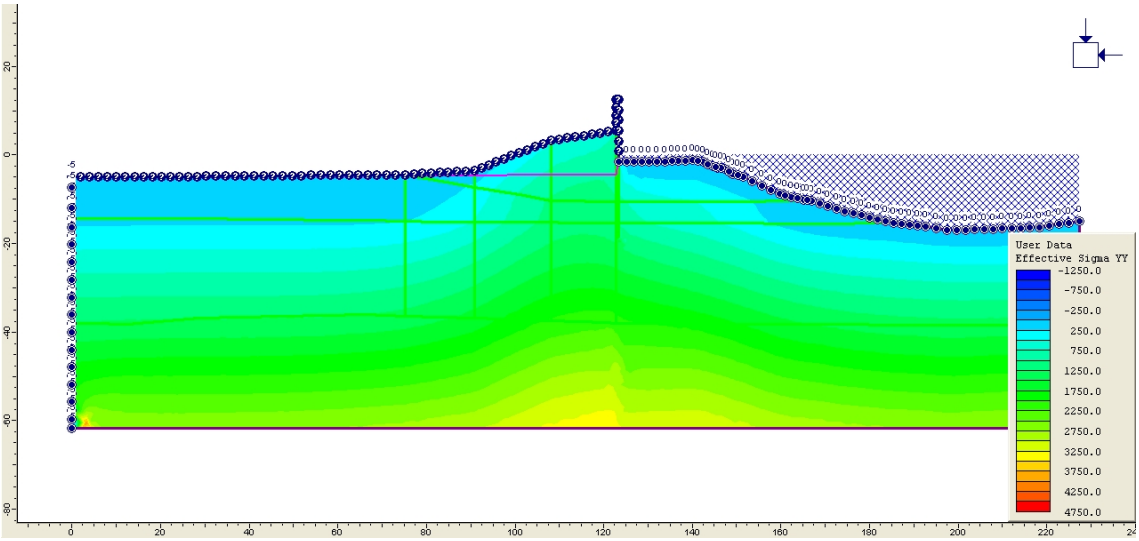

Figure A-4: Phase 2 Vertical Effective Stress figure for ESD w BC-5ft

ESD w BC-7ft

Model

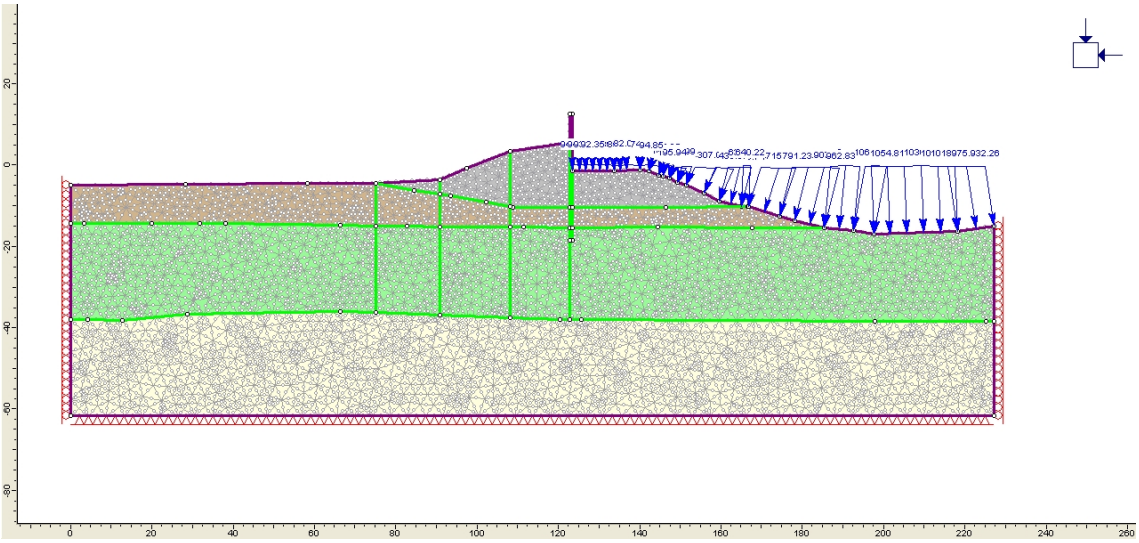

Figure A-5: Phase 2 Model for ESD w BC-7ft

Vertical Effective Stress

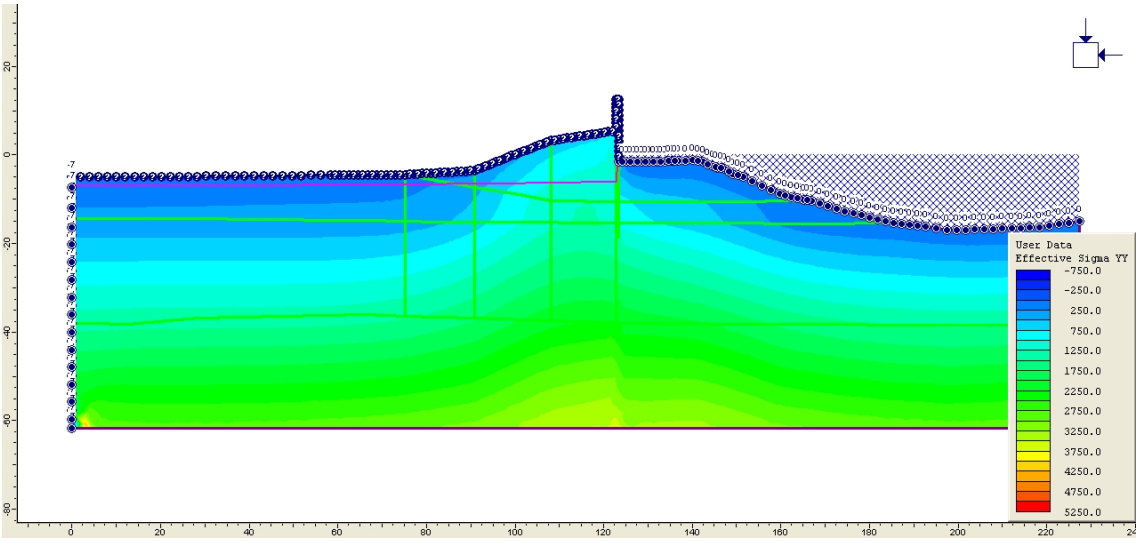

Figure A-6: Phase 2 Vertical Effective Stress figure for ESD w BC-7ft

Phase 2 Figures and Output Data: West Bank

ESD w BC-5ft

Model

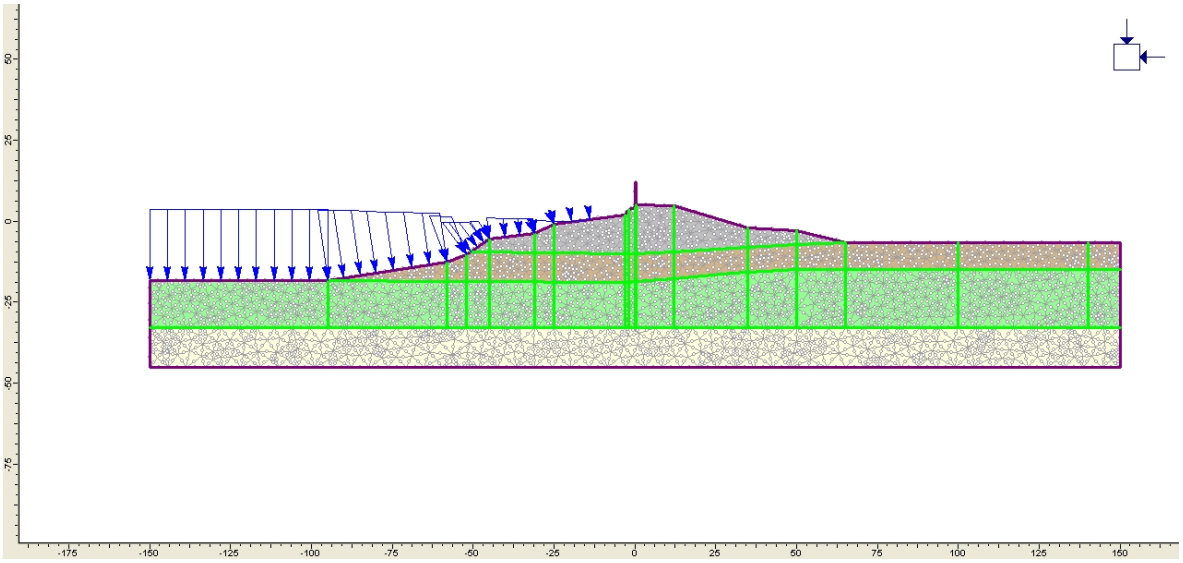

Figure A-7: Phase 2 Model for ESD w BC-7ft for West Bank

Vertical Effective Stress

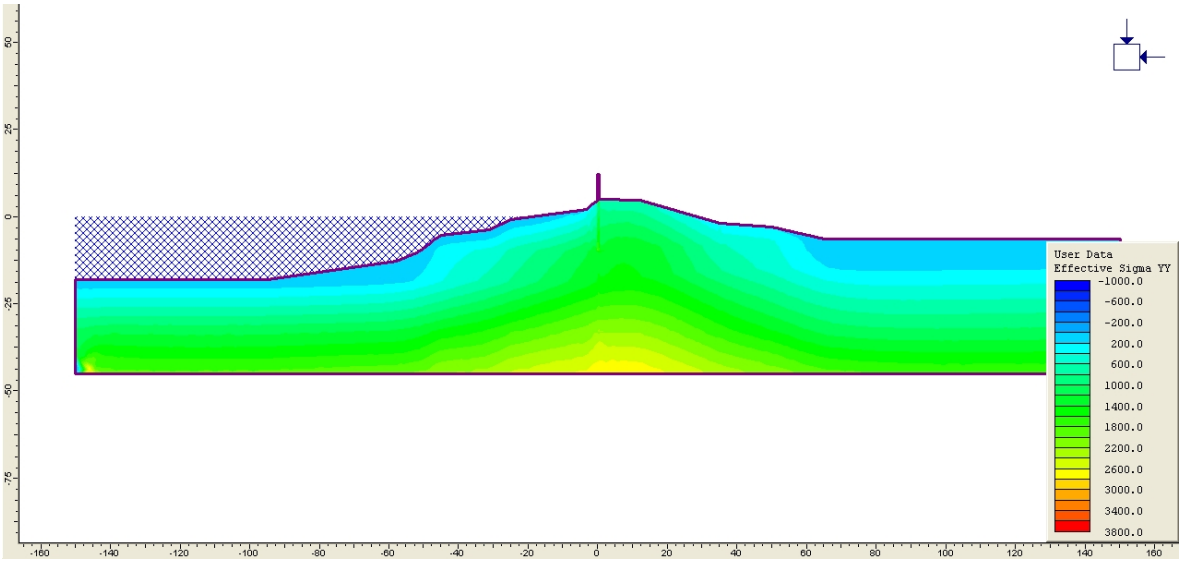

Figure A-8: Phase 2 Vertical Effective Stress figure for ESD w BC-7ft for West Bank

Appendix B

Computations and Sample Calculations

Sample Calculations

Vertical Effective Stress Calculation for IPET Strength Model

$$\sigma_v' = \gamma z$$

For marsh layer at an elevation of -5ft, $\gamma_{fill} = 109\,pcf$ and $\gamma_{marsh} = 80\,pcf$

$$\sigma_v' = \gamma_{fill}(17.5\,ft) + 5\,ft(\gamma_{marsh} - \gamma_{water})$$

$$\sigma_v' = 109\,pcf\,(17.5\,ft) + [5\,ft(80\,pcf - 62.4\,pcf)] = 1995.5\,psf$$

Undrained Shear Strength for IPET Strength Model

$$\frac{\left(\frac{S_u}{\sigma'_0}\right)_{OC}}{\left(\frac{S_u}{\sigma'_0}\right)_{NC}} = (OCR)^{0.8}$$

$$S_u = \left(\frac{S_u}{\sigma'_0}\right)_{NC} \sigma'_0\,(OCR)^{0.8}$$

$\left(\frac{S_u}{\sigma'_0}\right)_{NC}$ is assumed to be 0.24, then $S_u = 0.24\sigma'_0\,(OCR)^{0.8}$

For marsh layer at an elevation of -5ft and normally consolidated conditions:

$$S_u = 0.24(1995.5\,psf)(1)^{0.8} = 478.92\,psf$$

OCR Calculation

$$OCR = \frac{p_p}{\sigma'_0}$$

For a $p_p = 2394.6\,psf$:

$$OCR = \frac{2394.6\,psf}{1995.5\,psf} = 1.2$$

Appendix C

SLIDE5.0 Figures

SLIDE5.0 Figures: East Bank

IPET Strength Model (OCR=1)

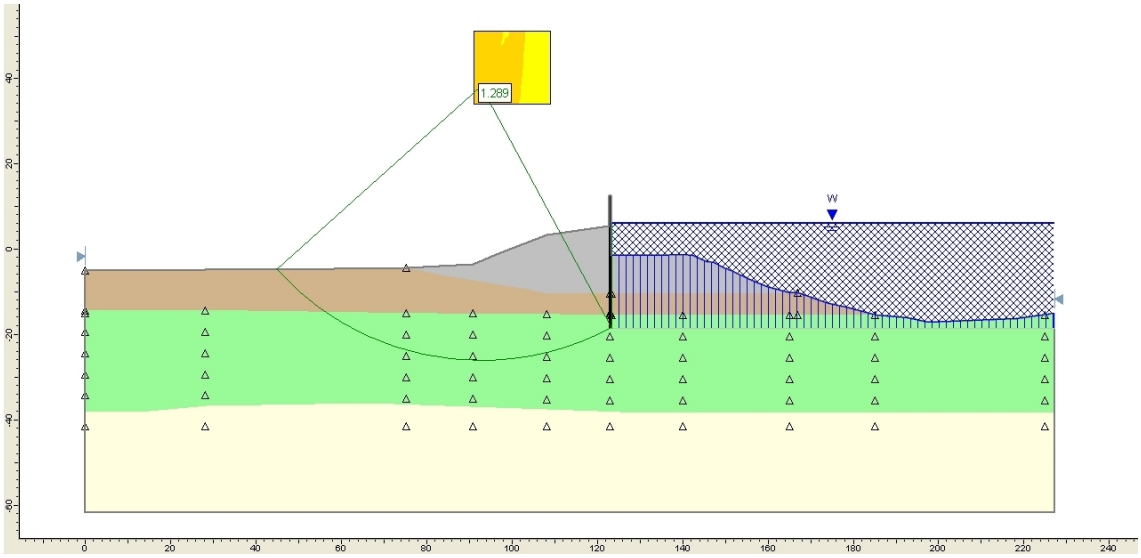

Figure C-1: Factor of safety for IPET Strength Model (OCR=1) at CWL=6ft

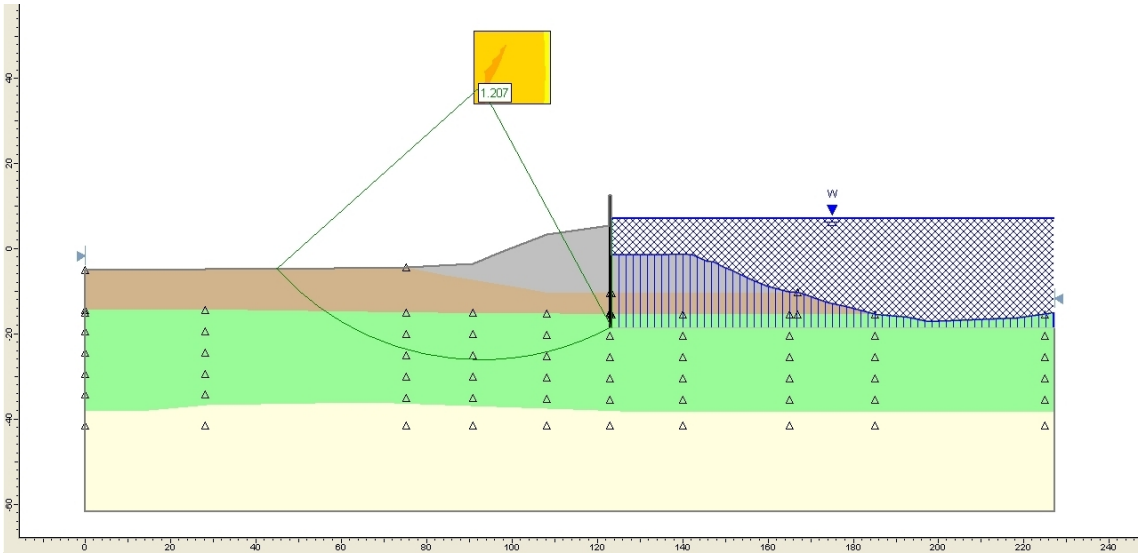

Figure C-2: Factor of safety for IPET Strength Model (OCR=1) at CWL=7ft

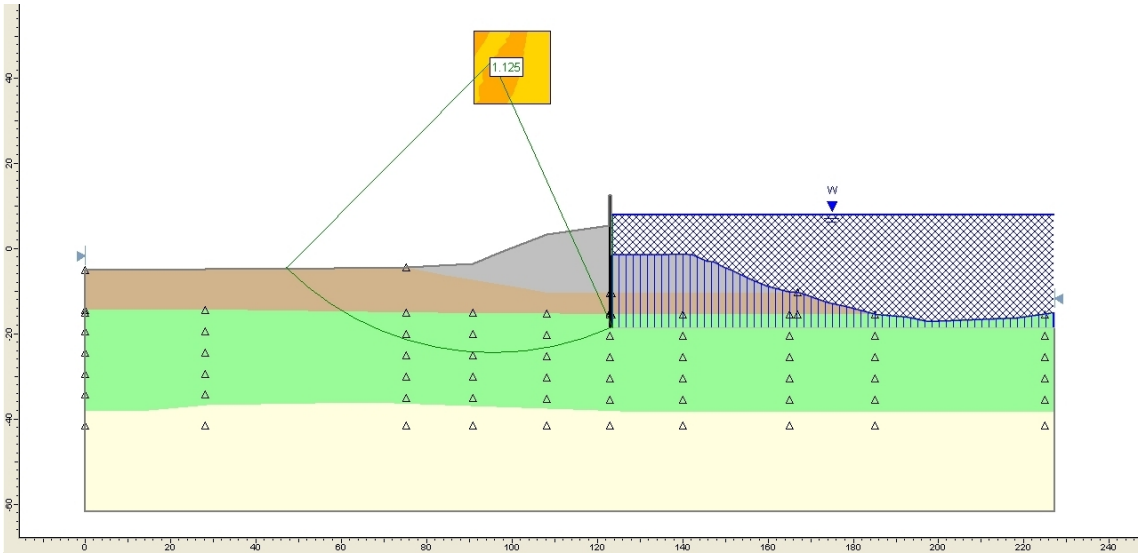

Figure C-3: Factor of safety for IPET Strength Model (OCR=1) at CWL=8ft

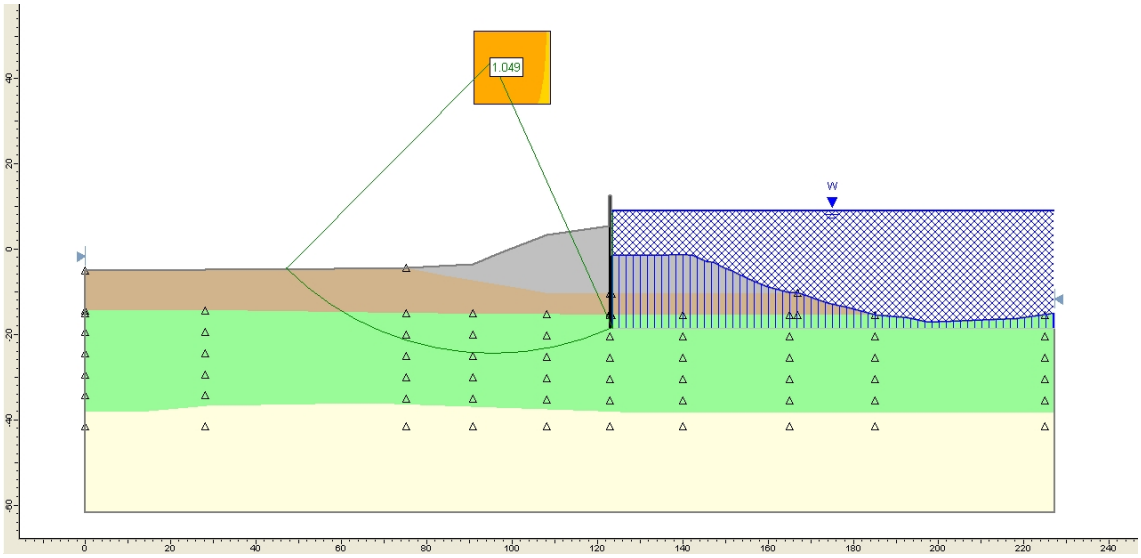

Figure C-4: Factor of safety for IPET Strength Model (OCR=1) at CWL=9ft

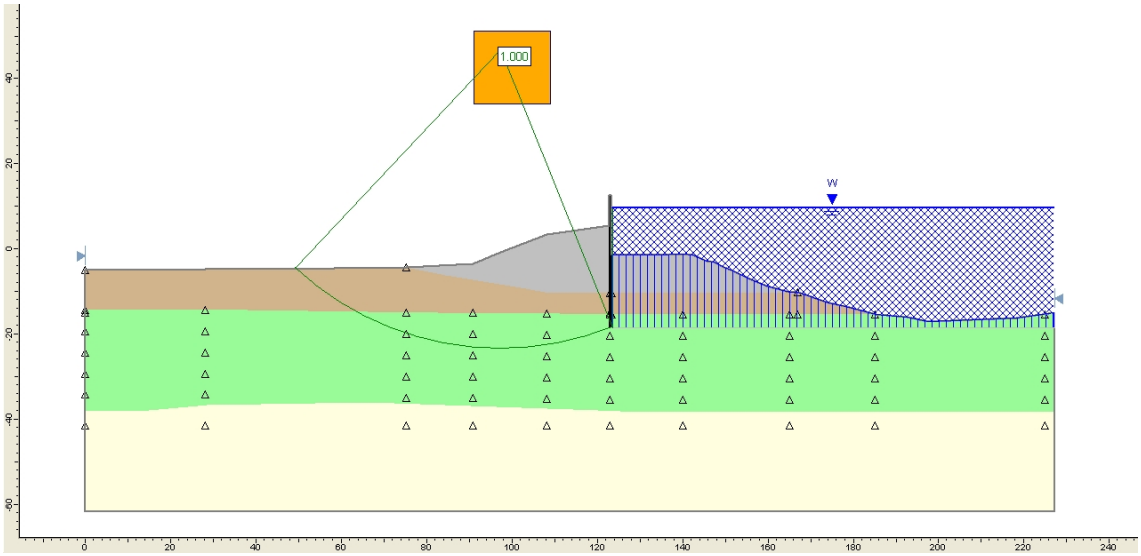

Figure C-5: Factor of safety for IPET Strength Model (OCR=1) at CWL=9.67ft

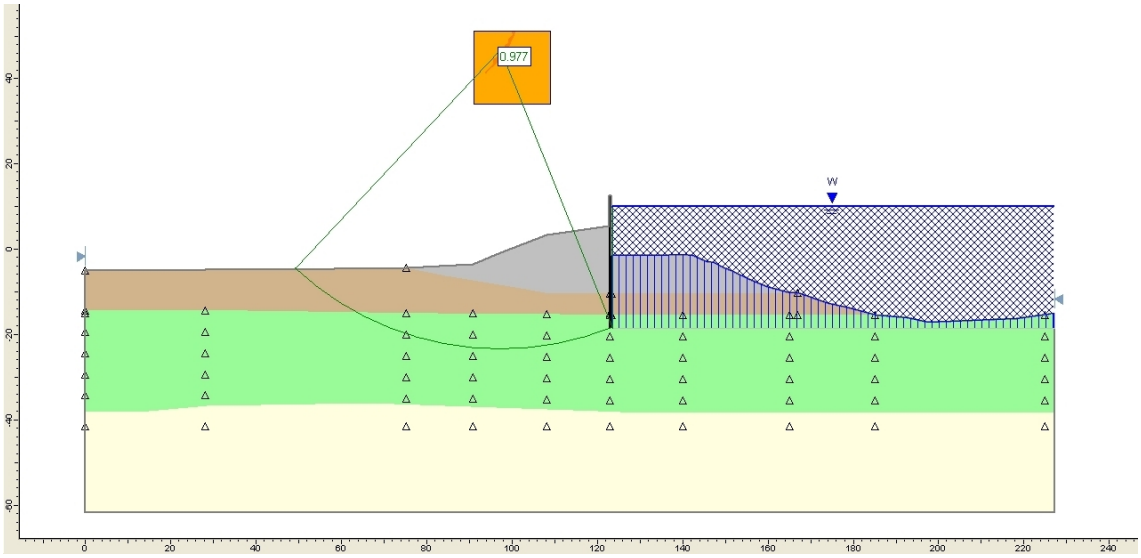

Figure C-6: Factor of safety for IPET Strength Model (OCR=1) at CWL=10ft

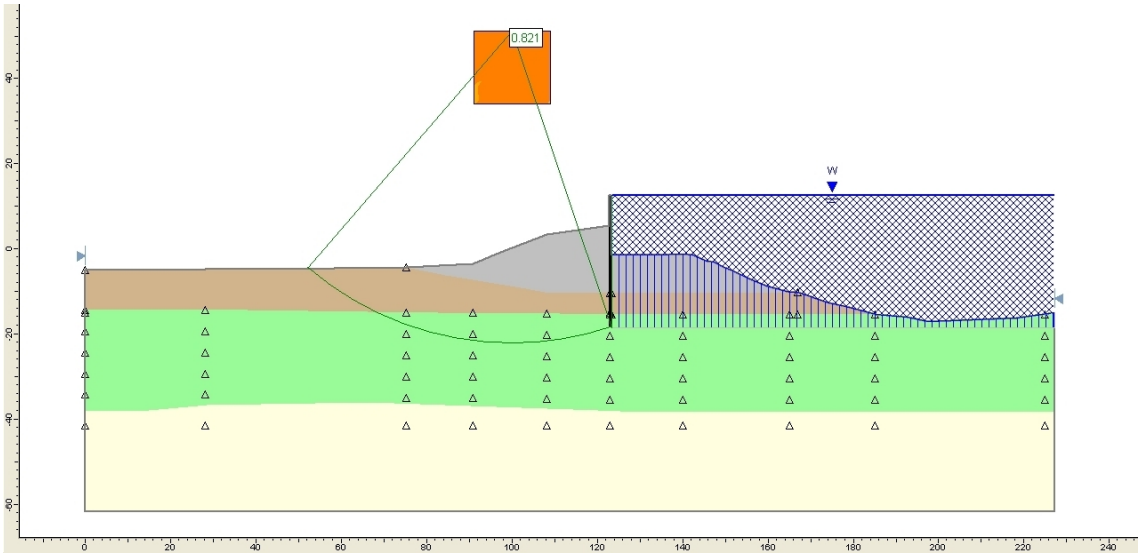

Figure C-7: Factor of safety for IPET Strength Model (OCR=1) at CWL=12.5ft

IPET Strength Model (OCR=1 to 1.2)

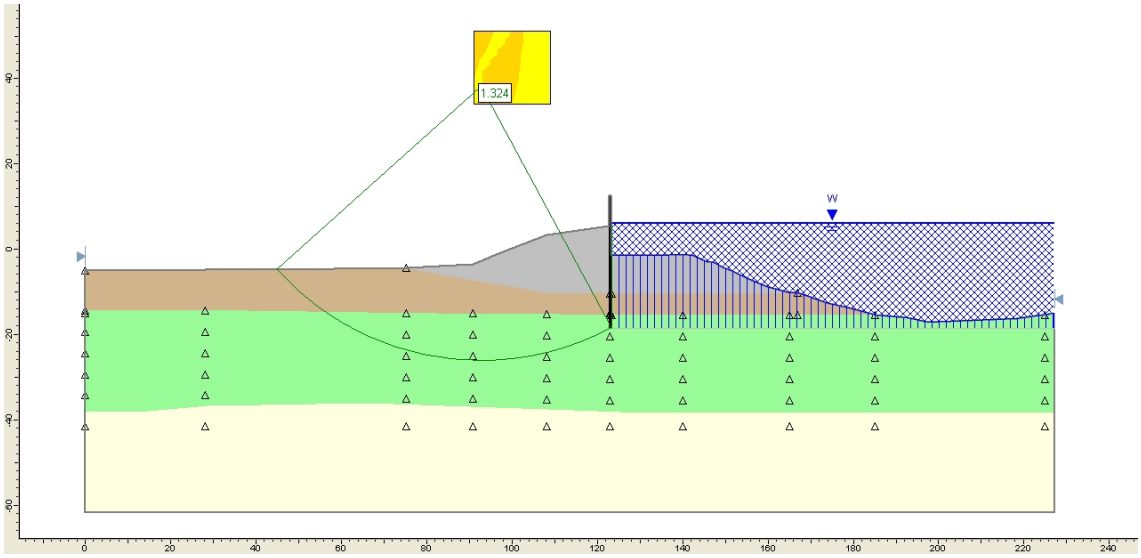

Figure C-8: Factor of safety for IPET Strength Model (OCR=1 to 1.2) at CWL=6ft

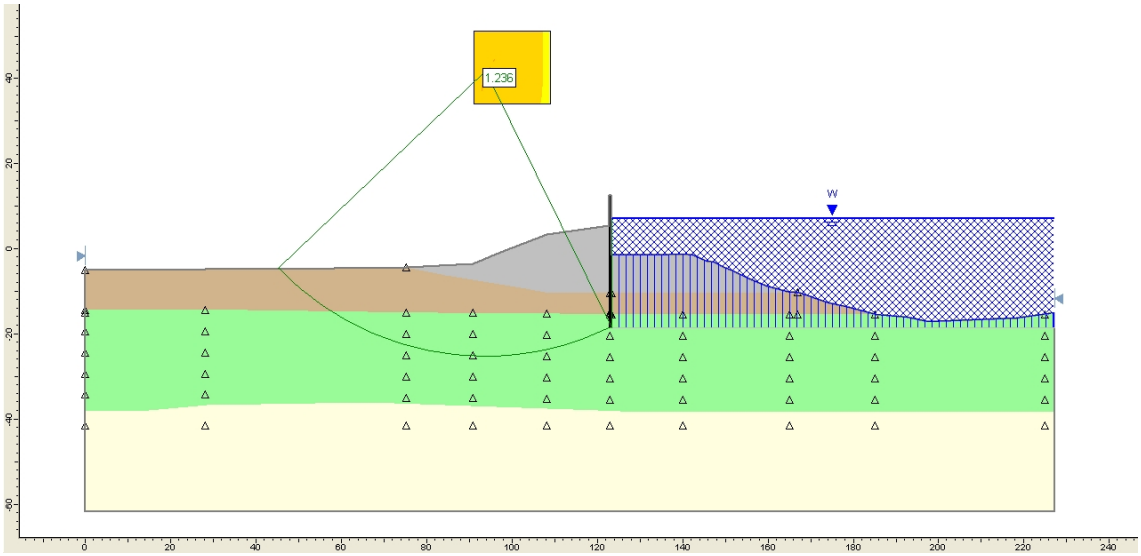

Figure C-9: Factor of safety for IPET Strength Model (OCR=1 to 1.2) at CWL=7ft

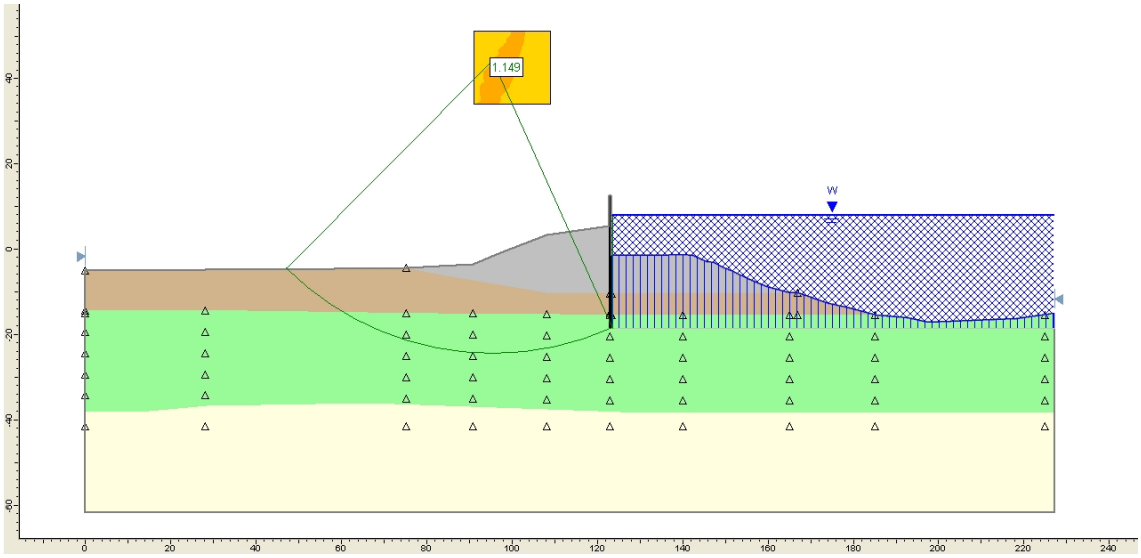

Figure C-10: Factor of safety for IPET Strength Model (OCR=1 to 1.2) at CWL=8ft

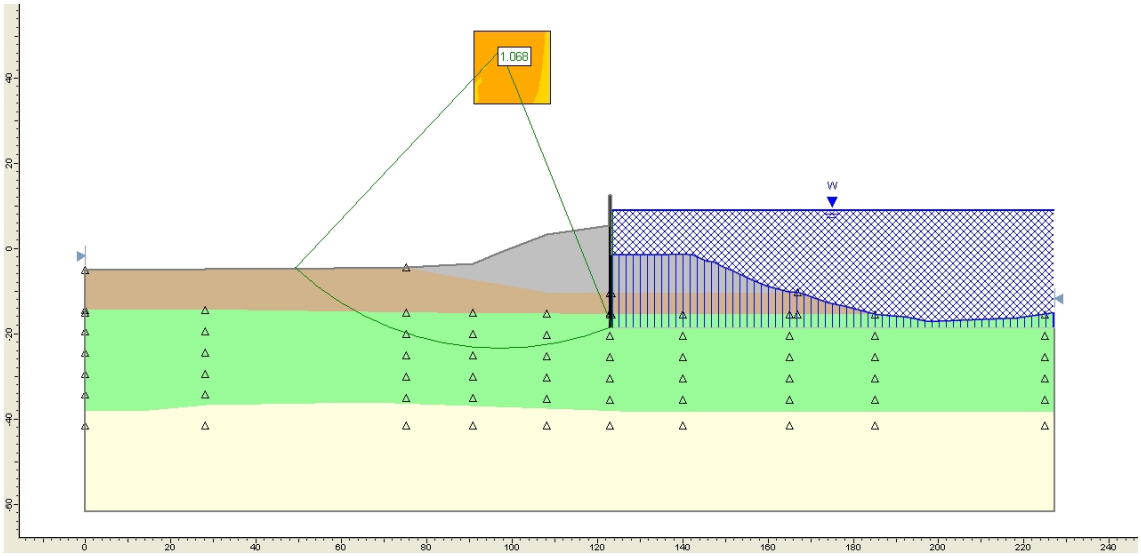

Figure C-11: Factor of safety for IPET Strength Model (OCR=1 to 1.2) at CWL=9ft

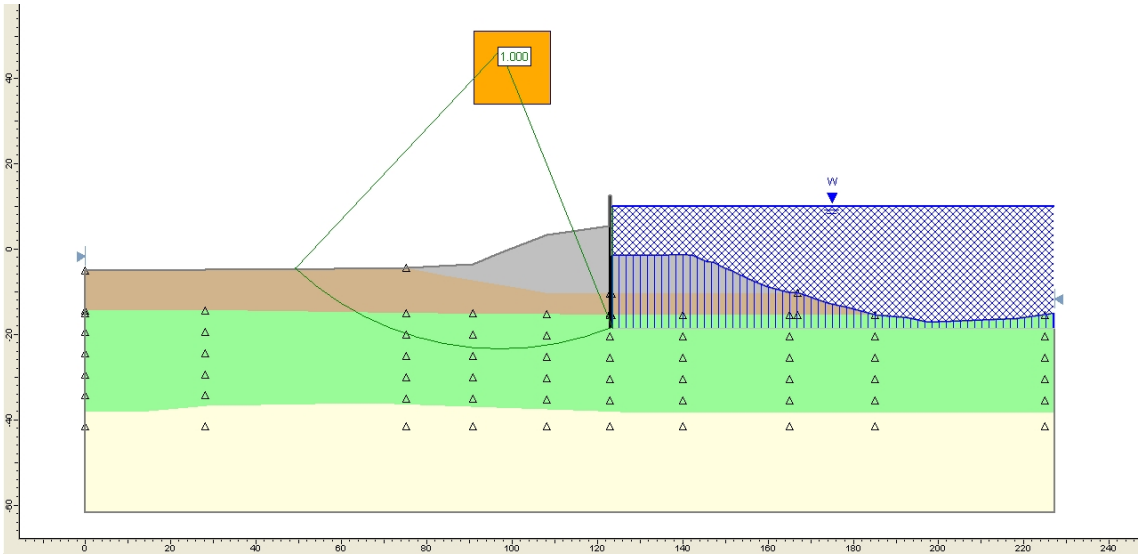

Figure C-12: Factor of safety for IPET Strength Model (OCR=1 to 1.2) at CWL=9.92ft

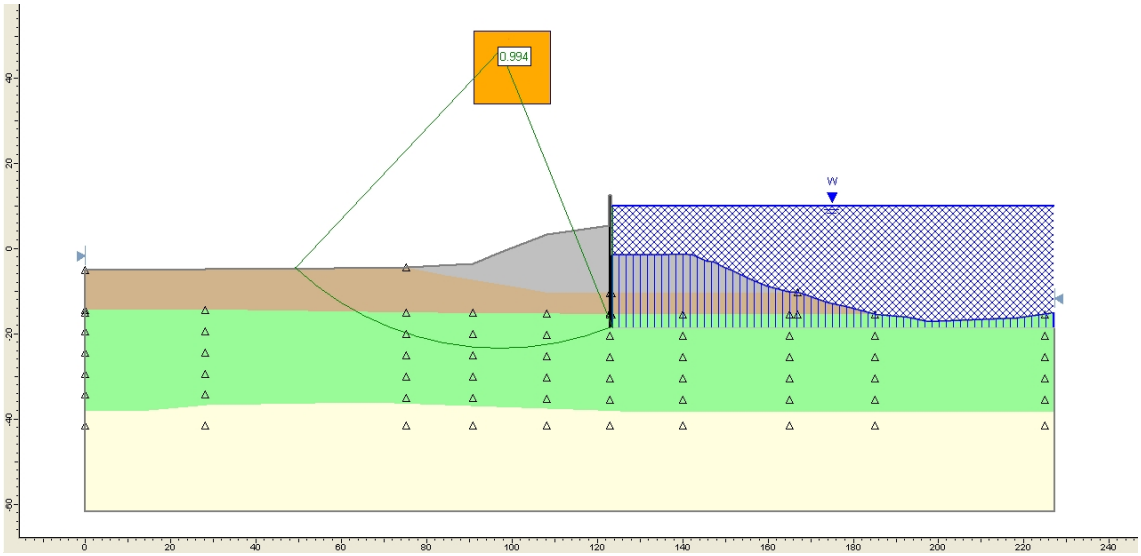

Figure C-13: Factor of safety for IPET Strength Model (OCR=1 to 1.2) at CWL=10ft

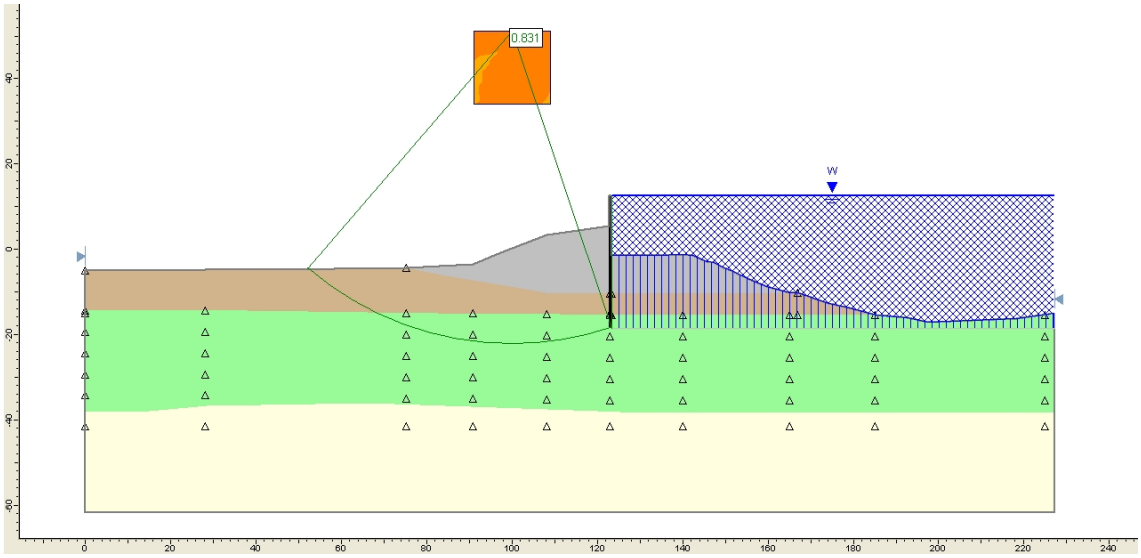

Figure C-14: Factor of safety for IPET Strength Model (OCR=1 to 1.2) at CWL=12.5ft

IPET Strength Model (OCR calculated)

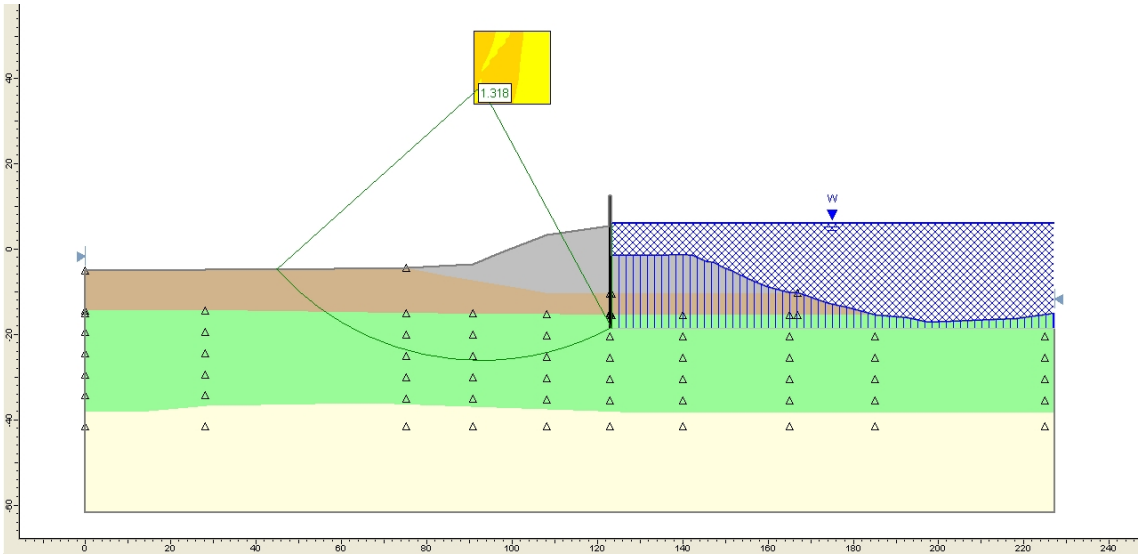

Figure C-15: Factor of safety for IPET Strength Model (OCR calculated) at CWL=6ft

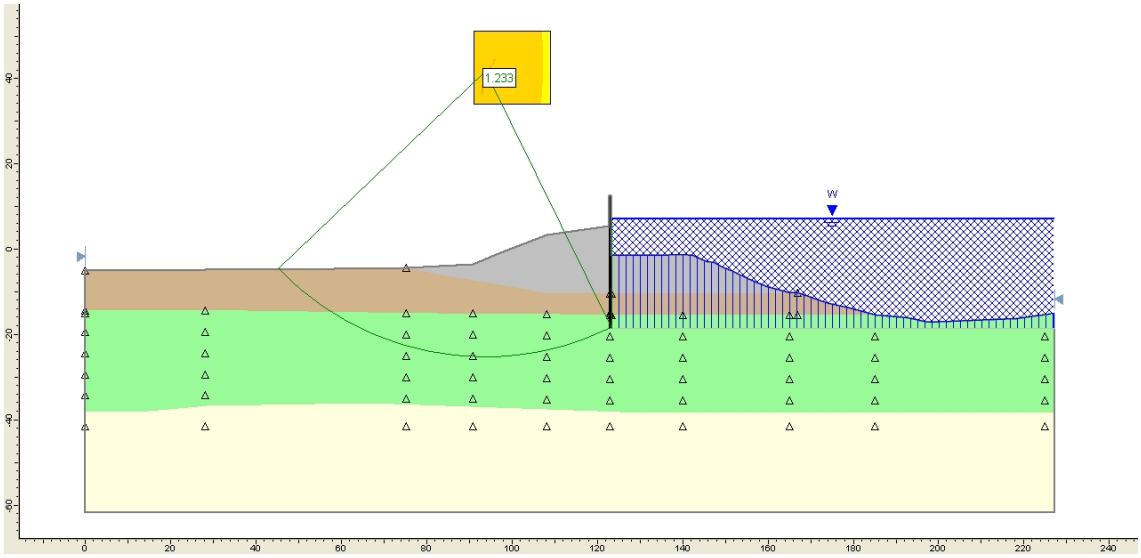

Figure C-16: Factor of safety for IPET Strength Model (OCR calculated) at CWL=7ft

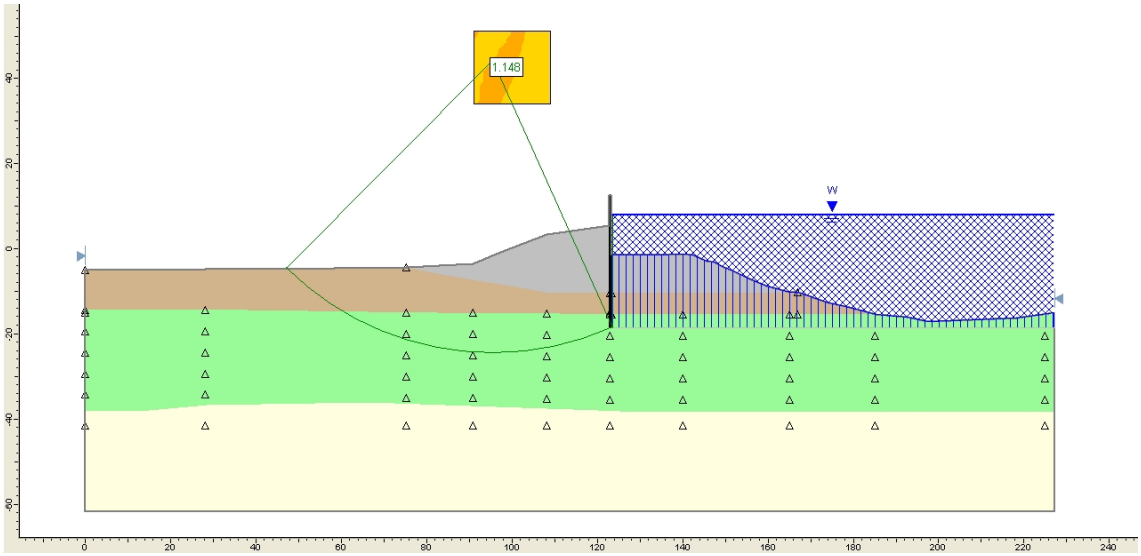

Figure C-17: Factor of safety for IPET Strength Model (OCR calculated) at CWL=8ft

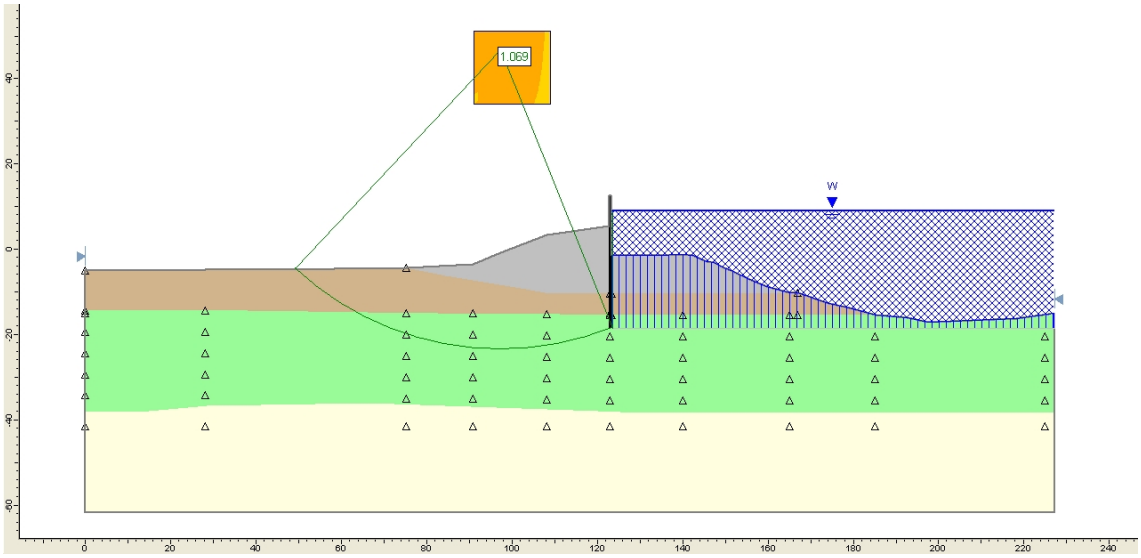

Figure C-18: Factor of safety for IPET Strength Model (OCR calculated) at CWL=9ft

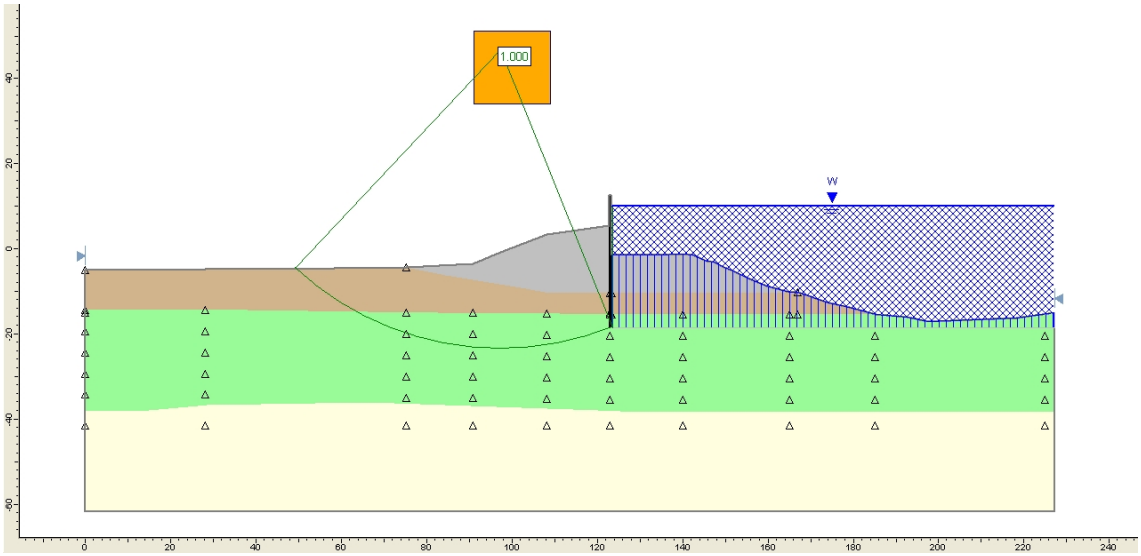

Figure C-19: Factor of safety for IPET Strength Model (OCR calculated) at CWL=9.92ft

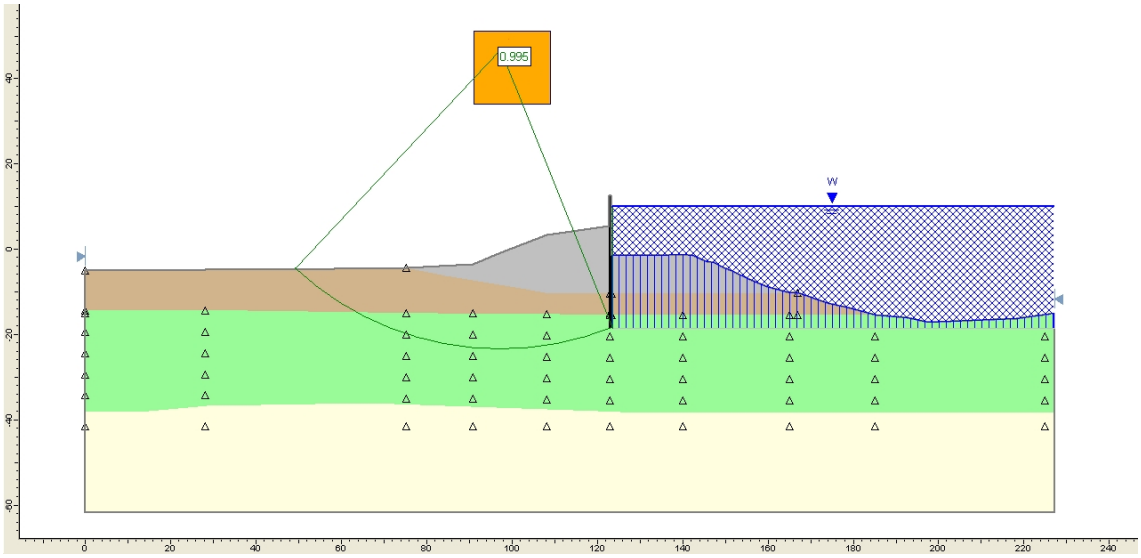

Figure C-20: Factor of safety for IPET Strength Model (OCR calculated) at CWL=10ft

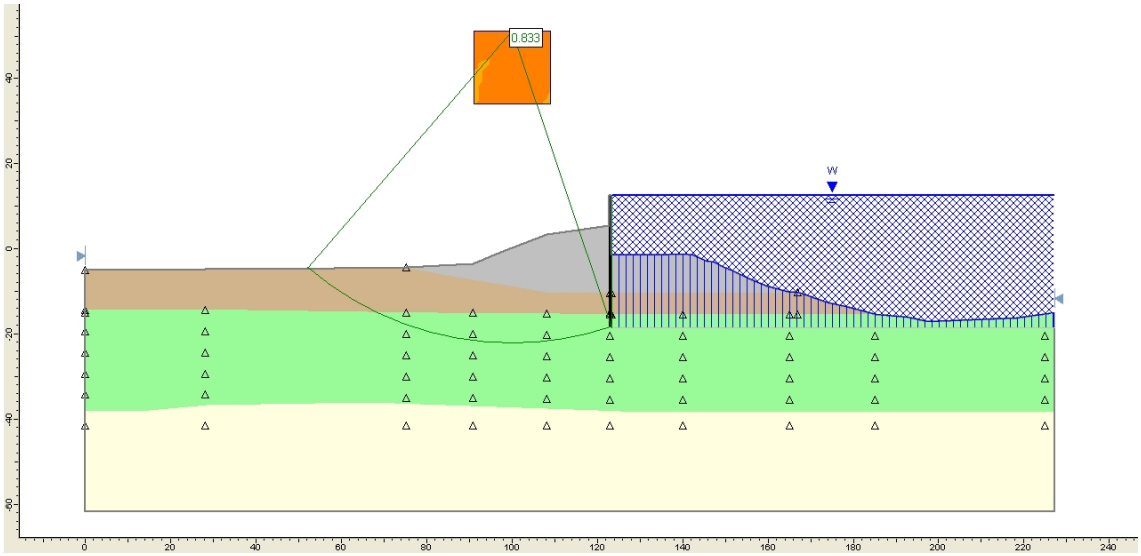

Figure C-21: Factor of safety for IPET Strength Model (OCR=1 to 1.2) at CWL=12.5ft

ESD w SWT (OCR=1)

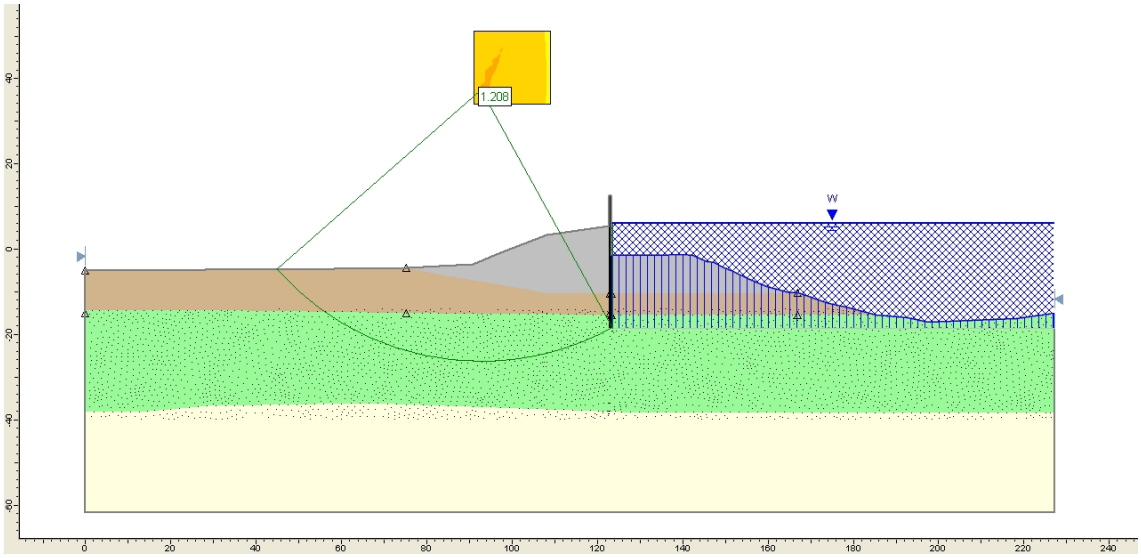

Figure C-22: Factor of safety for ESD w SWT (OCR=1) at CWL=6ft

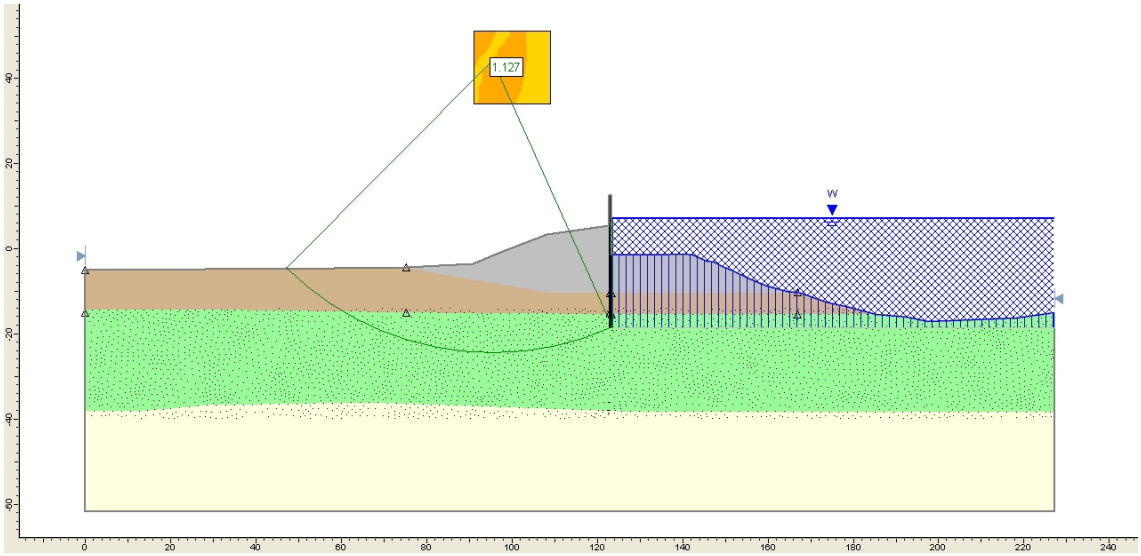

Figure C-23: Factor of safety for ESD w SWT (OCR=1) at CWL=7ft

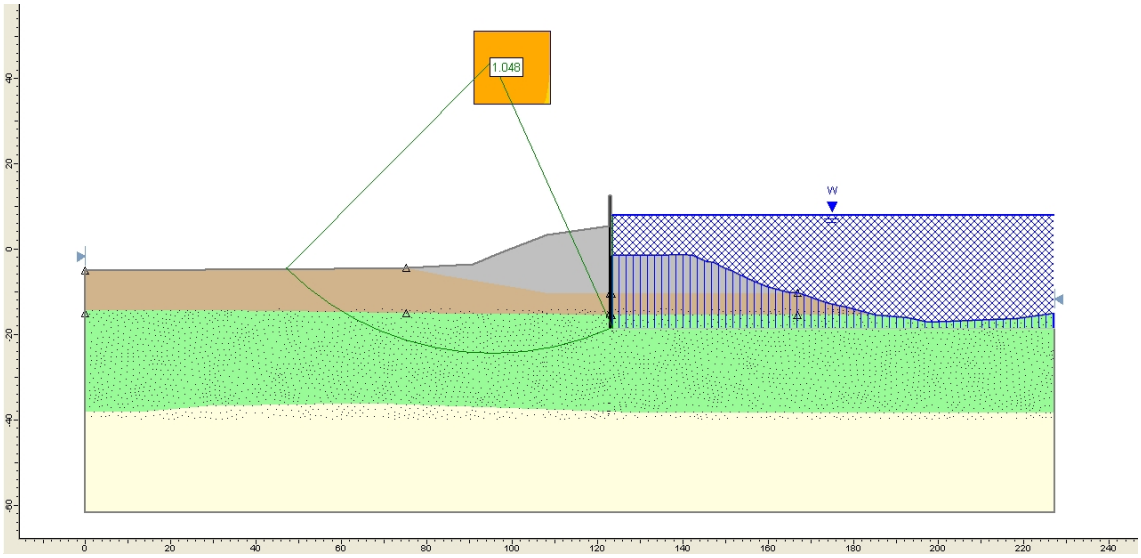

Figure C-24: Factor of safety for ESD w SWT (OCR=1) at CWL=8ft

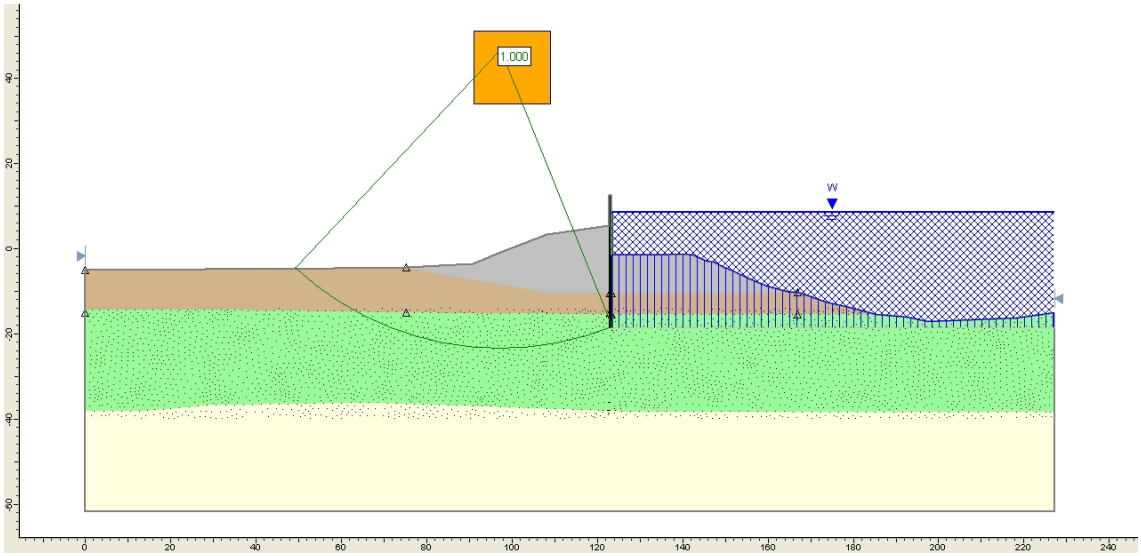

Figure C-25: Factor of safety for ESD w SWT (OCR=1) at CWL=8.65ft

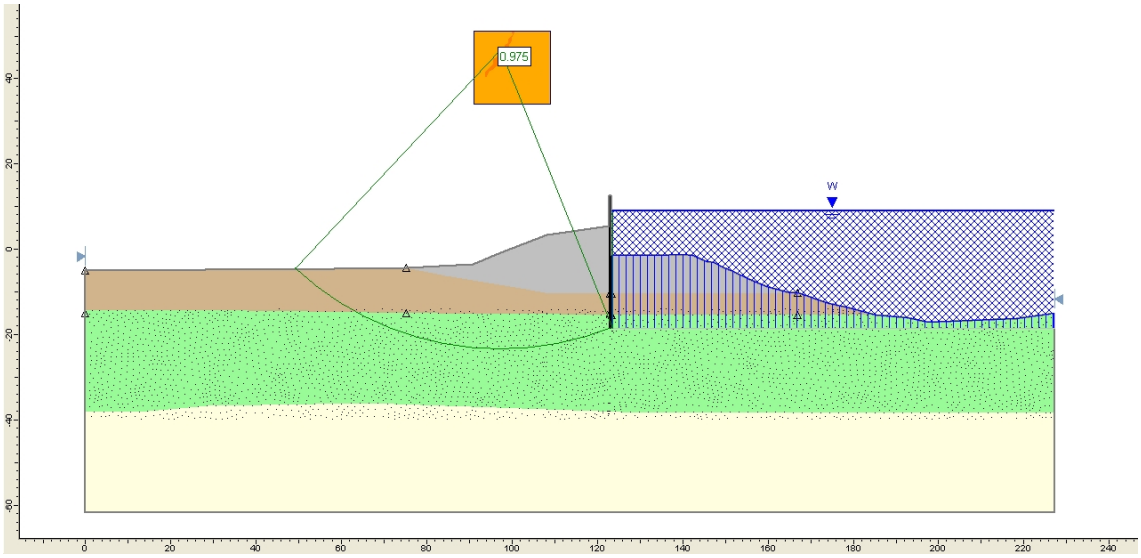

Figure C-26: Factor of safety for ESD w SWT (OCR=1) at CWL=9ft

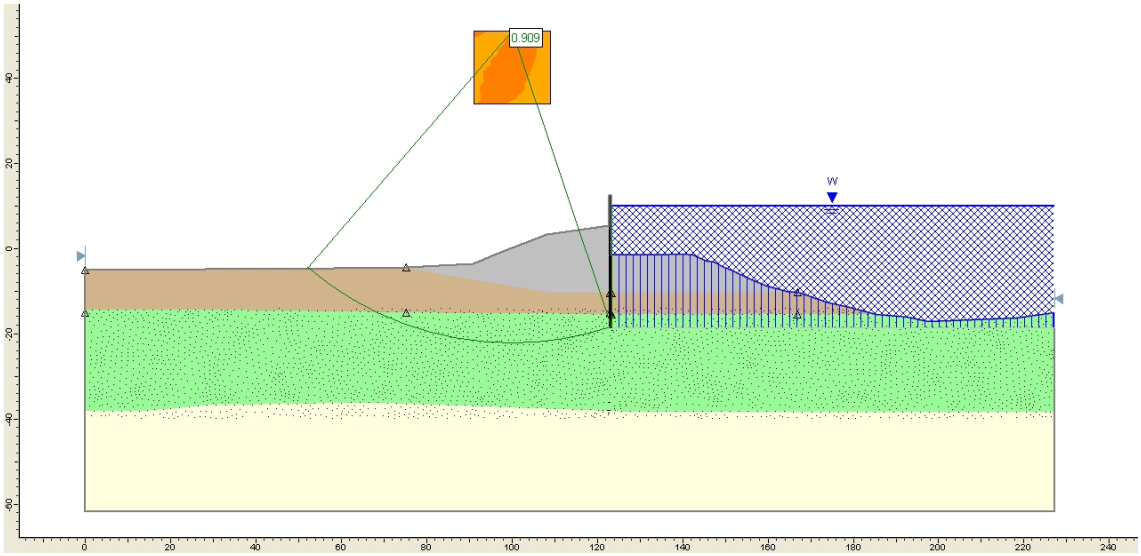

Figure C-27: Factor of safety for ESD w SWT (OCR=1) at CWL=10ft

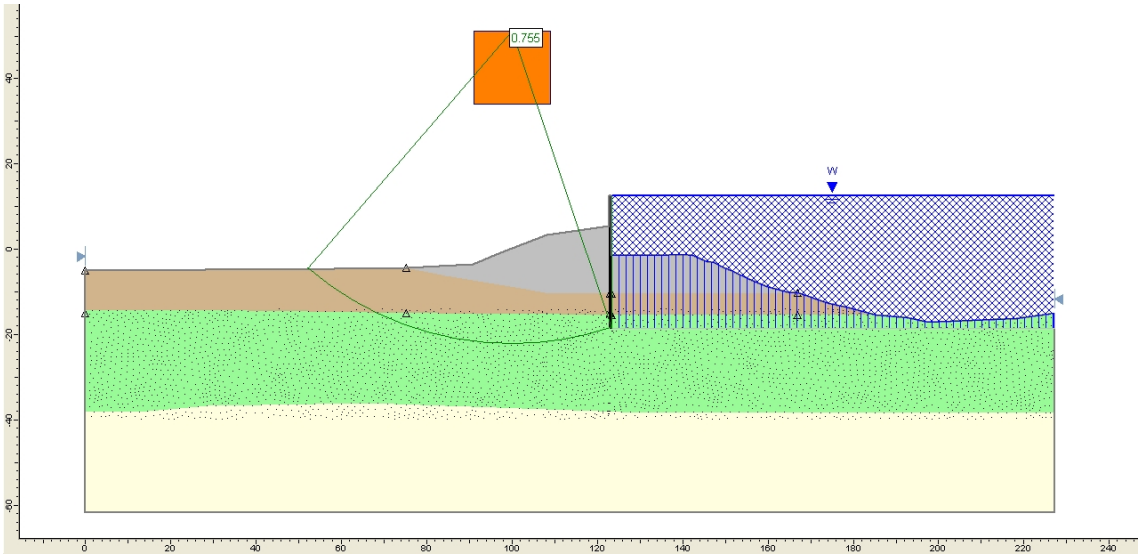

Figure C-28: Factor of safety for ESD w SWT (OCR=1) at CWL=12.5ft

ESD w SWT (OCR=1 to 1.2)

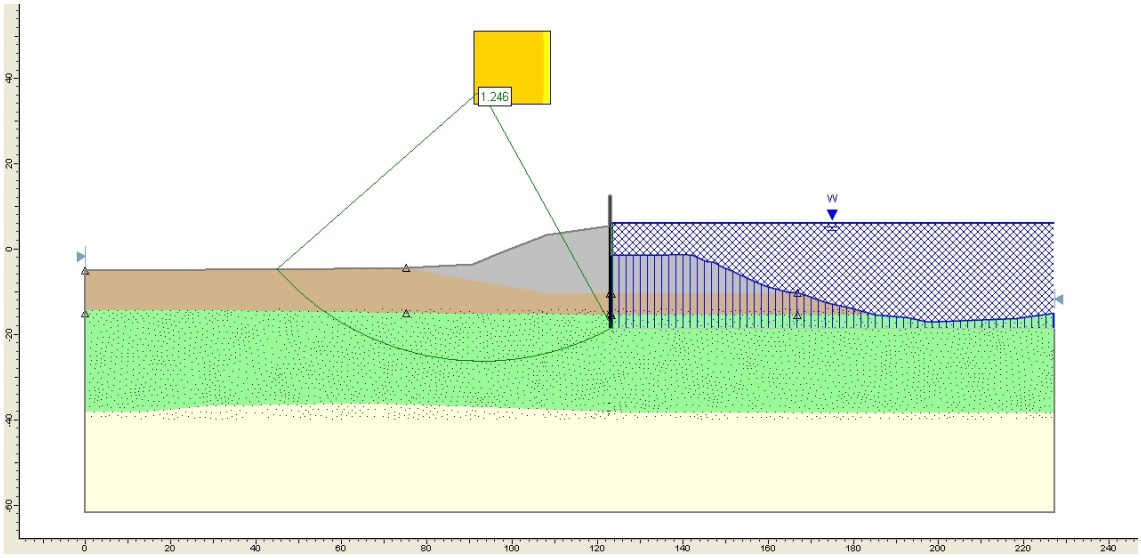

Figure C-29: Factor of safety for ESD w SWT (OCR=1 to 1.2) at CWL=6ft

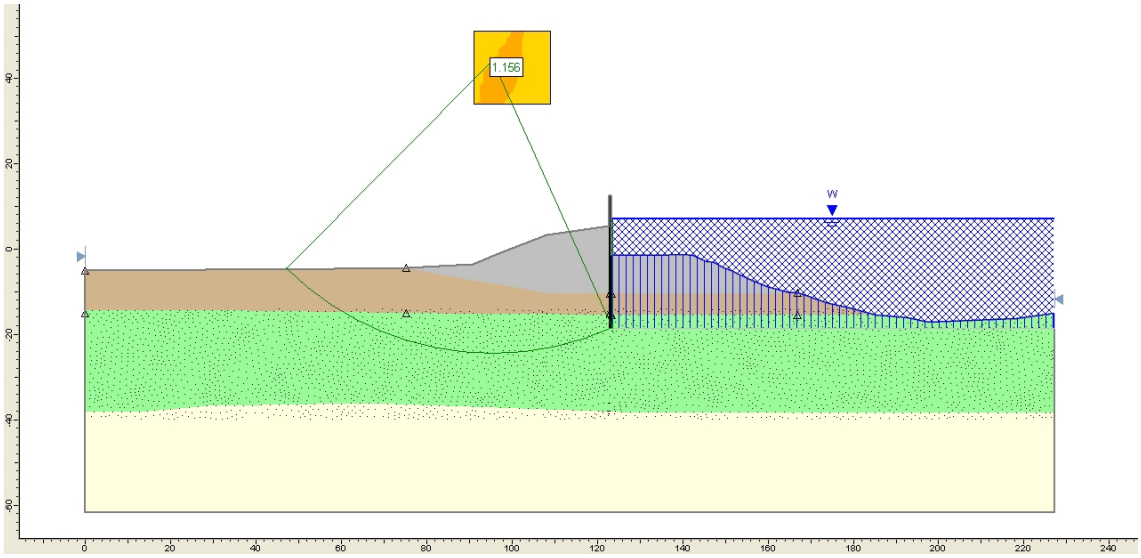

Figure C-30: Factor of safety for ESD w SWT (OCR=1 to 1.2) at CWL=7ft

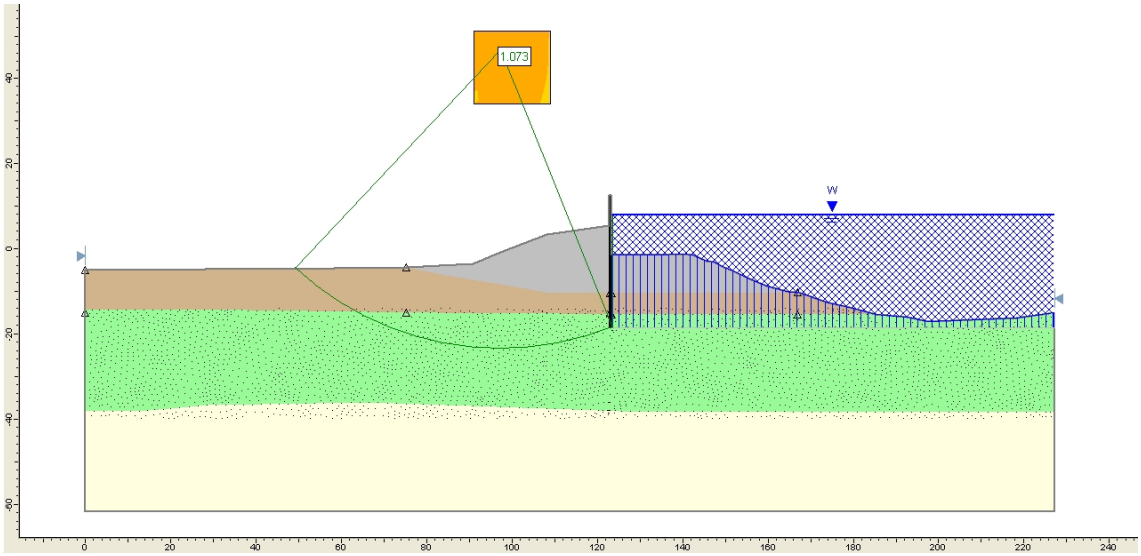

Figure C-31: Factor of safety for ESD w SWT (OCR=1 to 1.2) at CWL=8ft

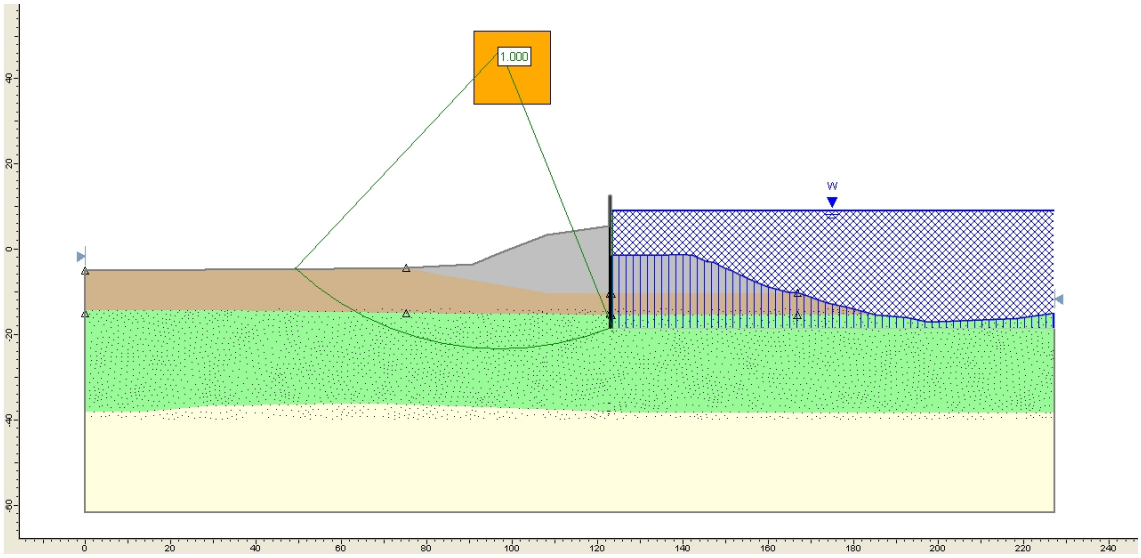

Figure C-32: Factor of safety for ESD w SWT (OCR=1 to 1.2) at CWL=8.94ft

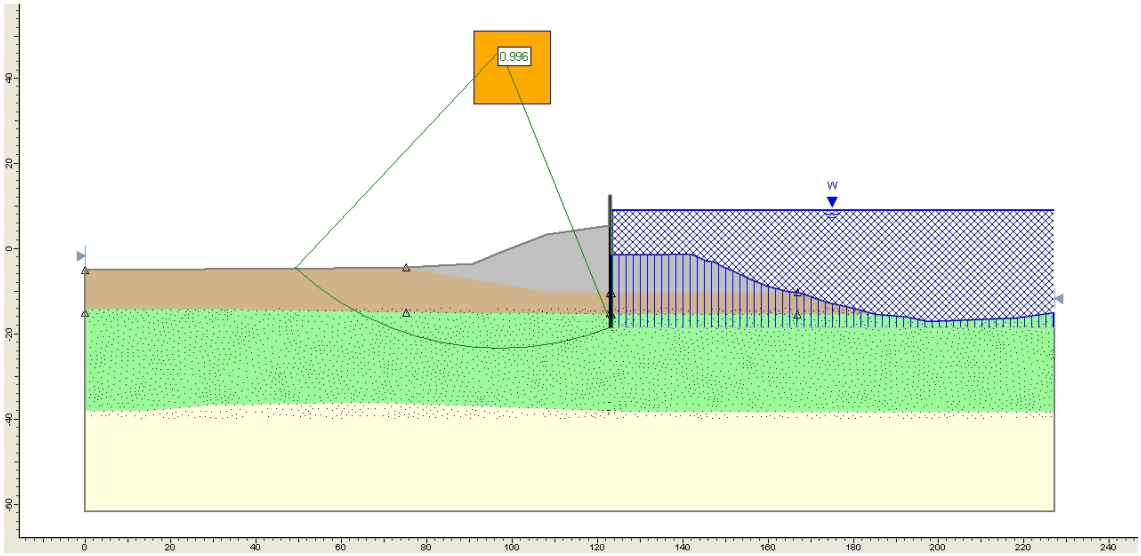

Figure C-33: Factor of safety for ESD w SWT (OCR=1 to 1.2) at CWL=9ft

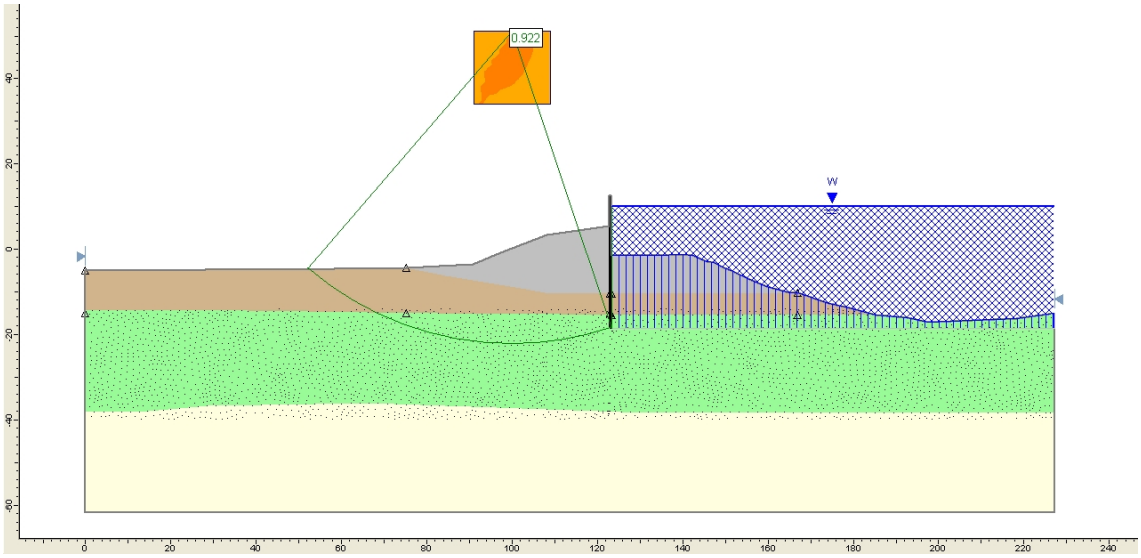

Figure C-34: Factor of safety for ESD w SWT (OCR=1 to 1.2) at CWL=10ft

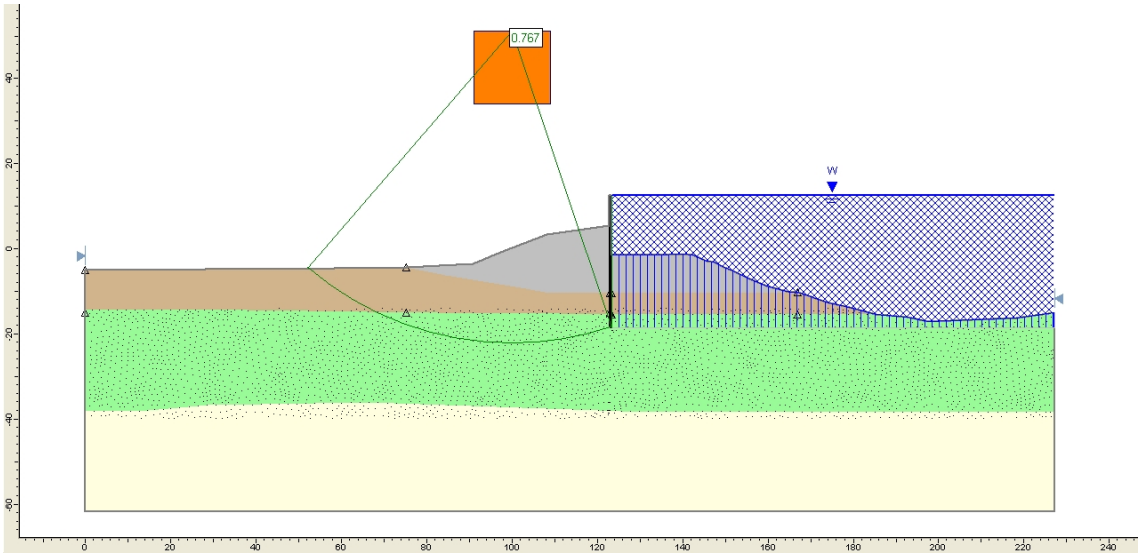

Figure C-35: Factor of safety for ESD w SWT (OCR=1 to 1.2) at CWL=12.5ft

ESD w SWT (OCR calculated)

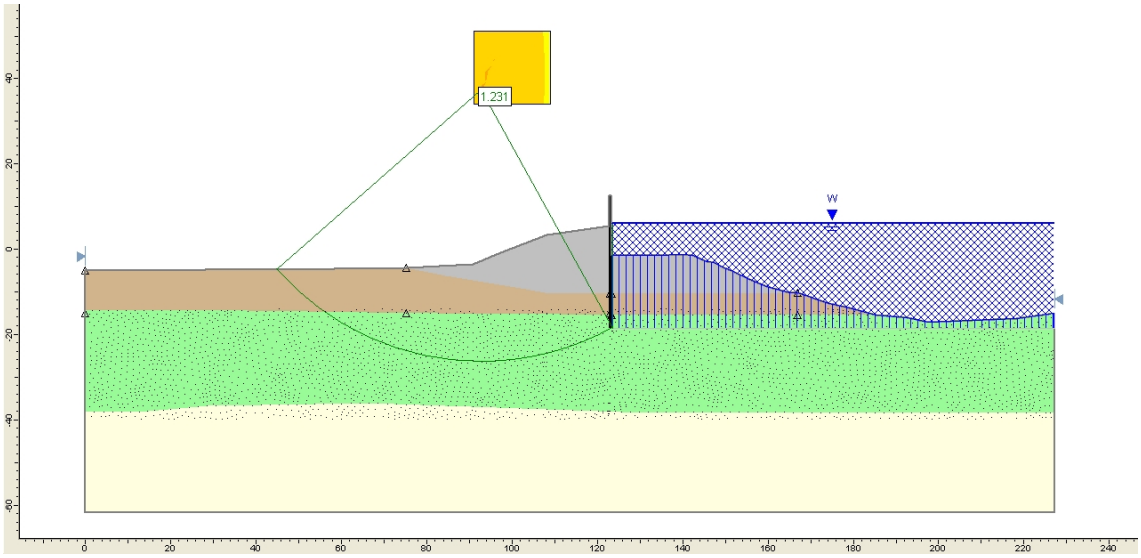

Figure C-36: Factor of safety for ESD w SWT (OCR calculated) at CWL=6ft

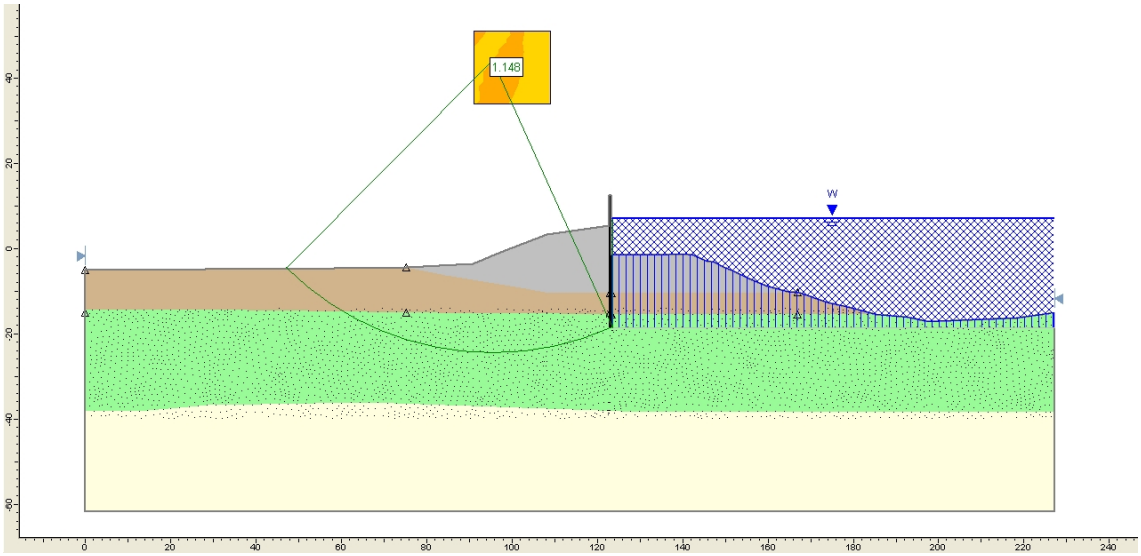

Figure C-37: Factor of safety for ESD w SWT (OCR calculated) at CWL=7ft

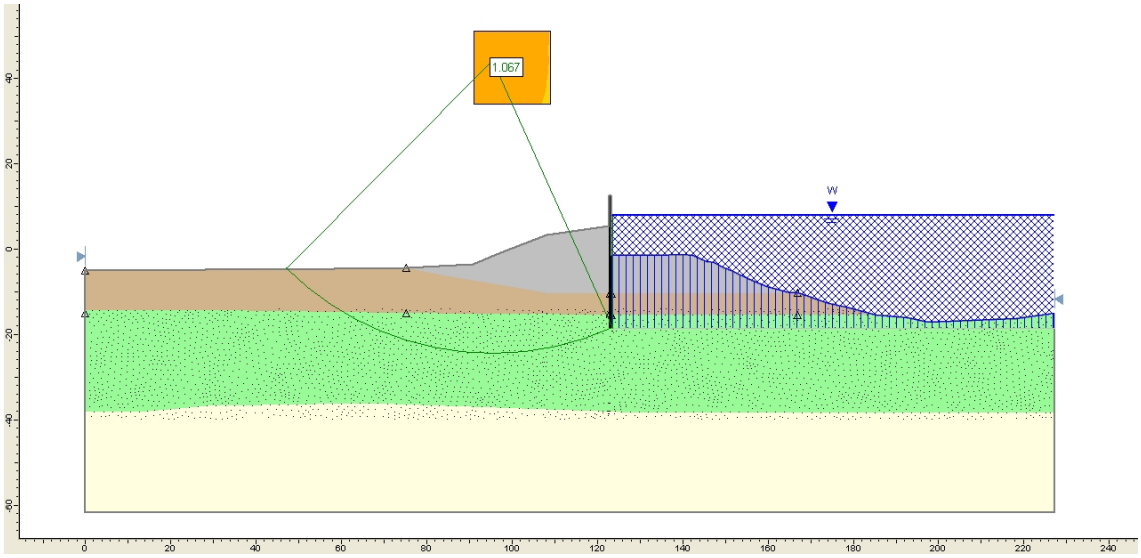

Figure C-38: Factor of safety for ESD w SWT (OCR calculated) at CWL=8ft

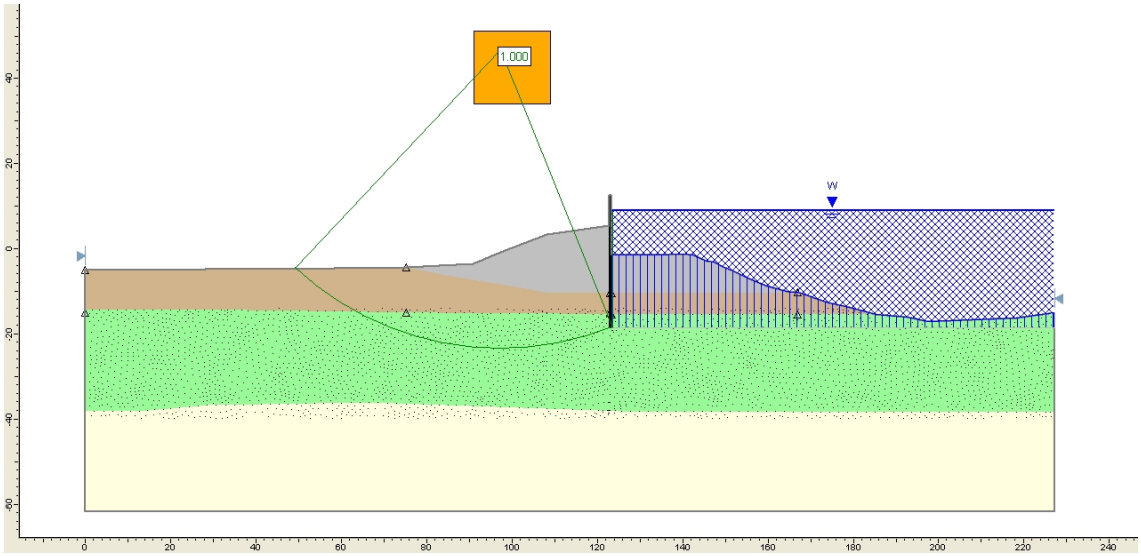

Figure C-39: Factor of safety for ESD w SWT (OCR calculated) at CWL=8.87ft

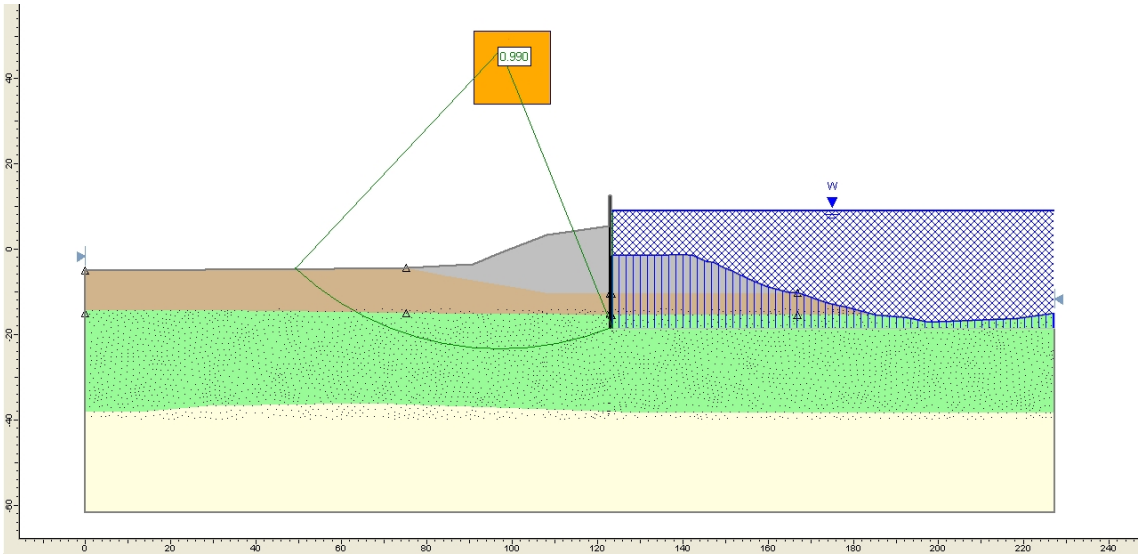

Figure C-40: Factor of safety for ESD w SWT (OCR calculated) at CWL=9ft

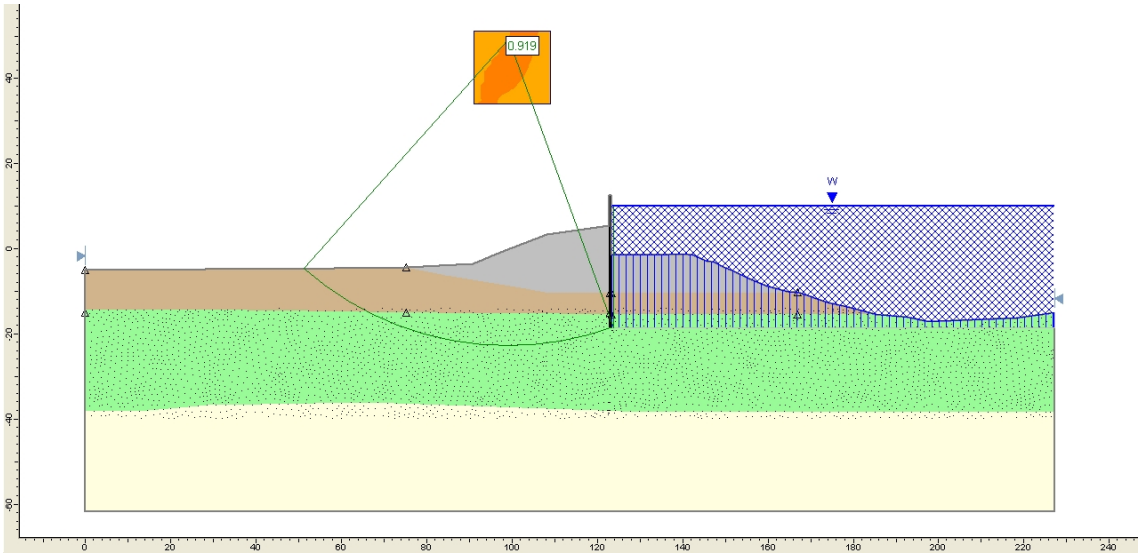

Figure C-41: Factor of safety for ESD w SWT (OCR calculated) at CWL=10ft

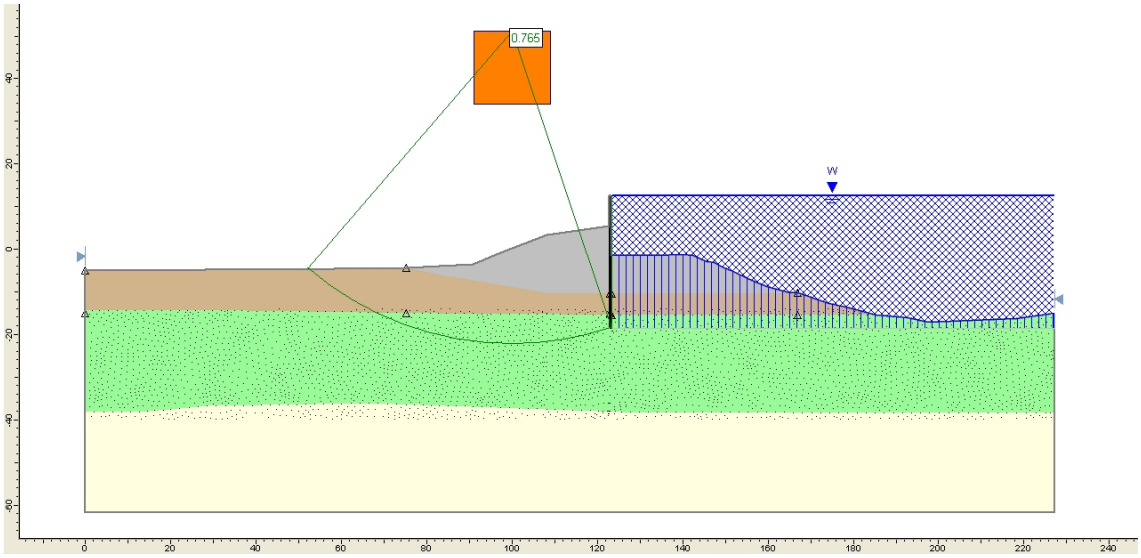

Figure C-42: Factor of safety for ESD w SWT (OCR calculated) at CWL=12.5ft

ESD w BC-5ft (OCR=1)

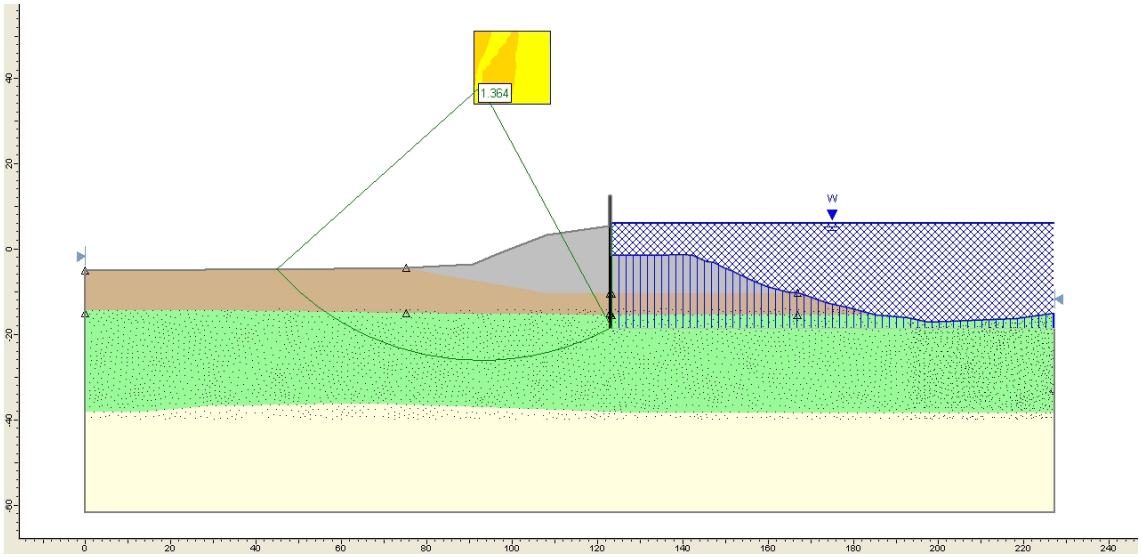

Figure C-43: Factor of safety for ESD w BC-5ft (OCR=1) at CWL=6ft

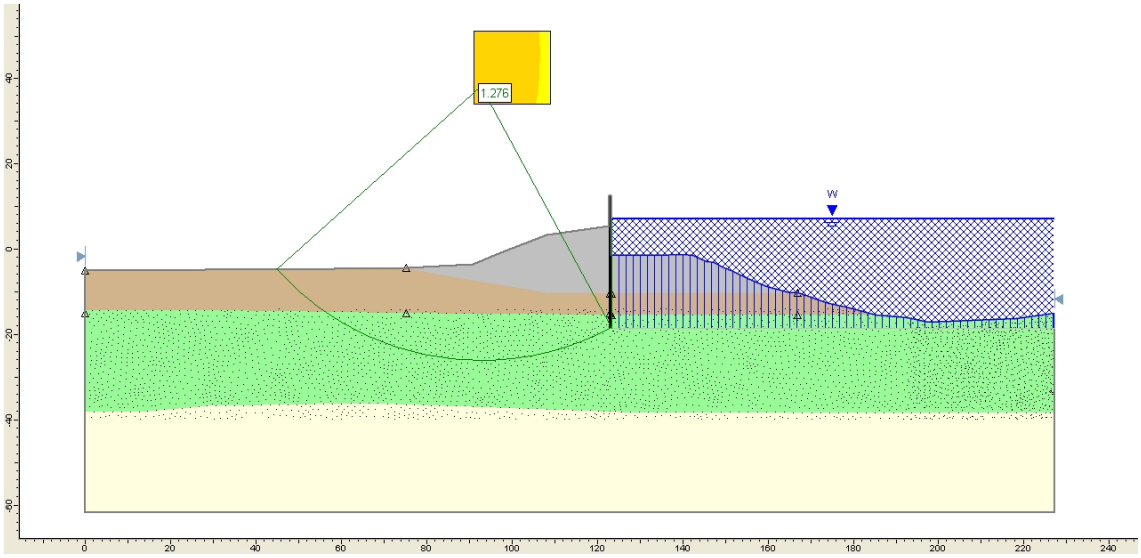

Figure C-44: Factor of safety for ESD w BC-5ft (OCR=1) at CWL=7ft

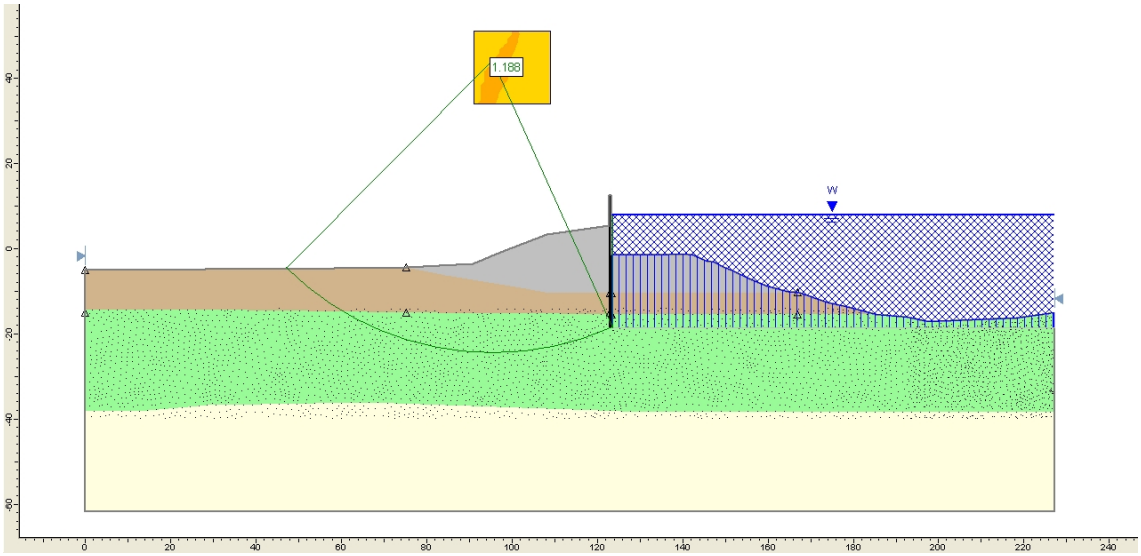

Figure C-45: Factor of safety for ESD w BC-5ft (OCR=1) at CWL=8ft

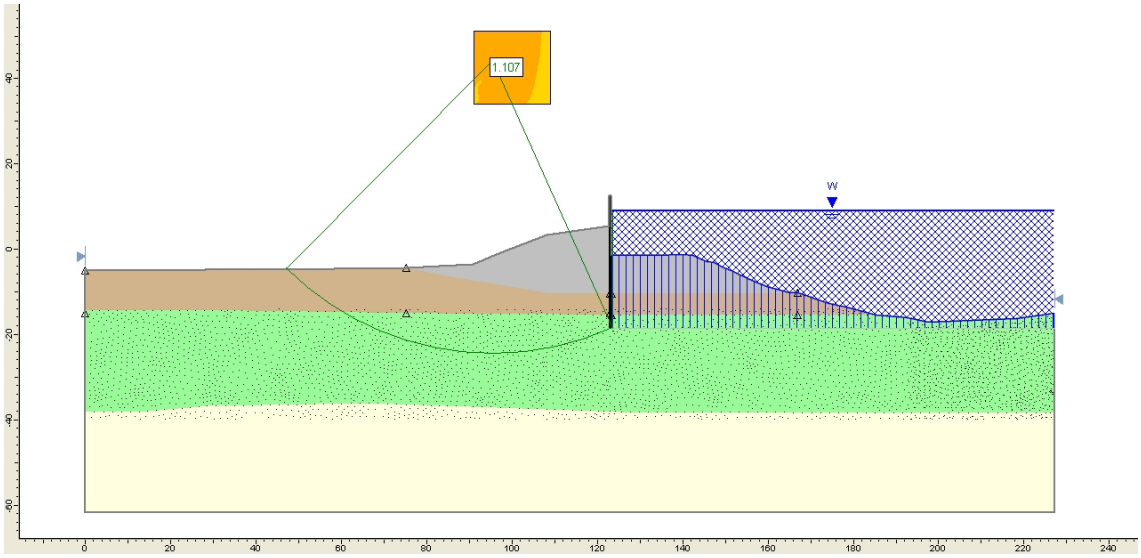

Figure C-46: Factor of safety for ESD w BC-5ft (OCR=1) at CWL=9ft

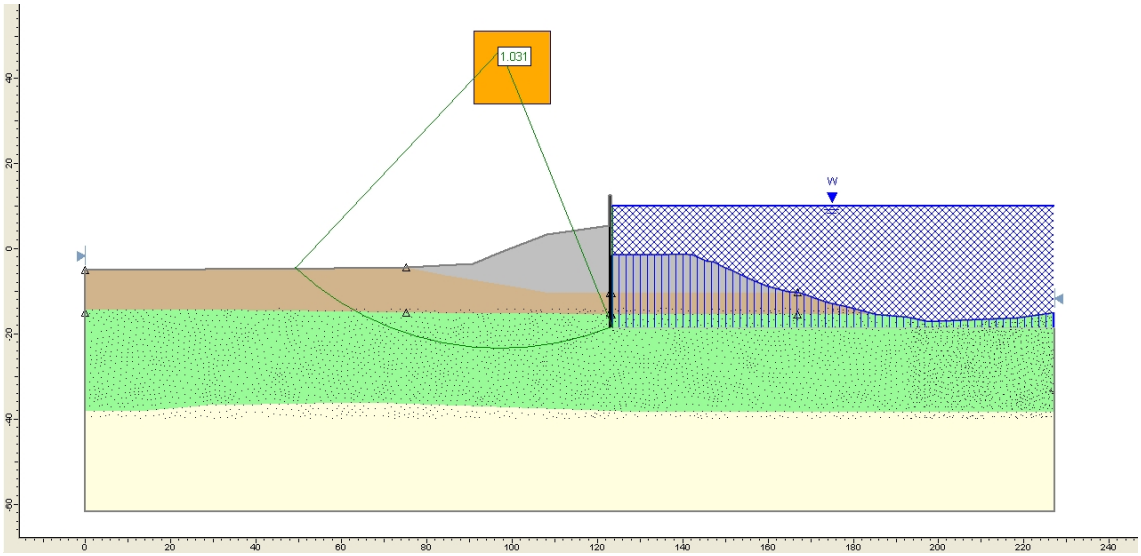

Figure C-47: Factor of safety for ESD w BC-5ft (OCR=1) at CWL=10ft

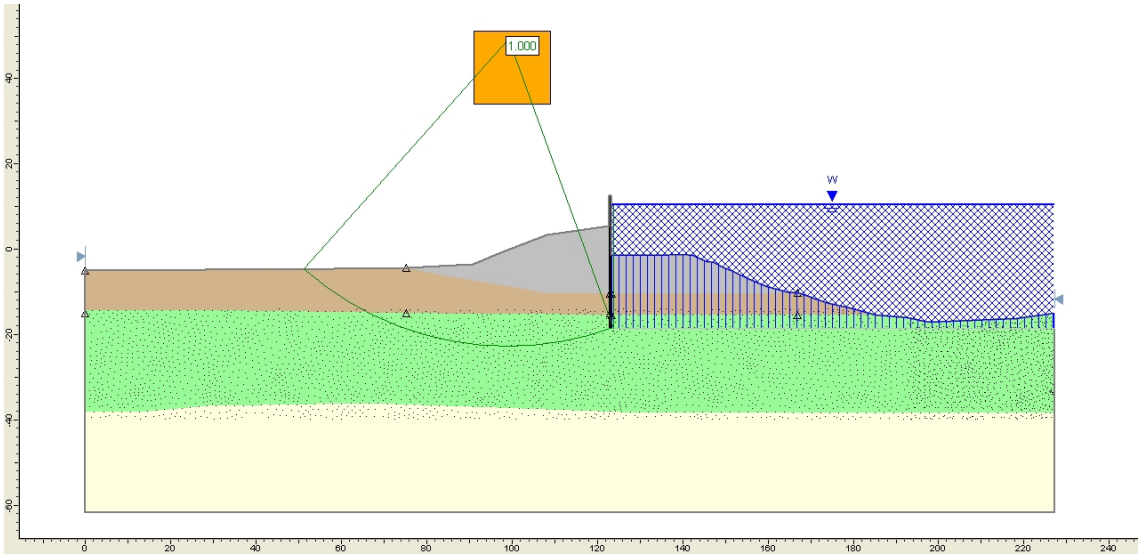

Figure C-48: Factor of safety for ESD w BC-5ft (OCR=1) at CWL=10.44ft

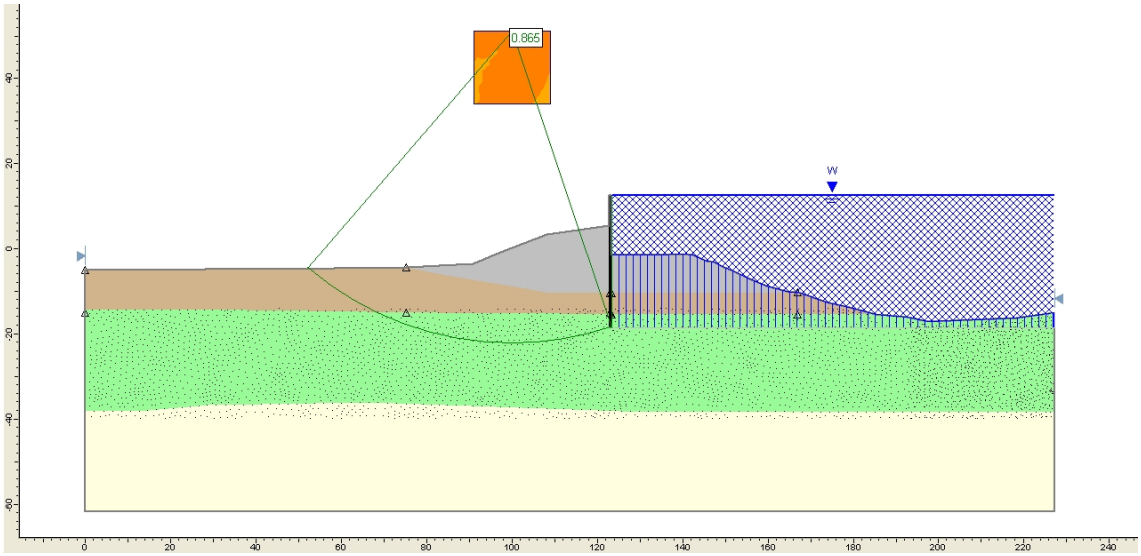

Figure C-49: Factor of safety for ESD w BC-5ft (OCR=1) at CWL=12.5ft

ESD w BC-5ft (OCR=1 to 1.2)

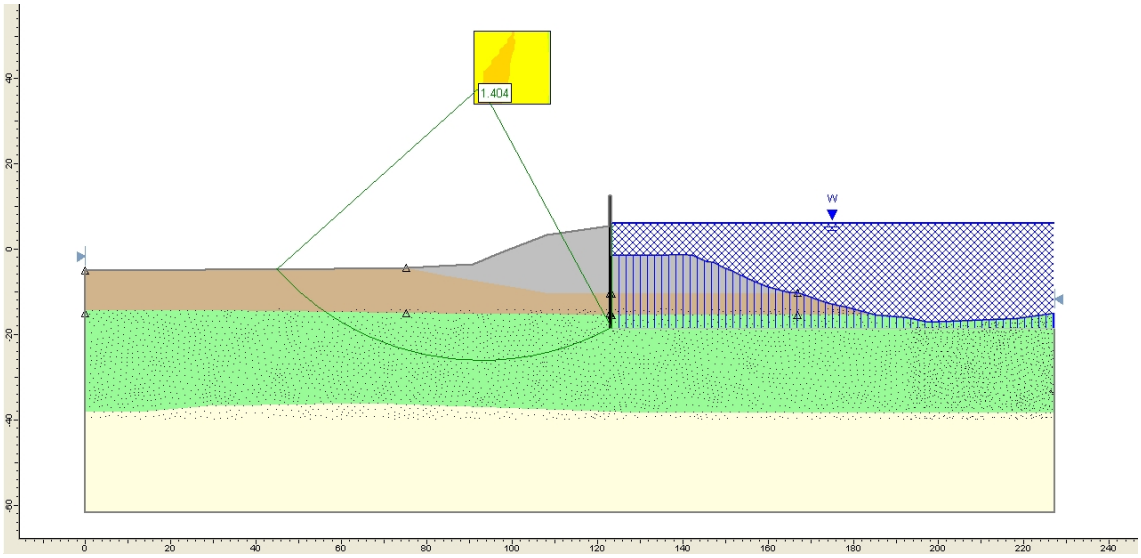

Figure C-50: Factor of safety for ESD w BC-5ft (OCR=1 to 1.2) at CWL=6ft

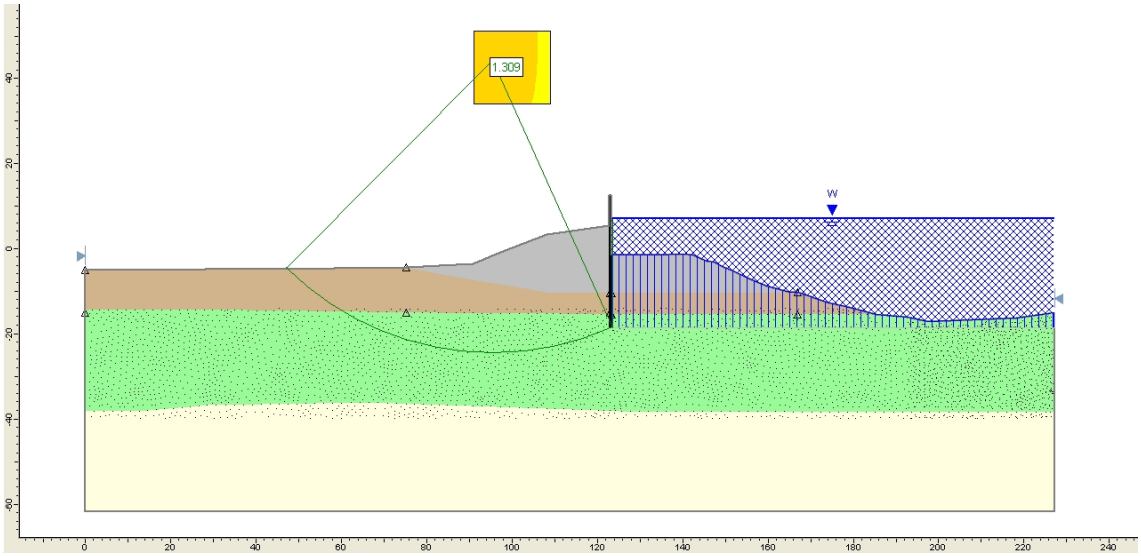

Figure C-51: Factor of safety for ESD w BC-5ft (OCR=1 to 1.2) at CWL=7ft

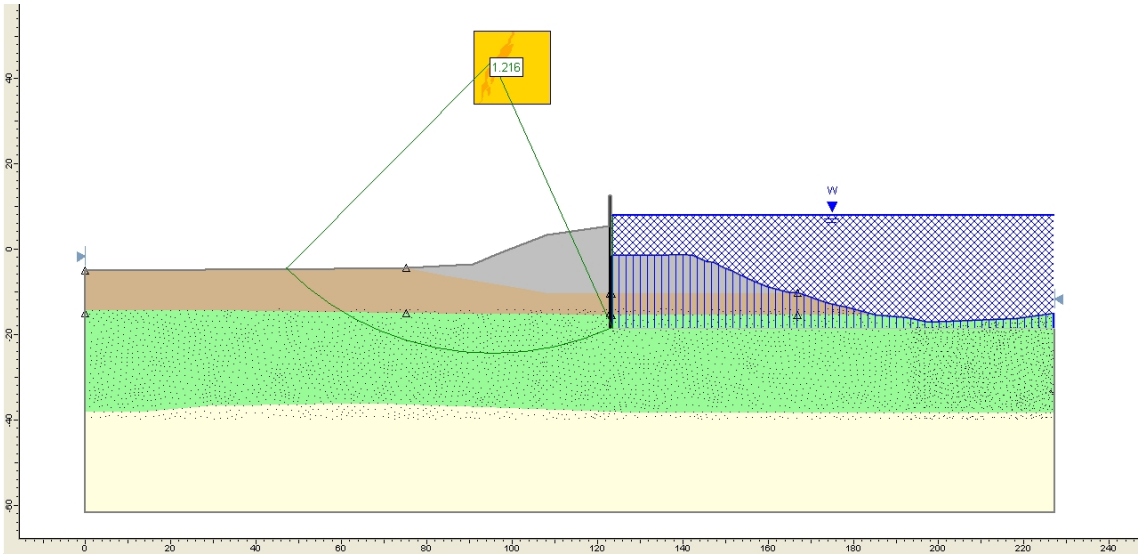

Figure C-52: Factor of safety for ESD w BC-5ft (OCR=1 to 1.2) at CWL=8ft

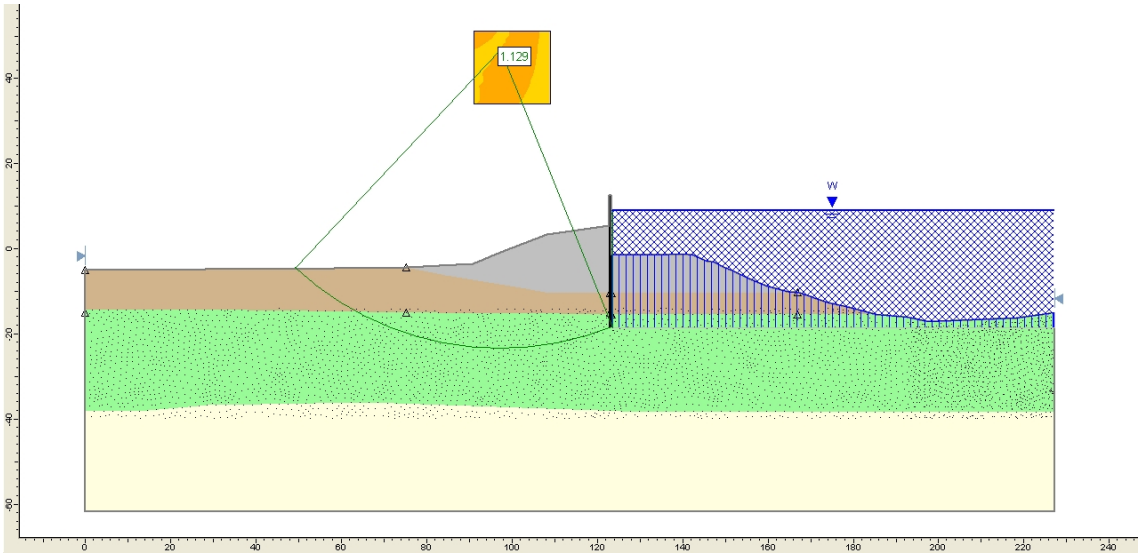

Figure C-53: Factor of safety for ESD w BC-5ft (OCR=1 to 1.2) at CWL=9ft

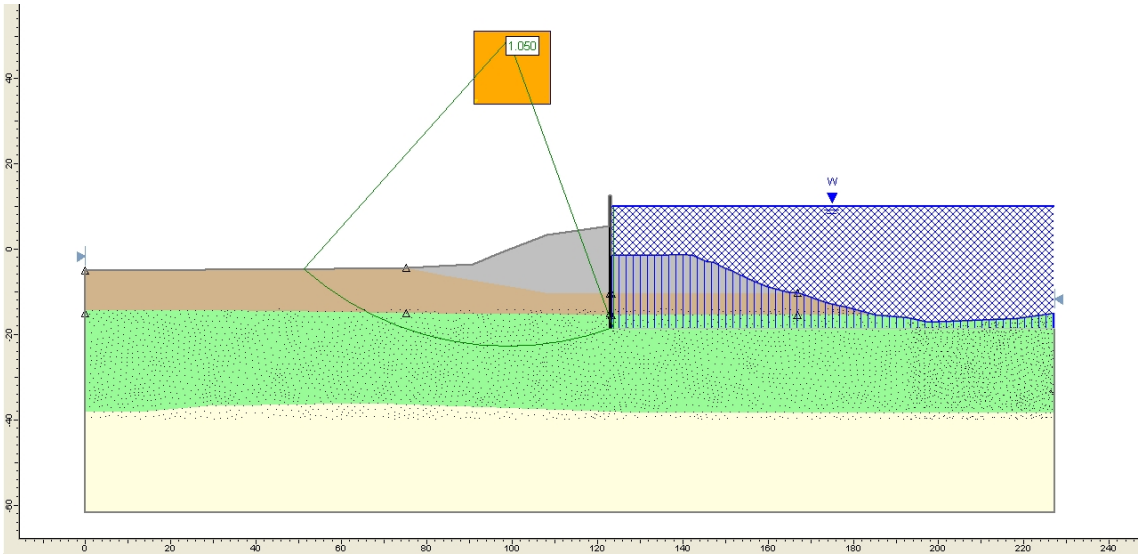

Figure C-54: Factor of safety for ESD w BC-5ft (OCR=1 to 1.2) at CWL=10ft

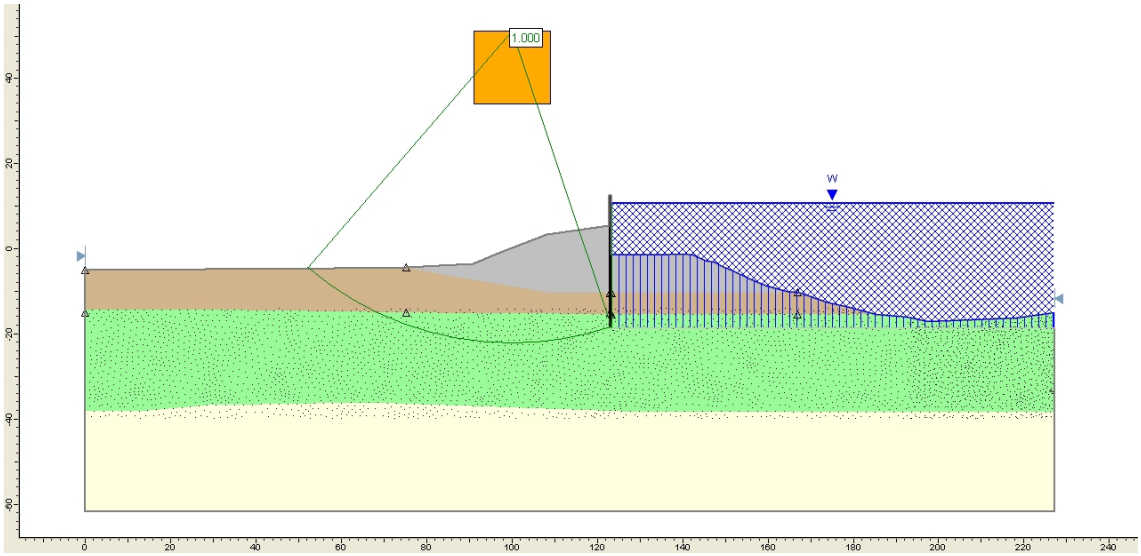

Figure C-55: Factor of safety for ESD w BC-5ft (OCR=1 to 1.2) at CWL=10.65ft

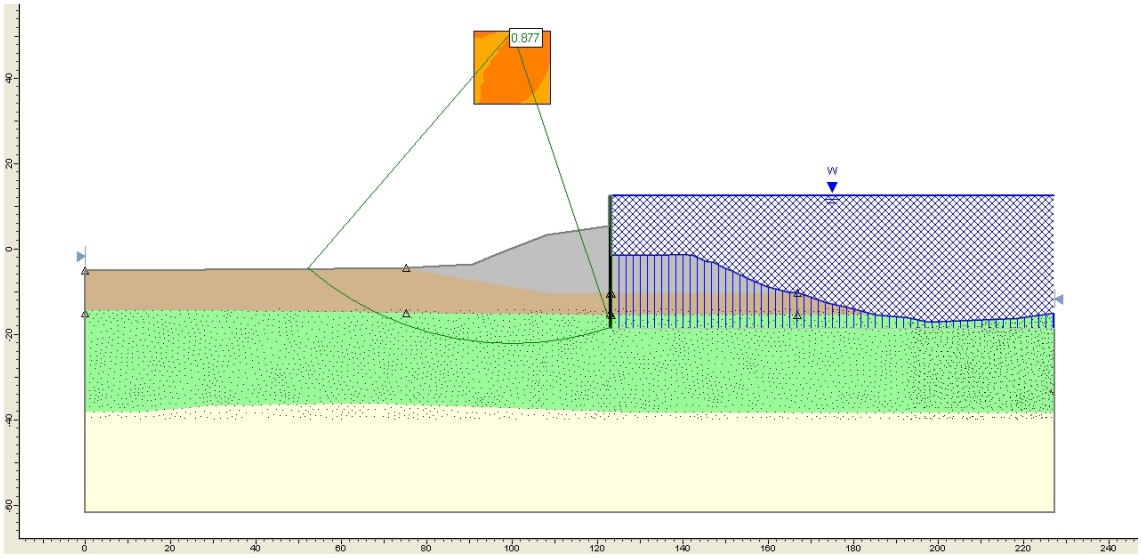

Figure C-56: Factor of safety for ESD w BC-5ft (OCR=1 to 1.2) at CWL=12.5ft

ESD w BC-5ft (OCR calculated)

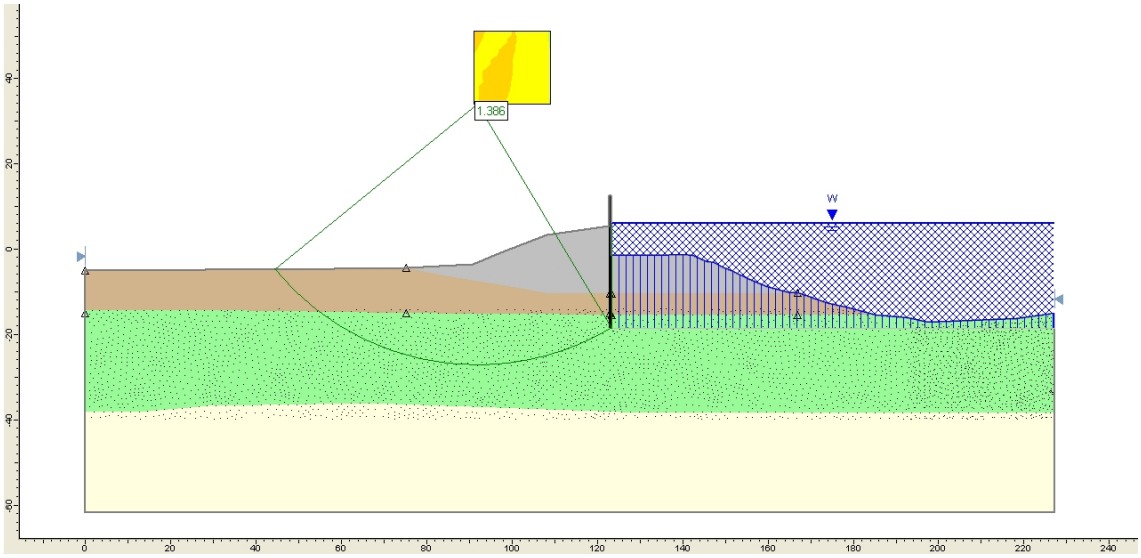

Figure C-57: Factor of safety for ESD w BC-5ft (OCR calculated) at CWL=6ft

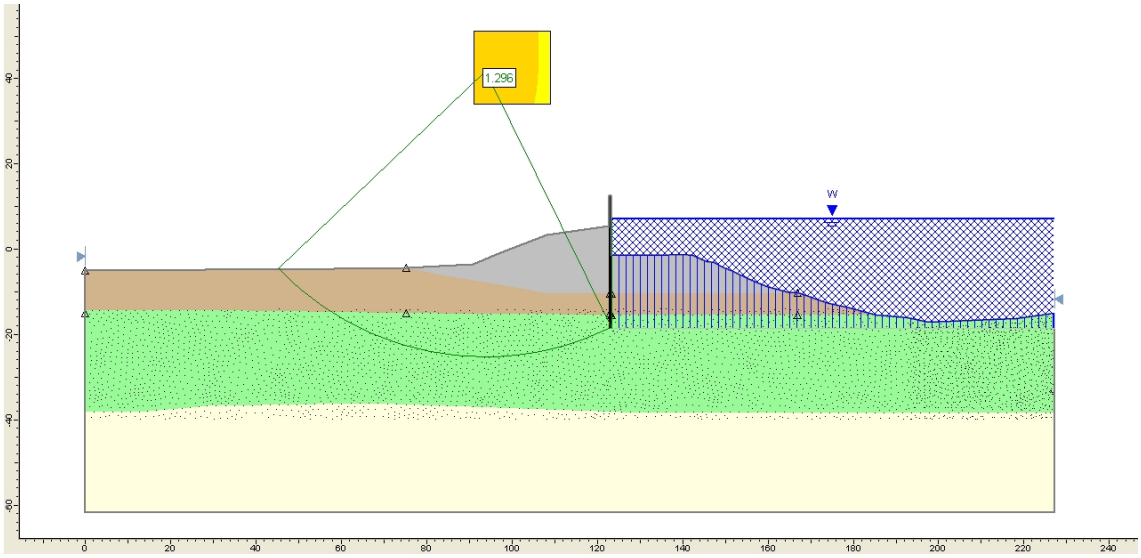

Figure C-58: Factor of safety for ESD w BC-5ft (OCR calculated) at CWL=7ft

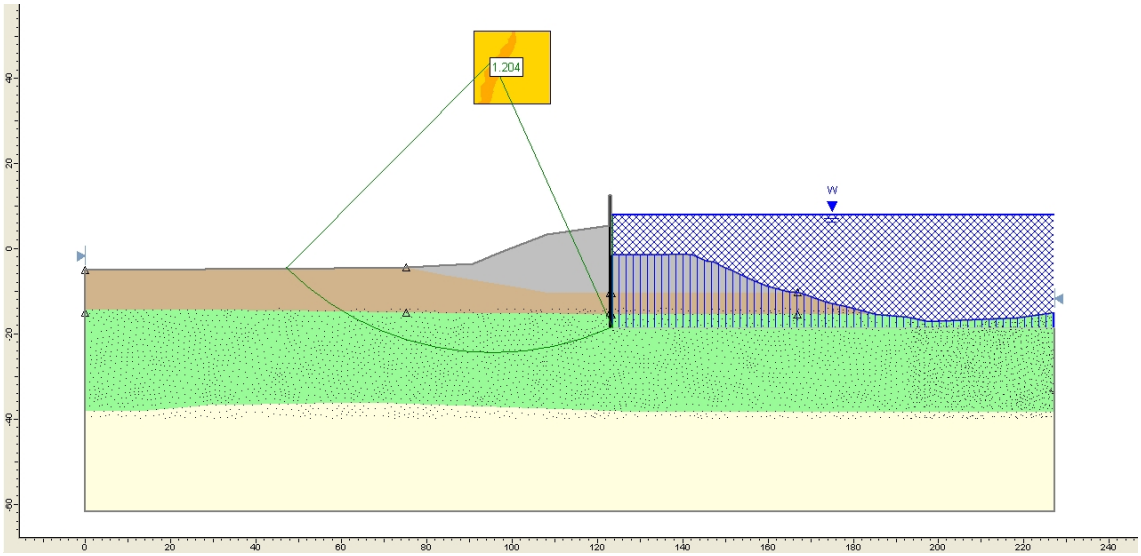

Figure C-59: Factor of safety for ESD w BC-5ft (OCR calculated) at CWL=8ft

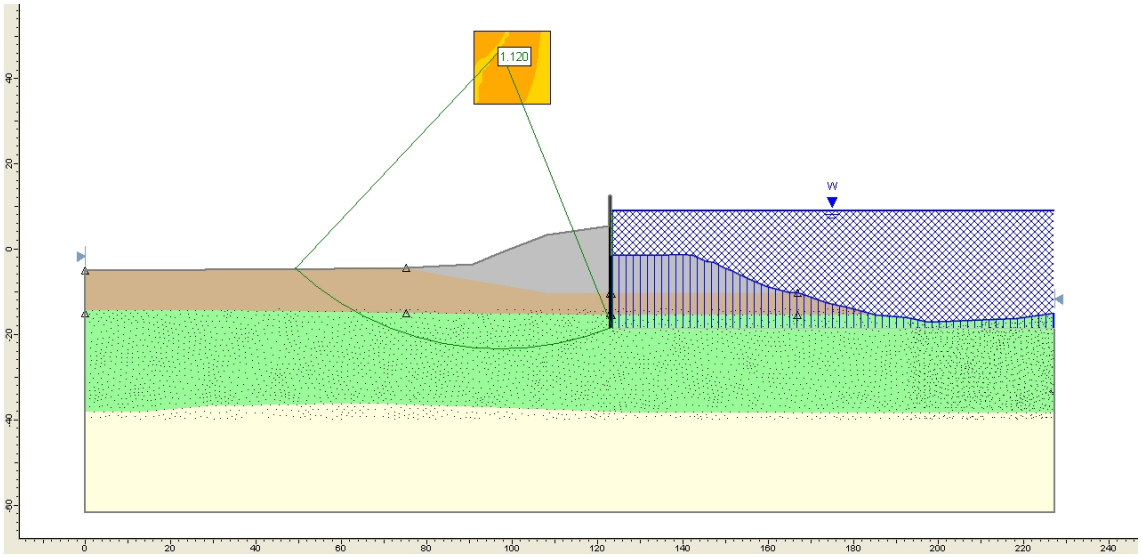

Figure C-60: Factor of safety for ESD w BC-5ft (OCR calculated) at CWL=9ft

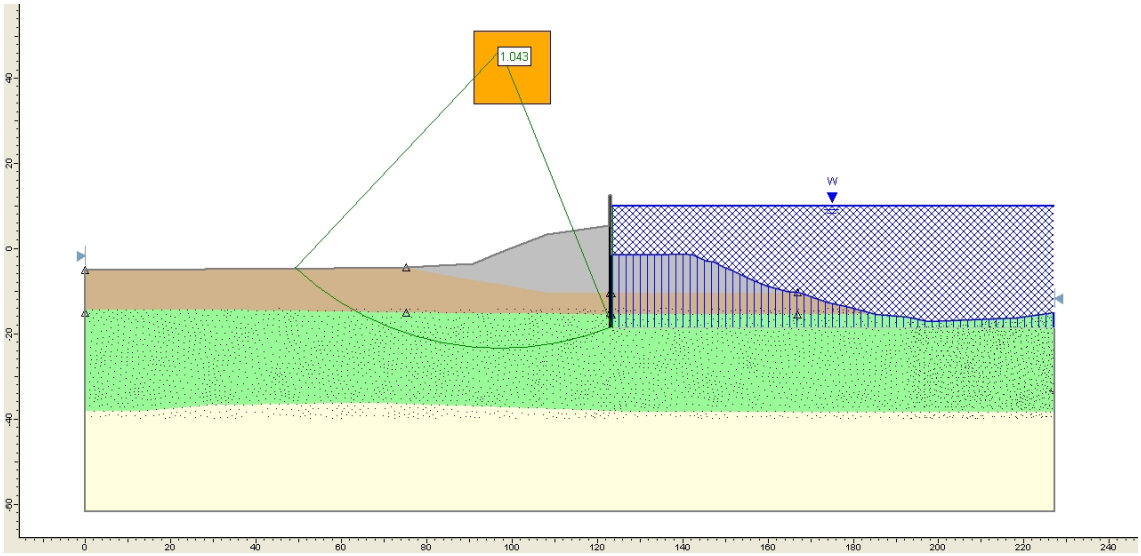

Figure C-61: Factor of safety for ESD w BC-5ft (OCR calculated) at CWL=10ft

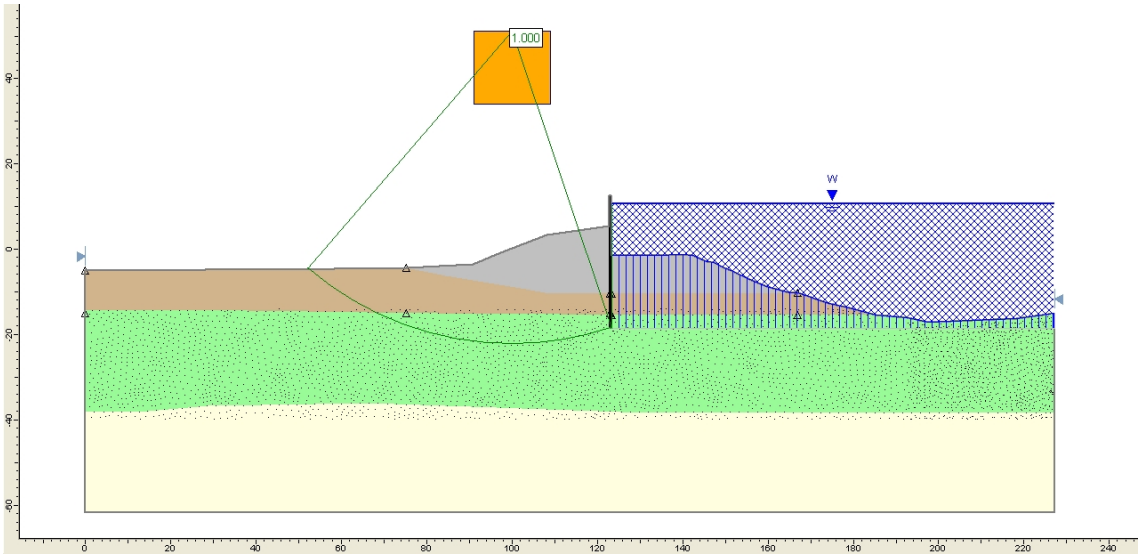

Figure C-62: Factor of safety for ESD w BC-5ft (OCR calculated) at CWL=10.57ft

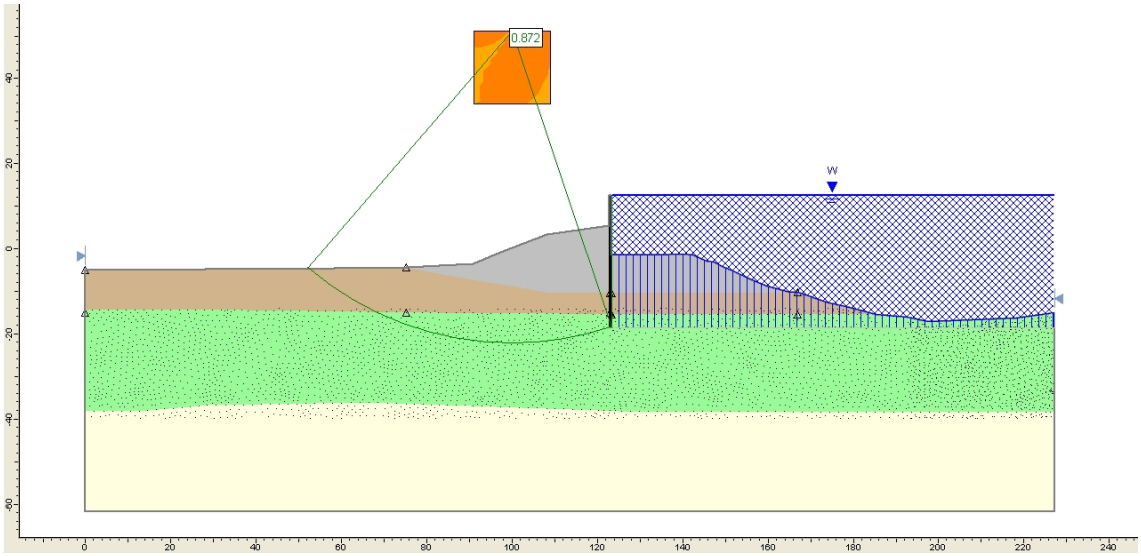

Figure C-63: Factor of safety for ESD w BC-5ft (OCR calculated) at CWL=12.5ft

ESD w BC-7ft (OCR=1)

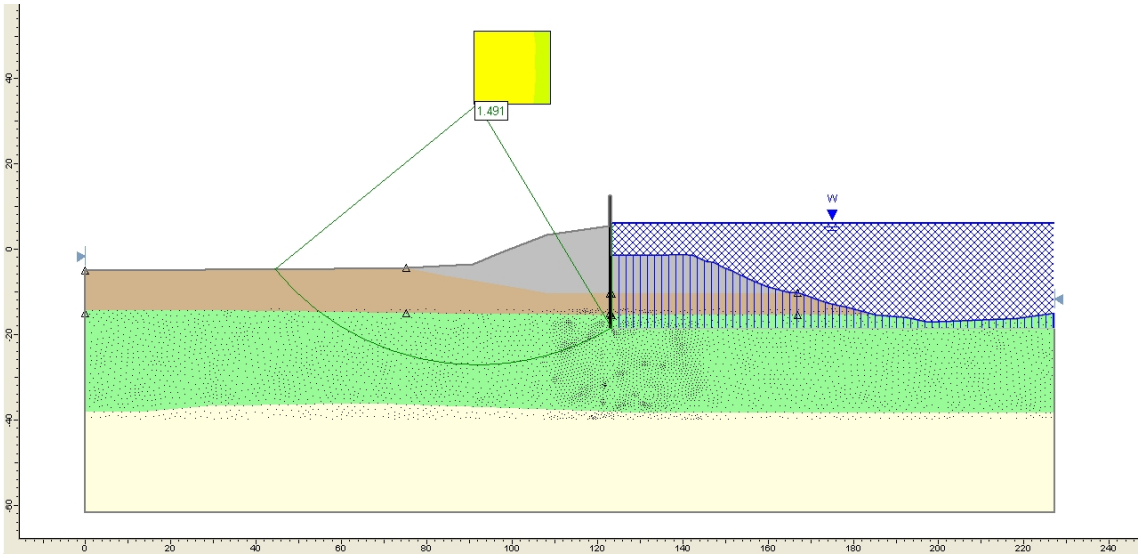

Figure C-64: Factor of safety for ESD w BC-7ft (OCR=1) at CWL=6ft

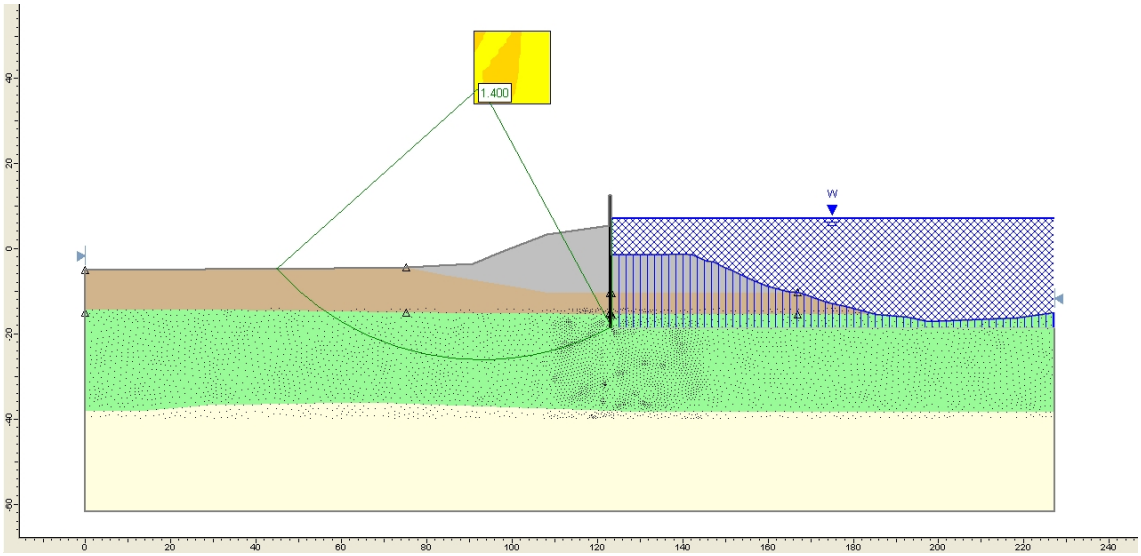

Figure C-65: Factor of safety for ESD w BC-7ft (OCR=1) at CWL=7ft

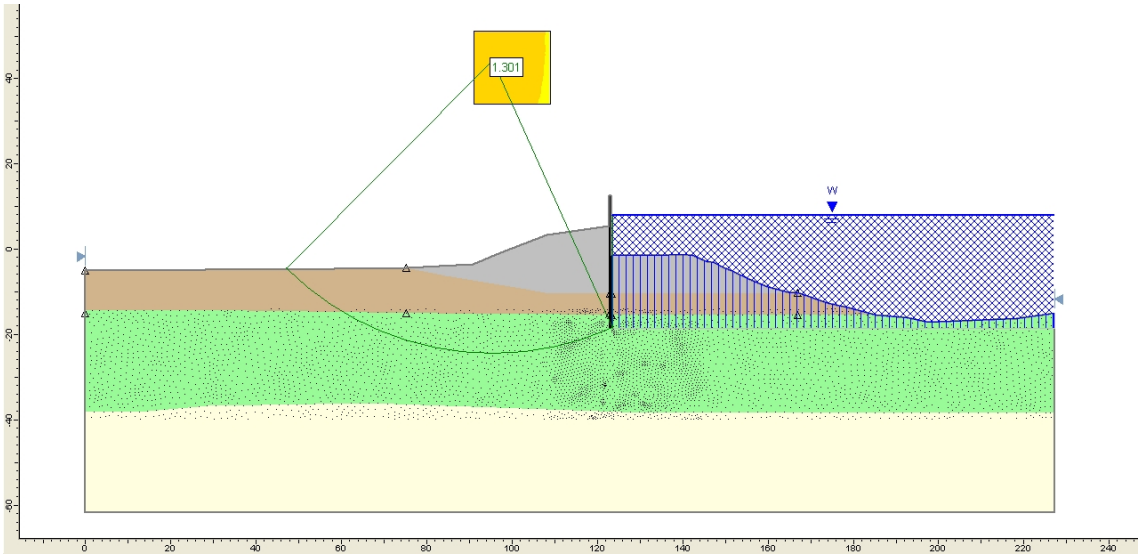

Figure C-66: Factor of safety for ESD w BC-7ft (OCR=1) at CWL=8ft

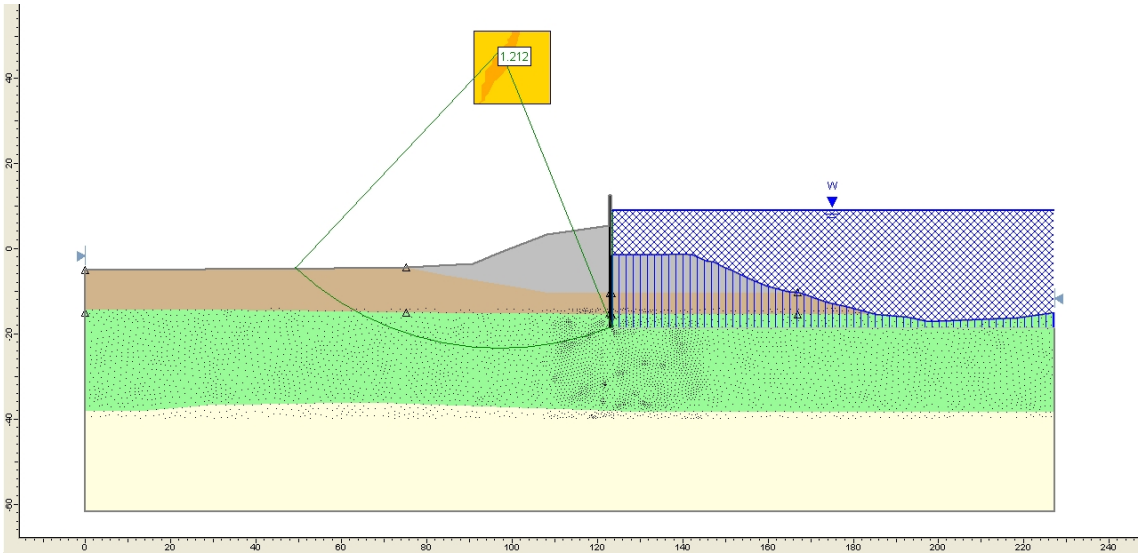

Figure C-67: Factor of safety for ESD w BC-7ft (OCR=1) at CWL=9ft

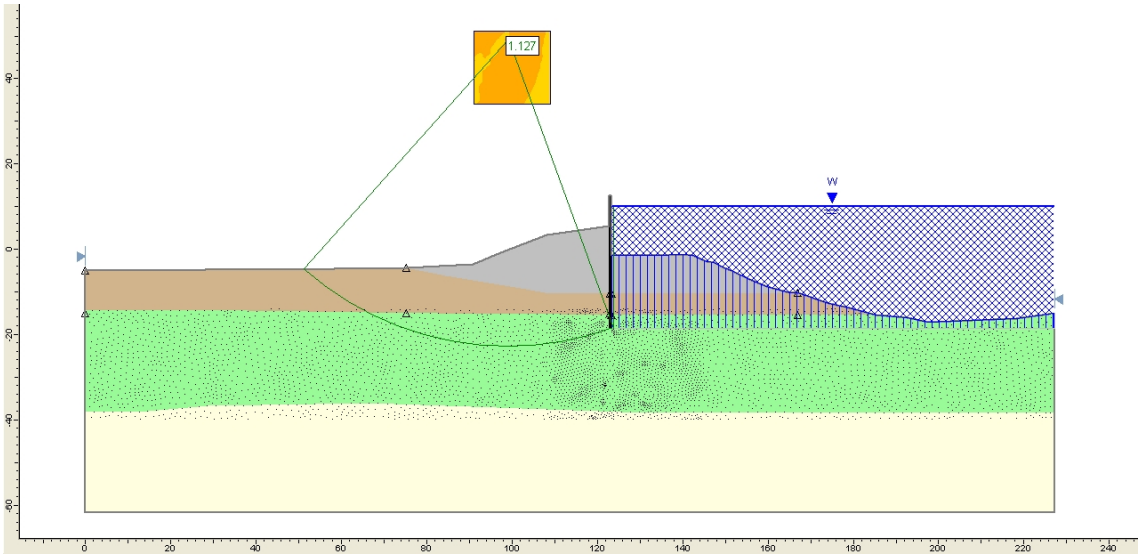

Figure C-68: Factor of safety for ESD w BC-7ft (OCR=1) at CWL=10ft

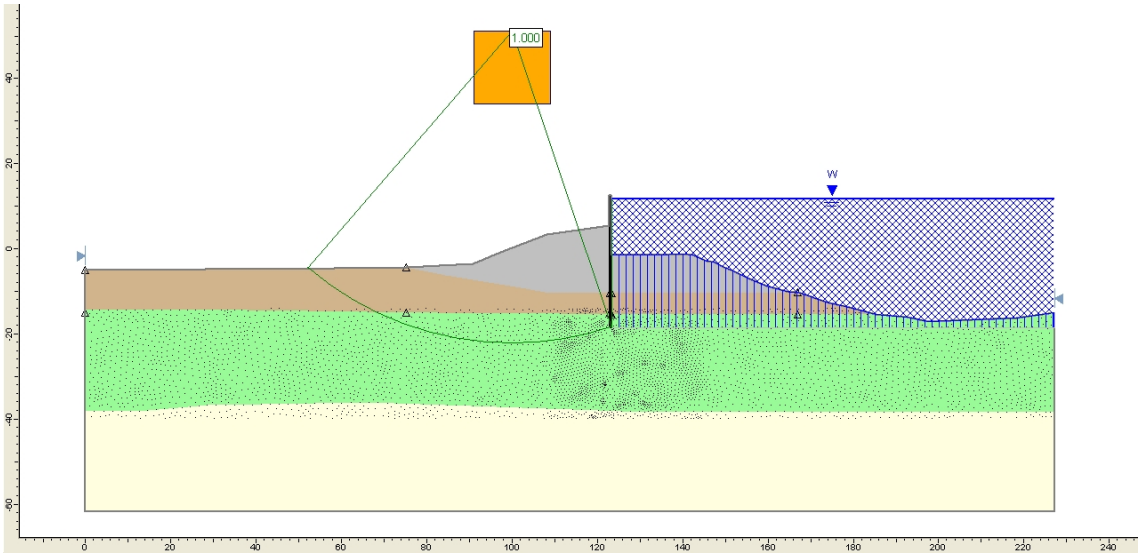

Figure C-69: Factor of safety for ESD w BC-7ft (OCR=1) at CWL=11.64ft

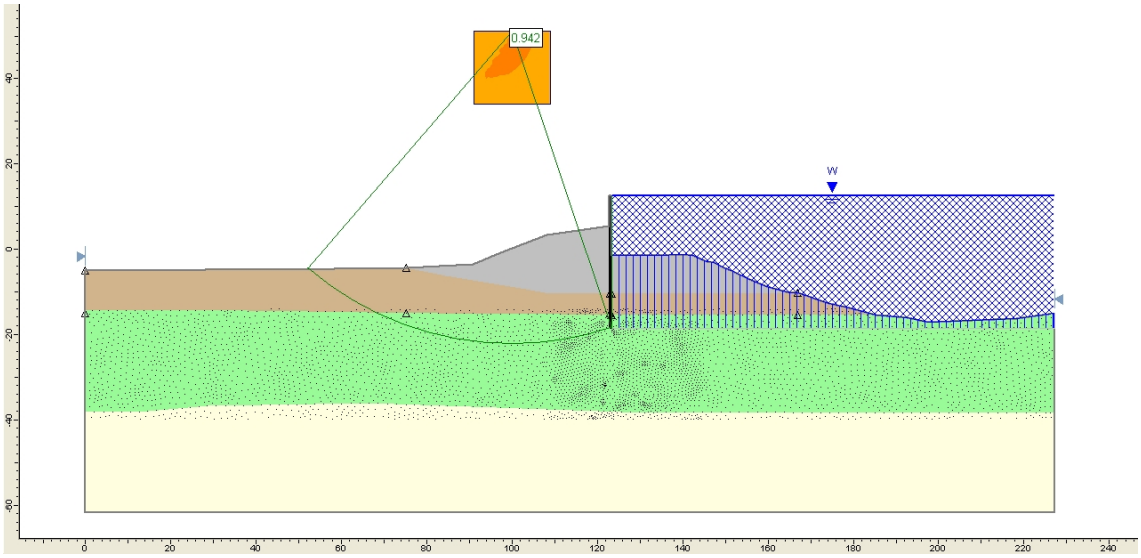

Figure C-70: Factor of safety for ESD w BC-7ft (OCR=1) at CWL=12.5ft

ESD w BC-7ft (OCR=1 to 1.2)

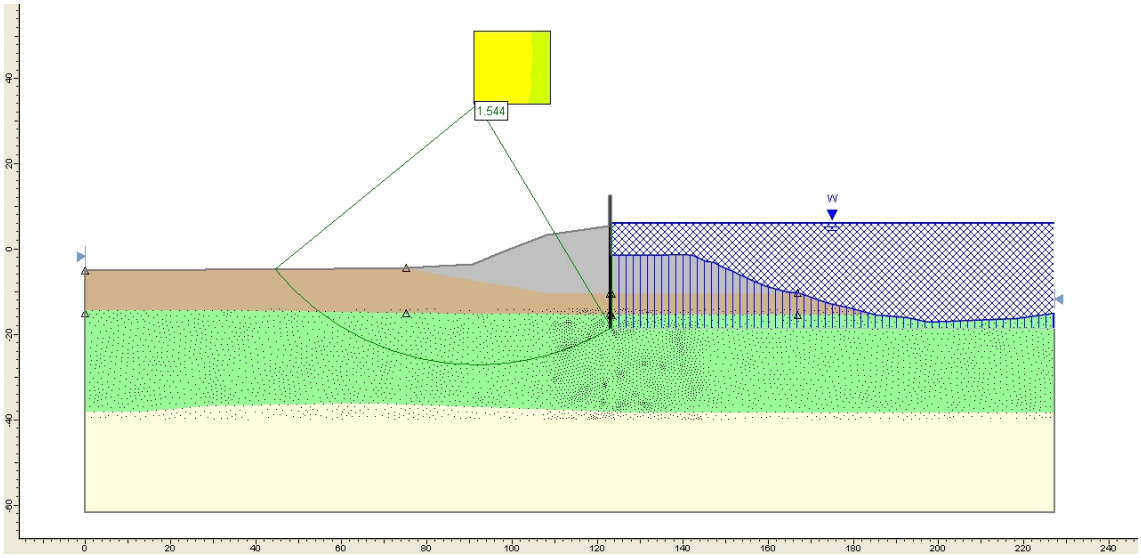

Figure C-71: Factor of safety for ESD w BC-7ft (OCR=1 to 1.2) at CWL=6ft

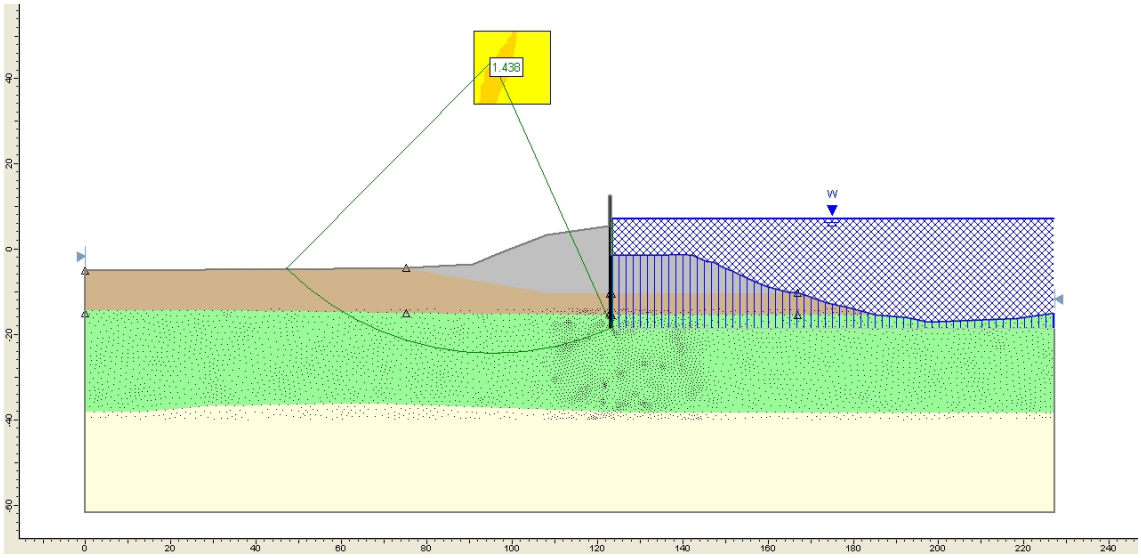

Figure C-72: Factor of safety for ESD w BC-7ft (OCR=1 to 1.2) at CWL=7ft

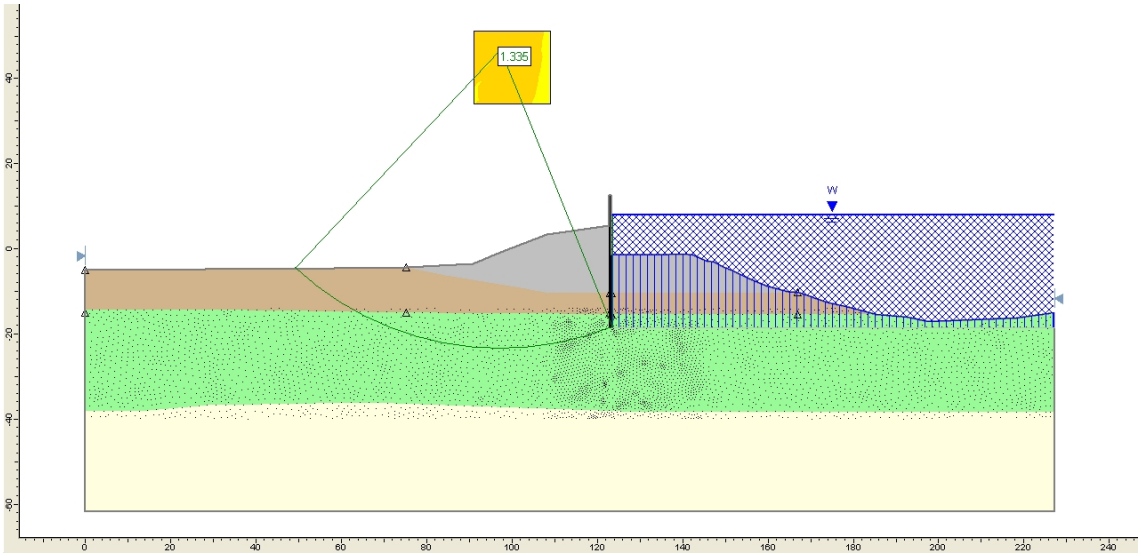

Figure C-73: Factor of safety for ESD w BC-7ft (OCR=1 to 1.2) at CWL=8ft

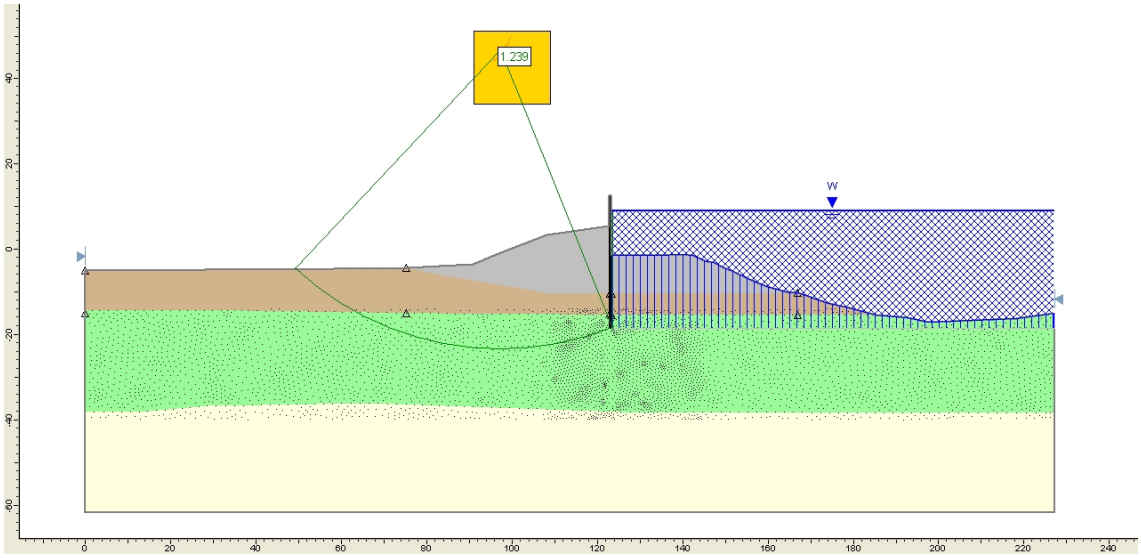

Figure C-74: Factor of safety for ESD w BC-7ft (OCR=1 to 1.2) at CWL=9ft

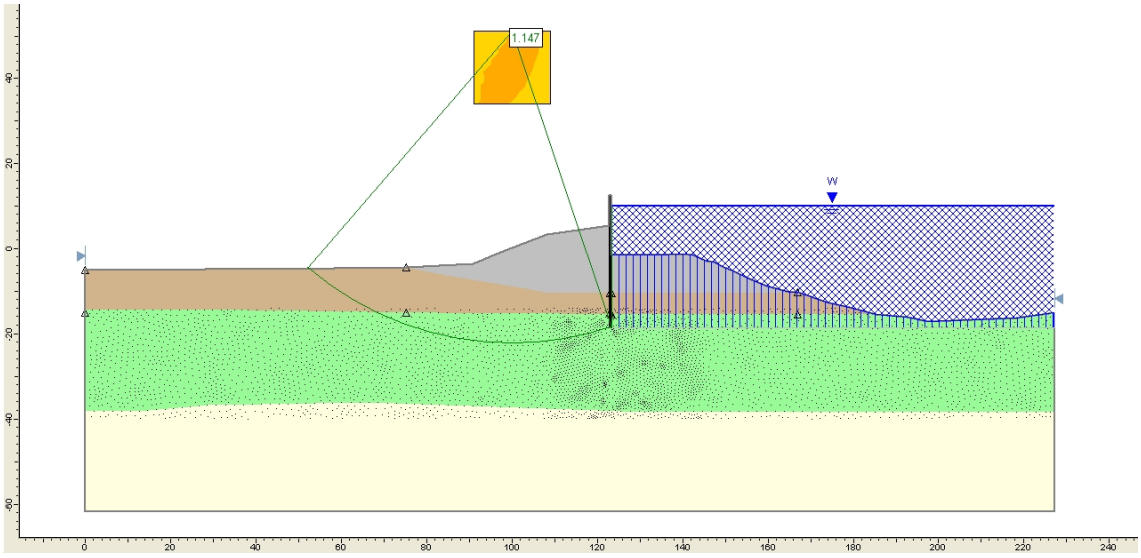

FigureC-75: Factor of safety for ESD w BC-7ft (OCR=1 to 1.2) at CWL=10ft

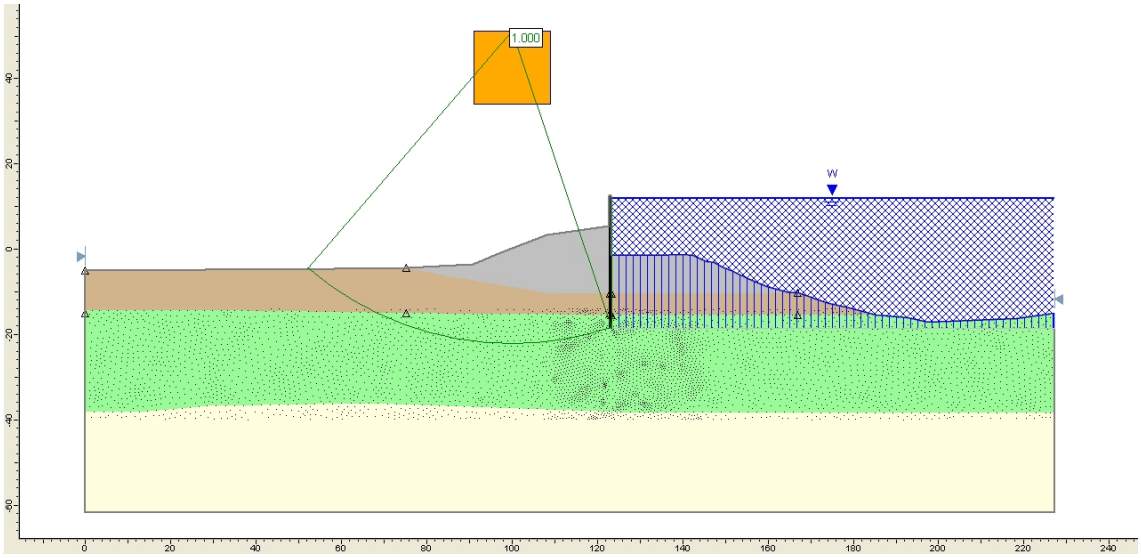

Figure C-76: Factor of safety for ESD w BC-7ft (OCR=1 to 1.2) at CWL=11.88ft

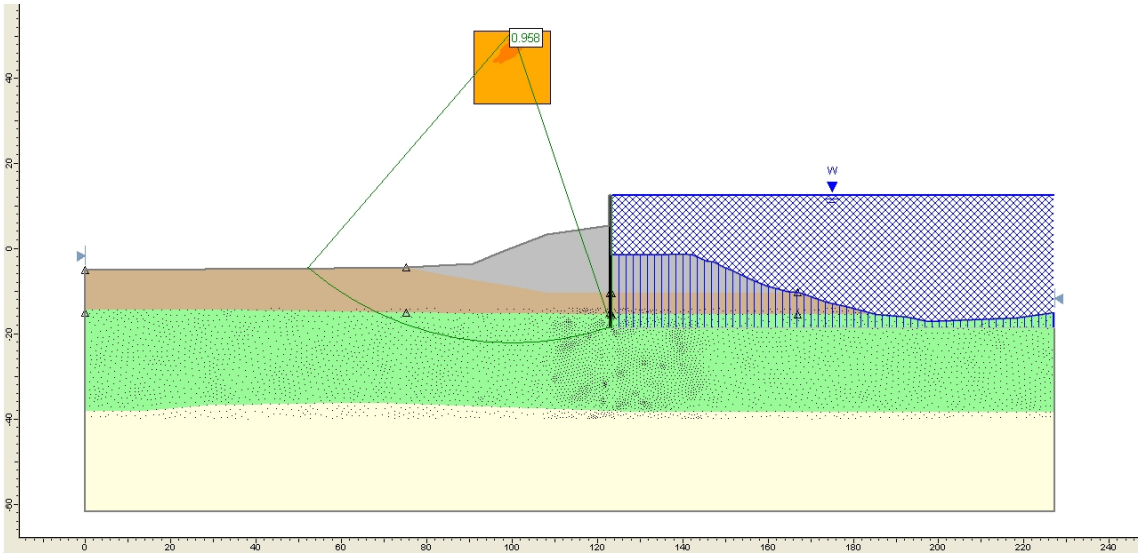

Figure C-77: Factor of safety for ESD w BC-7ft (OCR=1 to 1.2) at CWL=12.5ft

ESD w BC-7ft (OCR calculated)

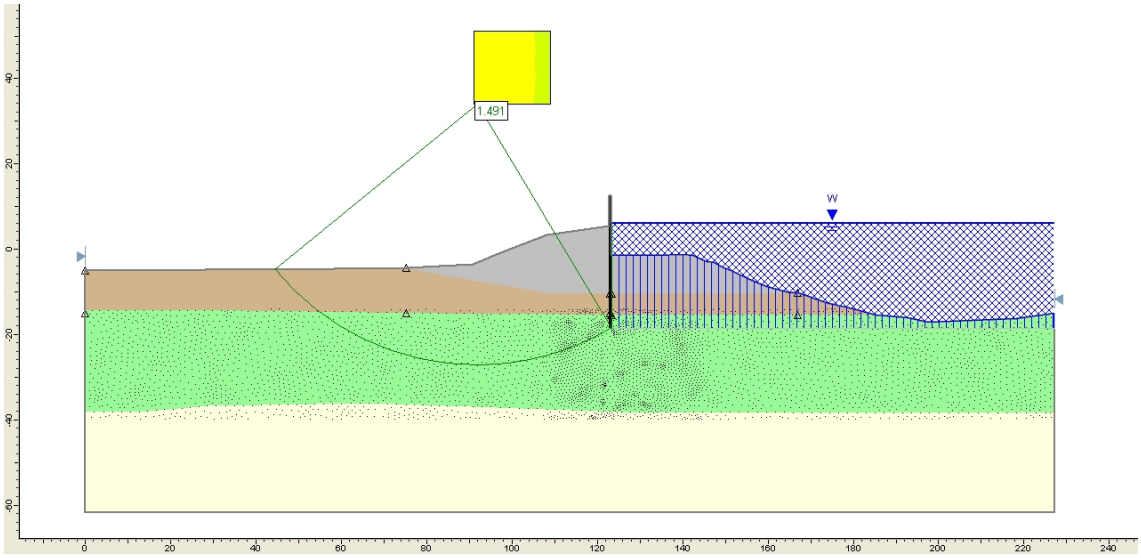

Figure C-78: Factor of safety for ESD w BC-7ft (OCR calculated) at CWL=6ft

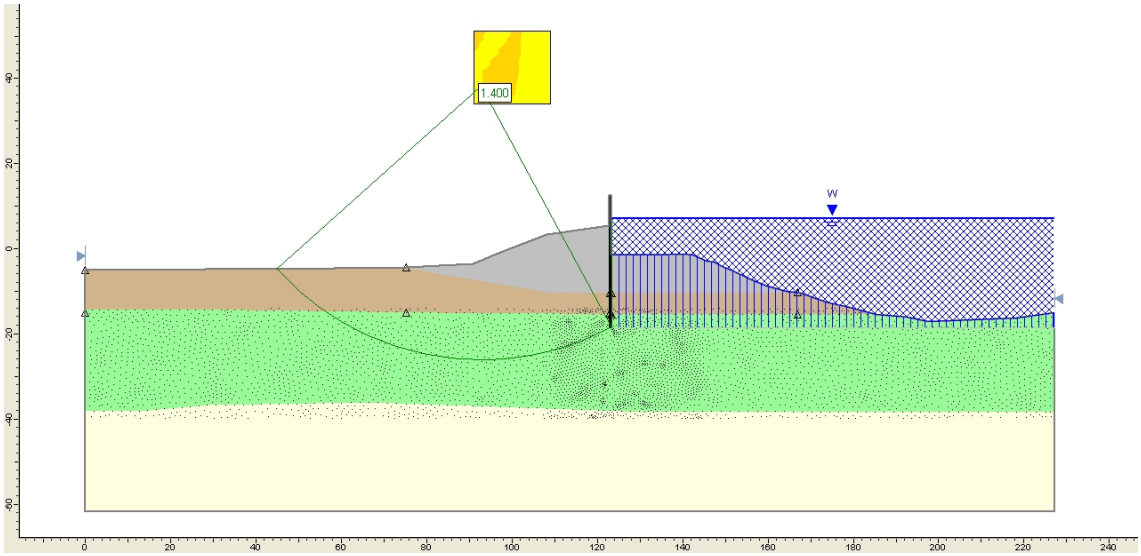

Figure C-79: Factor of safety for ESD w BC-7ft (OCR calculated) at CWL=7ft

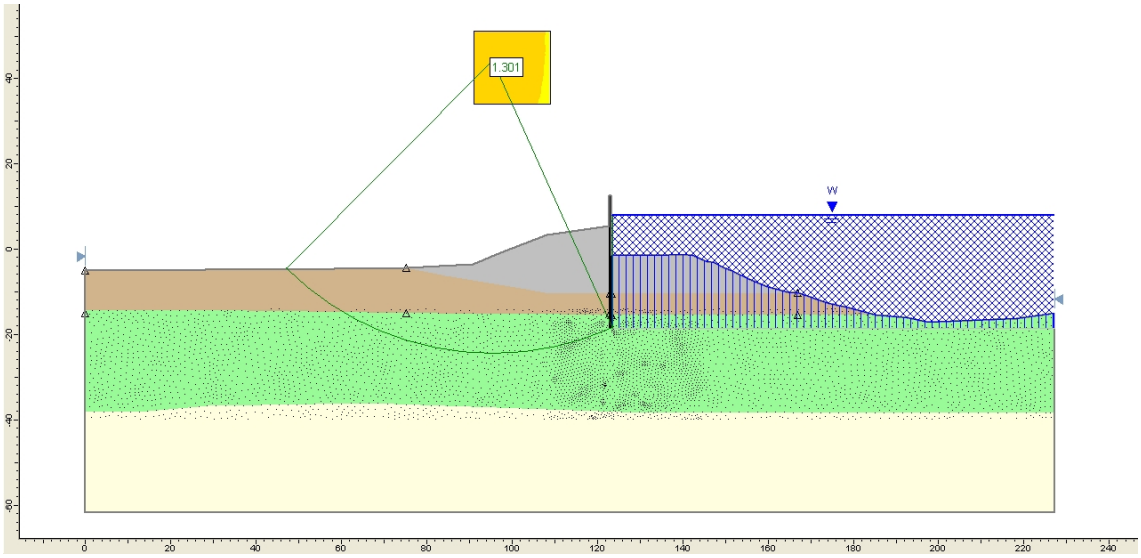

Figure C-80: Factor of safety for ESD w BC-7ft (OCR calculated) at CWL=8ft

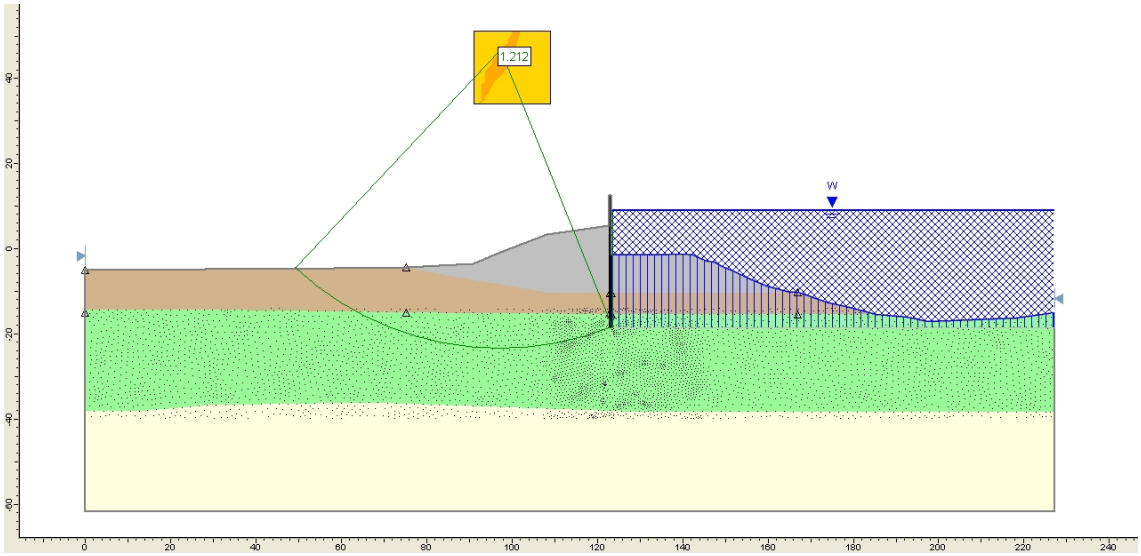

Figure C-81: Factor of safety for ESD w BC-7ft (OCR calculated) at CWL=9ft

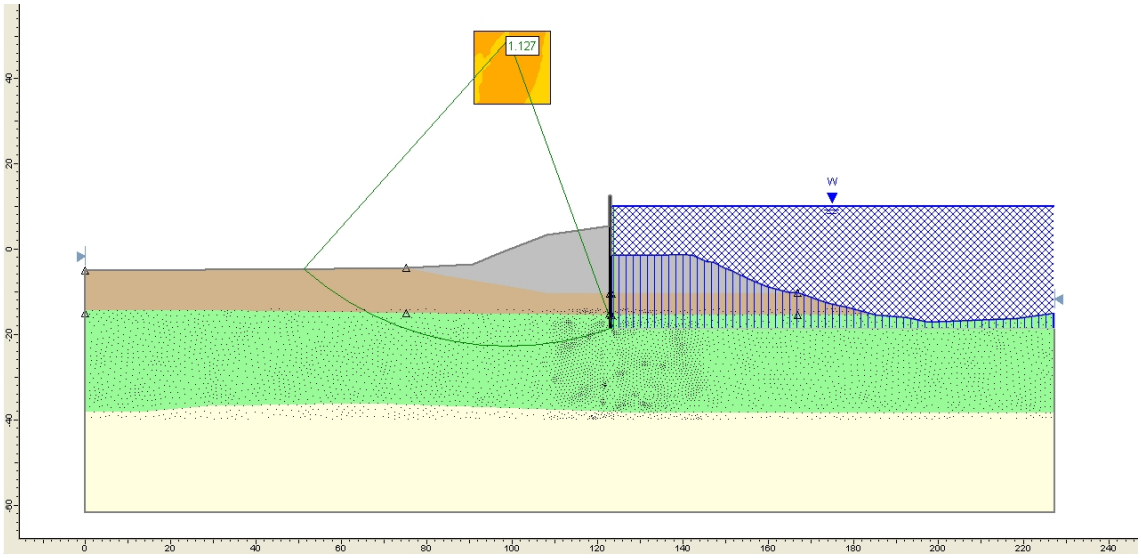

Figure C-82: Factor of safety for ESD w BC-7ft (OCR calculated) at CWL=10ft

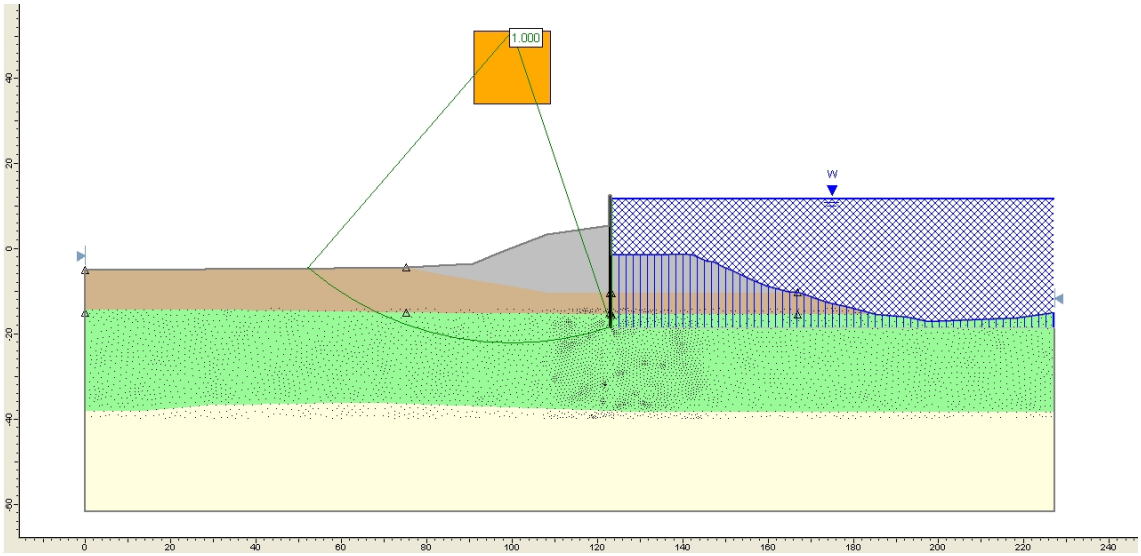

Figure C-83: Factor of safety for ESD w BC-7ft (OCR calculated) at CWL=11.64ft

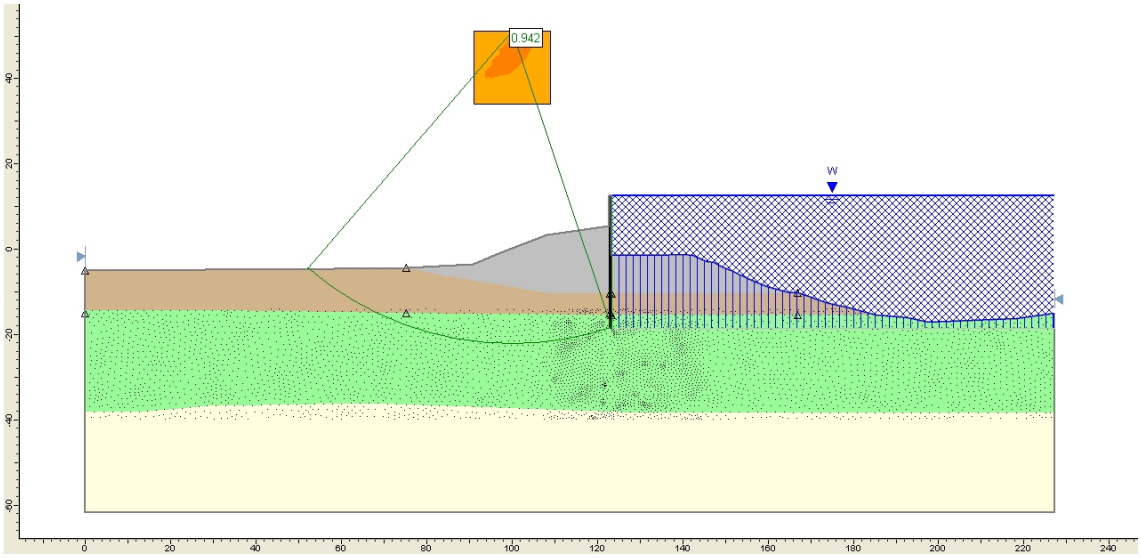

Figure C-84: Factor of safety for ESD w BC-7ft (OCR calculated) at CWL=12.5ft

SLIDE5.0 Figures: West Bank

ESD w BC-5ft (OCR calculated)

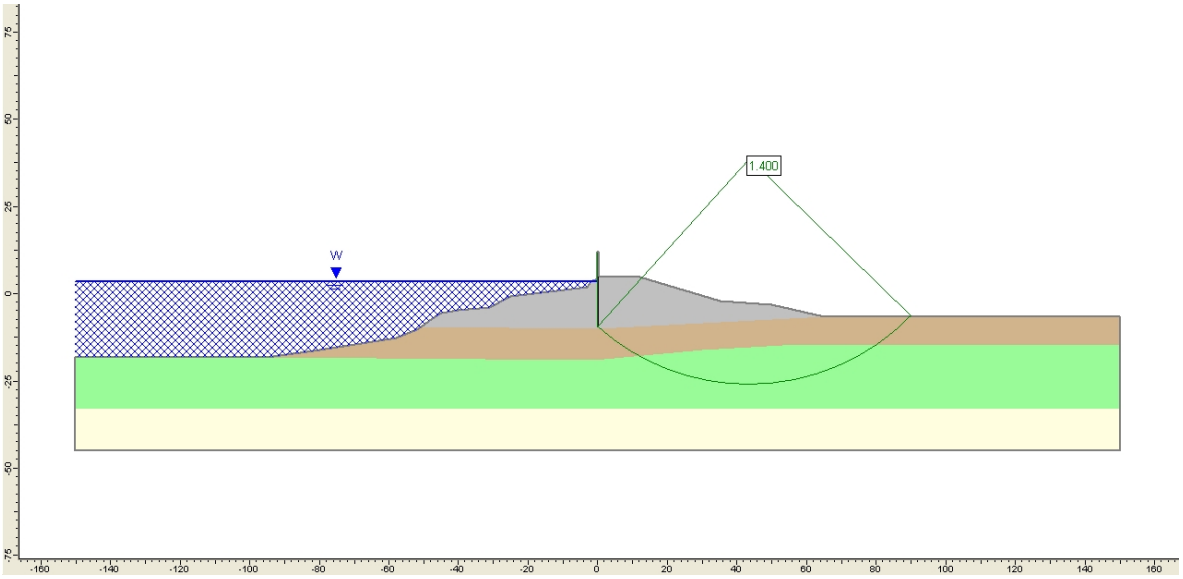

Figure C-85: Factor of safety for ESD w BC-5ft (OCR calculated) at CWL=3.39ft for West Bank

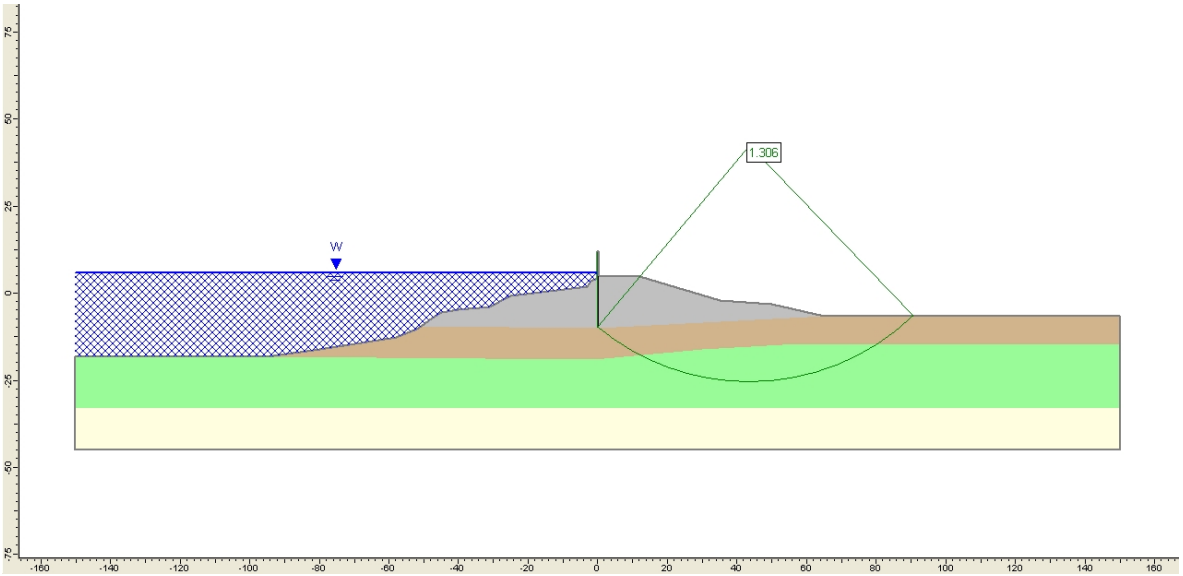

Figure C-86: Factor of safety for ESD w BC-5ft (OCR calculated) at CWL=6ft for West Bank

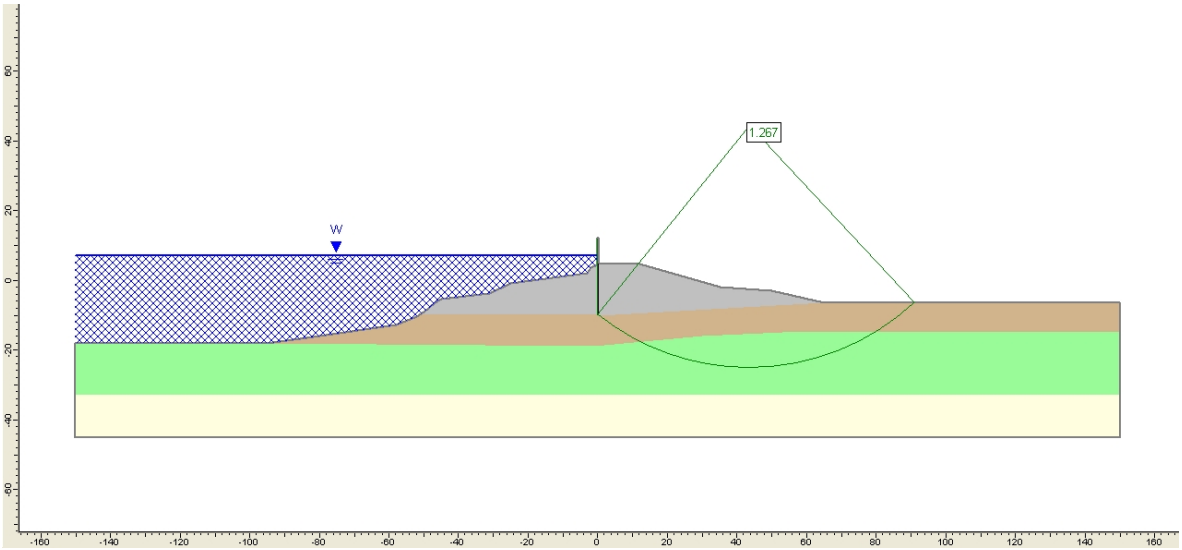

Figure C-87: Factor of safety for ESD w BC-5ft (OCR calculated) at CWL=7ft for West Bank

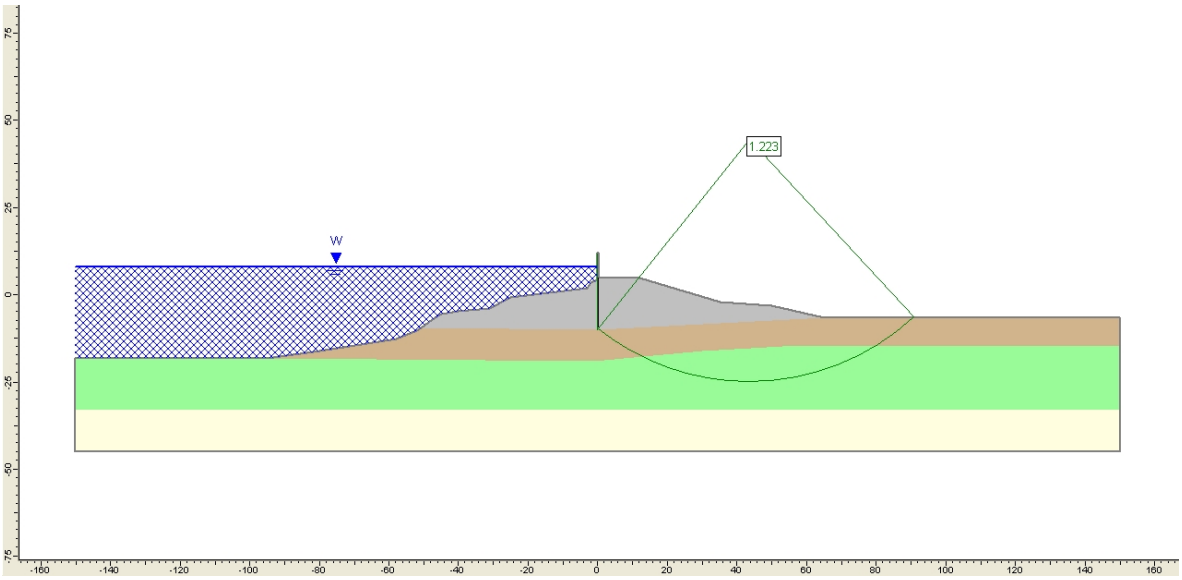

Figure C-88: Factor of safety for ESD w BC-5ft (OCR calculated) at CWL=8ft for West Bank

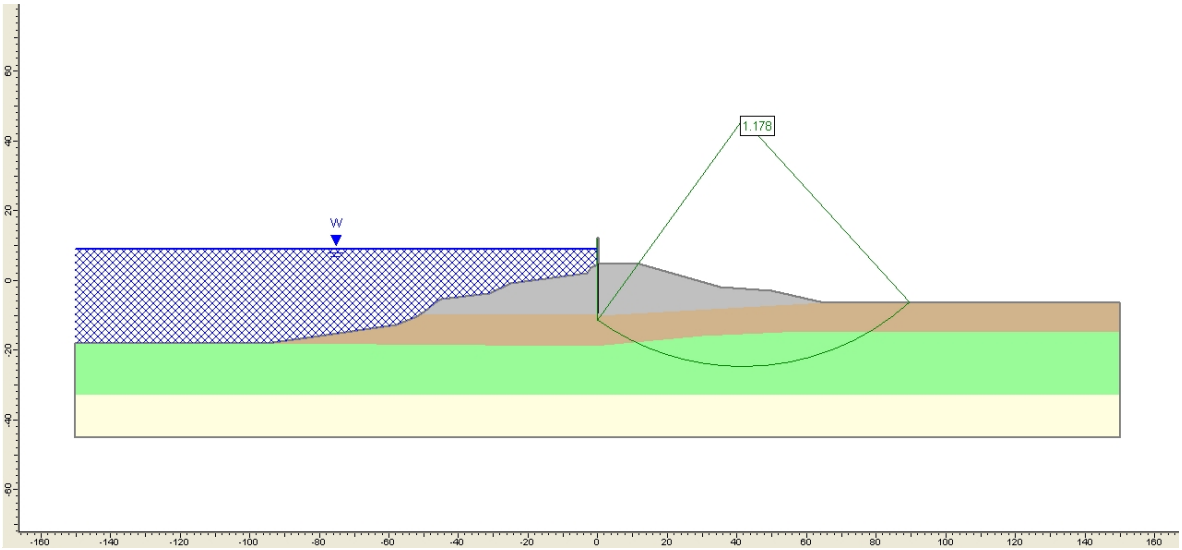

Figure C-89: Factor of safety for ESD w BC-5ft (OCR calculated) at CWL=9ft for West Bank

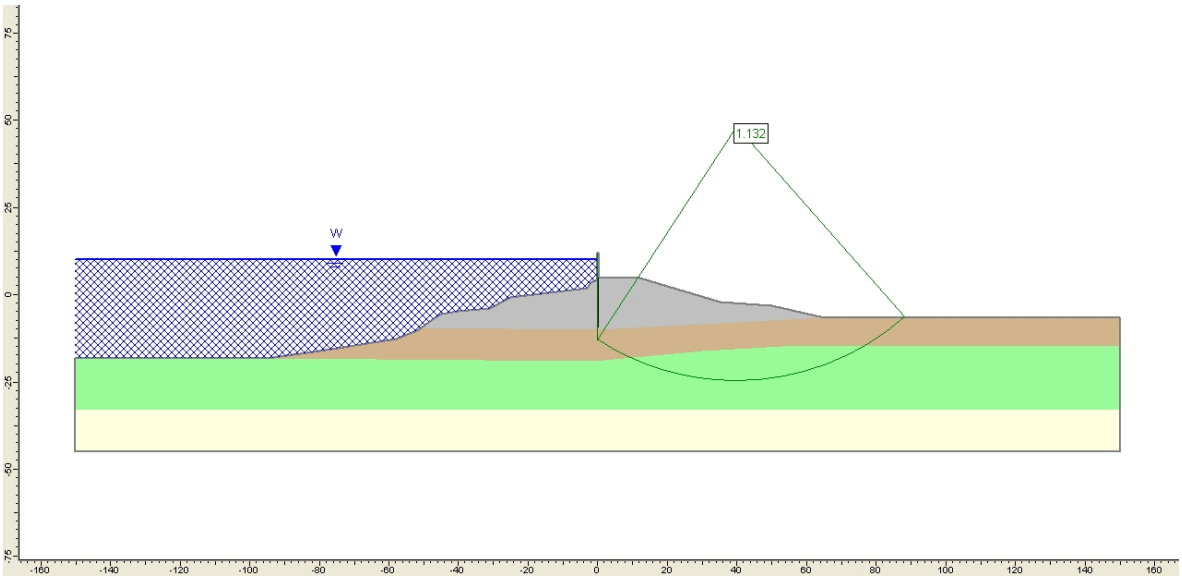

Figure C-90: Factor of safety for ESD w BC-5ft (OCR calculated) at CWL=10ft for West Bank

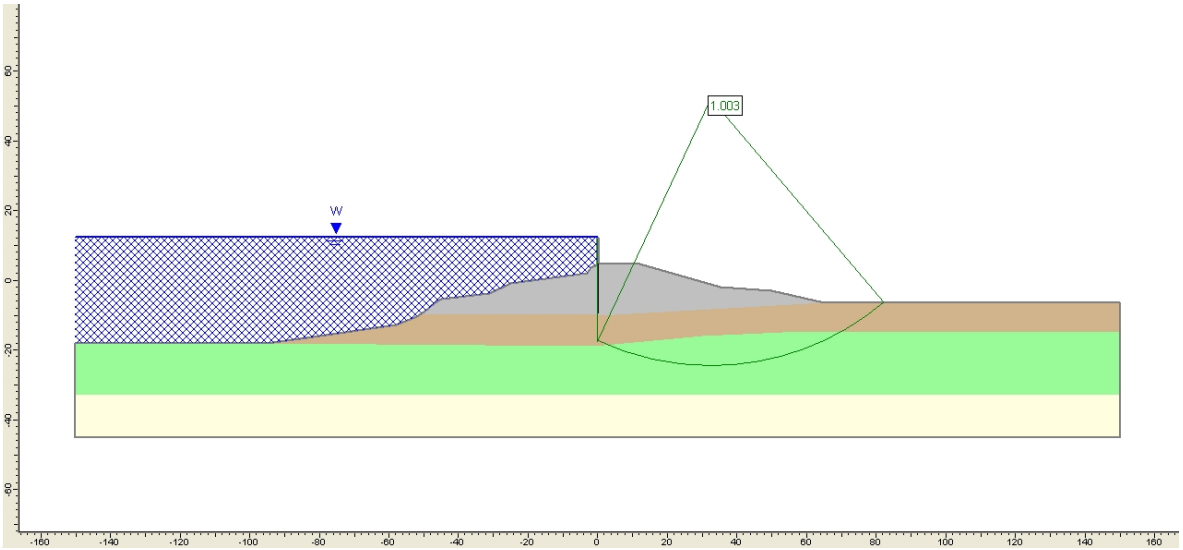

Figure C-91: Factor of safety for ESD w BC-5ft (OCR calculated) at CWL=12.5ft for West Bank